UC Berkeley
SEMM Reports Series

Title
Nonlinear Geometric Material and Time Dependent Analysis of Three Dimensional Reinforced and Prestressed Concrete Frames

Permalink
https://escholarship.org/uc/item/10n0w32g

Author
Mari, Antonio

Publication Date
1984-06-01

eScholarship.org Powered by the California Digital Library
University of California

REPORT NO.
UCB/SESM-84/12

STRUCTURAL ENGINEERING AND
STRUCTURAL MECHANICS

NONLINEAR GEOMETRIC, MATERIAL AND TIME DEPENDENT ANALYSIS OF THREE DIMENSIONAL REINFORCED AND PRESTRESSED CONCRETE FRAMES

by
ANTONIO R. MARI
Visiting Scholar

Faculty Investigator: A. C. Scordelis

JUNE 1984

DEPARTMENT OF CIVIL ENGINEERING
UNIVERSITY OF CALIFORNIA
BERKELEY, CALIFORNIA

TECHNICAL REPORT STANDARD TITLE PAGE

1. Report No.	2. Government Accession No.	3. Recipient's Catalog No.

4. Title and Subtitle
Nonlinear Geometric, Material and Time Dependent Analysis of Three Dimensional Reinforced and Prestressed Concrete Frames

5. Report Date
June 1984

6. Performing Organization Code

7. Author(s)
Antonio R. Mari

8. Performing Organization Report No.
UCB/SESM-84/12

9. Performing Organization Name and Address
Department of Civil Engineering
University of California
Berkeley, California 94720

10. Work Unit No.

11. Contract or Grant No.

12. Type of Report and Period Covered

12. Sponsoring Agency Name and Address
Fulbright Council and Spanish Ministry of Education and Science
Cartagena 83-85, Madrid, Spain

14. Sponsoring Agency Code

15. Supplementary Notes
This study was made during the author's stay at Berkeley as a Visiting Scholar from the Polytechnic University of Barcelona, Spain

16. Abstract

A method of analysis for three dimensional reinforced and prestressed concrete frames based upon the finite element displacement formulation is presented. The frames may have arbitrary geometry and be subjected to applied loads and imposed displacements in any direction. The method recognizes the material nonlinearities due to cracking of the concrete and yielding of the steel reinforcement. The effects of prestressing are also taken into account for postensioned bonded frames including instantaneous and time dependent prestress losses. A straight beam element with an arbitrary cross section made up of longitudinal filaments to represent the concrete and reinforcing steel is used. The element has six degrees of freedom at each end. An incremental and iterative solution scheme based either upon constant imposed load or displacement can be used as a nonlinear strategy. The procedure is capable of predicting the response of these structures throughout their service load history as well as throughout their elastic, cracking, inelastic and ultimate ranges. Several numerical examples analyzed by the computer program PCF3D developed are presented to demonstrate the validity and applicability of the method.

17. Key Words	18. Distribution Statement
Reinforced Concrete; Prestressed Concrete, Frame; Nonlinear analysis; Cracking, Creep; Finite element.	Unlimited

19. Security Classif. (of this report)	20. Security Classif. (of this page)	21. No. of Pages	22. Price
unclassified	unclassified		

Form DOT F 1700.7 (8-69)

Department of Civil Engineering
Division of Structural Engineering
and
Structural Mechanics

UCB/SESM Report No. 84-12

NONLINEAR GEOMETRIC, MATERIAL AND TIME DEPENDENT ANALYSIS OF THREE DIMENSIONAL REINFORCED AND PRESTRESSED CONCRETE FRAMES

by

Antonio R. Marí
Visiting Scholar

Faculty Investigator:

A. C. Scordelis

College of Engineering
Office of Research Services
University of California
Berkeley, California

June, 1984

ABSTRACT

A method of analysis for three dimensional reinforced and prestressed concrete frames based upon the finite element displacement formulation is presented. The frames may have arbitrary geometry and be subjected to applied loads and imposed displacements in any direction. The method recognizes the material nonlinearities due to cracking of the concrete and yielding of the steel reinforcement. The effects of prestressing are also taken into account for postensioned bonded frames including prestress losses due to anchorage slip, friction and time dependent behaviour. The procedure is capable of predicting the response of these structures throughout their service load history as well as throughout their elastic, cracking, inelastic and ultimate load ranges.

A straight beam element with an arbitrary cross-section made up of longitudinal filaments to represent the concrete and reinforcing steel is used. The element has six degrees of freedom at each end. Changing element properties at any time are evaluated by a filament integration. The contribution of each prestressing tendon is added directly.

An incremental and iterative solution scheme based either upon constant imposed load or displacement can be used as a nonlinear strategy, so that structures with local instabilities or strain softening can be analysed.

Several numerical examples analysed by the computer program developed are presented to demonstrate the validity and applicability of the method.

ACKNOWLEDGEMENTS

The author wishes to express his sincere gratitude to Professor A.C. Scordelis for his constant guidance and encouragement throughout the course of this study. His constructive suggestions, criticism and his friendship are highly appreciated.

The author also extends his deepest appreciation and gratitude to his colleagues, Esmond Chan and Mark Ketchum for their help and useful suggestions.

A special word of thanks is also extended to Francesca Torrella and Eduardo González for their skillful typing of the manuscript and drawing of the figures.

This research was sponsored by a Post-doctoral Fulbright-Spanish Ministry of Education and Science Fellowship. The Computer Center at the University of California, Berkeley provided the facilities for the numerical work.

Finally, the love, support and encouragement of the author's wife and friends have played a major role in making it possible to complete this study.

TABLE OF CONTENTS

1. INTRODUCTION

1.1 General

It is well known that the behaviour of reinforced and prestressed concrete structures deviates, even for relative low loading levels, from the linear elastic behaviour that classically has been assumed as valid. For ultimate loading levels the behaviour of concrete structures is highly non-linear not only because of the material properties but also because sometimes the magnitude of the displacements and strains no longer can be considered "small".

When designing a concrete structure both safety and serviciability conditions must be satisfied. In order to ensure the serviciability requirements, an accurate prediction of displacements, internal forces and deformations of the structure subjected to service loads throughout its service life is necessary. To assess the safety of the structure against failure, an accurate estimation of the ultimate load has to be made. Therefore the prediction of the behaviour of the structure through the elastic, inelastic and ultimate ranges is desirable.

There are two ways, essentially, of studying the structural behaviour: the experimental and the analytical; both are necessary and complementary of each other. Since the appearance of digital computers, the development of numerical methods and mathematical models trying to represent accurately the structural behaviour has been favoured. It is possible to use

these models as a complement and even as a substitute for some experimental studies that could be very expensive. The Finite Element Method, (FEM) with its power and generality, has played an important role in the advancement of structural analysis and specifically, in the analysis of reinforced and prestressed concrete structures.

Since the first application of the Finite Element Method to the analysis of reinforced concrete structures, made by Ngo and Scordelis |1| in 1967, numerous studies have been developed covering all the aspects of structural behaviour of concrete structures. These aspects can be classified into three major groups:

- Modeling of material properties (constitutive equations, multiaxial stress states, time dependent behaviour, etc.)
- Studies at a micro-structure level (bond slip, shear transfer, tension stiffening, local effects, etc.)
- Studies at a macro-structure level, which try to model the overall structural behaviour rather than local effects.

There is an extensive literature about the application of finite elements to the analysis of concrete structures. Comprehensive reviews have been made by Scordelis |2| and |3|, Schnobrich |4|, Bazant Schnobrich and Scordelis |5|, ASCE Committee on Finite Element Analysis of Reinforced Concrete Structures |6|, Kang |10|, Chan |14| and other researchers.

In the specific field of reinforced and prestressed concrete frames most of the studies have dealt with planar frames. Selna |7| analyzed this kind of structure, including creep and

shrinkage, Aas-Jackobsen |8| studied slender reinforced concrete frames including creep and geometric nonlinearity, Aldstedt |9| included the effects of bond slip, creep and geometric nonlinearity, and Kang |10| studied reinforced and prestressed concrete planar frames including material and geometric nonlinearities as well as time dependent effects of load and temperature histories including creep, shrinkage and aging of concrete and relaxation of prestressing steel. Hellesland |11| used the model developed by Kang to analyze bridge columns under imposed deformations and Ketchum |12| studied also with this model the behaviour of prestressed concrete bridge structures for time dependent effects.

In the case of three dimensional frames Buckle and Jackson |13| developed a filamented beam element with a rectangular cross section for the analysis of beam slab systems, and Chan |14| developed a similar element with a trilinear torque-twist relationship to model concentric and eccentric edge beams in shell structures, taking into account geometric and material nonlinearities and time dependent behaviour.

1.2 OBJECTIVE AND SCOPE OF THE PRESENT STUDY

The objective of the present study is to develop a numerical procedure for the nonlinear geometric, material and time dependent analysis of reinforced and prestressed concrete three dimensional frames with member of arbitrary cross section, taking into account the time dependent effects of load history, temperature history, creep, shrinkage and aging of concrete and relaxation

of prestressing steel. An accurate prediction of the response of these structures throughout their service load history as well as through their elastic, inelastic and ultimate load ranges is the desired goal.

The study has been based on previous work by Kang |10| and Chan |14|, extending it to the case of three dimensional reinforced and prestressed concrete frames with member of arbitrary cross section. For this purpose a computer program in FORTRAN IV language has been developed trying to include the advantages of the existing programs PCFRAME |10| and NASHL |14|.

A filamented reinforced concrete beam element is used. The element has six degrees of freedom (DOF) at each end and one internal DOF at mid length that is eliminated by static condensation. The element can have an arbitrary cross section defined by a special shape matrix. A trilinear torque-twist relationship is used to model the torsional behaviour of the element.

Postensioned bonded structures can be analyzed taking into account prestressing losses due to friction, anchorage slip and time dependent effects. The prestressing effect is introduced by means of an equivalent load vector and the participation of the prestressing steel to the element stiffness is added directly.

Each concrete and steel filament is considered to be subjected to a uniaxial stress-state. Parabolic-linear, bilinear and multilinear approximations of the stress-strain

curves are utilized for concrete, reinforcing steel and prestressing steel respectively. A simple model for inelastic load reversal is incorporated. Perfect bond between concrete and steel is assumed. Tension stiffening and the effect of confinement in concrete are not taken into account in the present study. A tangent stiffness formulation, coupled with a time integration solution is used. In order to solve the nonlinear equations either load control or displacement control can be used to allow the complete load-displacement curve to be traced.

Several examples are presented to verify and compare the results of the computer program with other analytical or experimental results.

2. MODELLING OF MATERIAL PROPERTIES

2.1 General Remarks

The behaviour of concrete and steel, the components of reinforced and prestressed concrete structures is very complex due to several reasons, such as:

- Heterogeneity of concrete material.
- Nonlinearity in the stress-strain relationship for concrete and steel, and difference between this curve in tension and compression in concrete.
- Time and environmental dependent properties of concrete.
- Unloading and reloading characteristics of concrete and steel.
- Imperfect bond between concrete and steel.
- Discrete character of cracking. (tension stiffening effect).
- Friction between internal faces of cracks, etc.

Reinforcing and prestressing steel are considered homogeneous materials and their properties are generally well defined. In this study concrete is considered homogeneous in a macroscopic sense by defining its average properties by statistical grounds. Thus, we can study the composite action of different homogeneous materials, concrete and steel.

It is assumed that perfect bond exists between concrete and steel (reinforcing and prestressing); thus the displacement field within a reinforced or prestressed concrete element can be considered continuous.

The material properties of concrete and steel depend on the stress state of the material due to the effect of the nonlinear stress-strain relationships, cracking of concrete and yielding of steel. In order to incorporate the varied material properties within a frame in evaluating element properties, the element is divided into a discrete number of concrete and reinforcing steel filaments, as will be shown in chapter no.3. Each of these filaments is assumed to be in a state of uniaxial stress and the deformation due to shearing strain is neglected.

2.2 Properties of Concrete

2.2.1 Deformation of Concrete

One of the most important assumptions in studying the deformation of concrete is that the strain of concrete may be considered as being composed of strains caused by different phenomena. For the present study total uniaxial concrete strain $\varepsilon(t)$ at any time is assumed to be composed of the following contributions:

$$\varepsilon(t) = \varepsilon^{m}(t) + \varepsilon^{nm}(t) \qquad (2.1)$$

$$\varepsilon^{nm}(t) = \varepsilon^{c}(t) + \varepsilon^{s}(t) + \varepsilon^{a}(t) + \varepsilon^{t}(t) \qquad (2.2)$$

Where $\varepsilon^{m}(t)$ is the mechanical strain or instantaneous strain caused by a short-time loading and is the independent variable in the stress-strain relationship:

$$\sigma(t) = f(\varepsilon^{m}(t)) \tag{2.3}$$

Where $\sigma(t)$ is the uniaxial concrete stress at time t.

Non-mechanical strain $\varepsilon^{nm}(t)$ consists of creep strain $\varepsilon^{c}(t)$, shrinkage strain $\varepsilon^{s}(t)$, aging strain $\varepsilon^{a}(t)$ and thermal strain $\varepsilon^{t}(t)$.

In this study, for the time dependent analysis, the time domain is divided into a discrete number of time intervals each of which may not be of the same length of time. The junctions of this intervals are called time steps. A step forward integration is performed by adding the results obtained for each time step successively, starting from the first time step to arrive to the final solution. The calculation of strains and stresses at a typical time step, t_n, is performed as follows:

1. Total strain at time step t_n is obtained by adding the increment of total strain, obtained from the incremental structural analysis, $\Delta\varepsilon_n$ occuring during the time interval t_{n-1} to t_n, to the total strain ε_{n-1} at time t_{n-1}

$$\varepsilon_n = \varepsilon_{n-1} + \Delta\varepsilon_n \tag{2.4}$$

2. The increment of non-mechanical strain $\Delta\varepsilon_n^{nm}$ occuring between time steps t_{n-1} to t_n is obtained by adding contributions due to creep, shrinkage, aging and temperature:

$$\Delta\varepsilon^{nm} = \Delta\varepsilon^{c} + \Delta\varepsilon^{s} + \Delta\varepsilon^{a} + \Delta\varepsilon^{t} \qquad (2.5)$$

3. Non-mechanical strain at time step t_n is then obtained by adding the increment $\Delta\varepsilon_n^{nm}$ to the previous total:

$$\varepsilon_n^{nm} = \varepsilon_{n-1}^{nm} + \Delta\varepsilon_n^{nm} \qquad (2.6)$$

4. Mechanical strain ε_n^m at time t_n is obtained by substracting non-mechanical strain ε_n^{nm} from total strain ε_n:

$$\varepsilon_n^m = \varepsilon_n - \varepsilon_n^{nm} \qquad (2.7)$$

5. Stress at time t_n is then obtained from the stress-strain relationship valid at time step n:

$$\sigma_n = f_n(\varepsilon_n^m)$$

2.2.2 Stress-Strain Relationship

The mathematical formula used in this study to represent the stress-strain relationship is the one suggested by Hognestad and used by Kang [10] in his study.

The effects of dynamic cyclic loading, such as seismic load or wind load, are not considered in this study, but loading and reloading due to live load history or temperature history are accounted for by a simple load reversal model of the stress-strain curve. The load reversal model utilized in

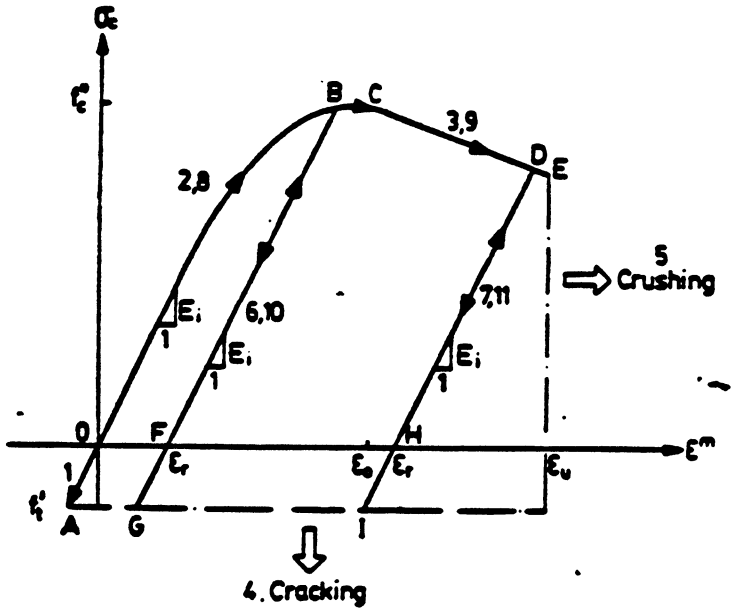

Fig. 2.1. Stress-Strain Curve of Concrete Assumed in the Present Study. (Numbers Represent the Material State of Concrete).

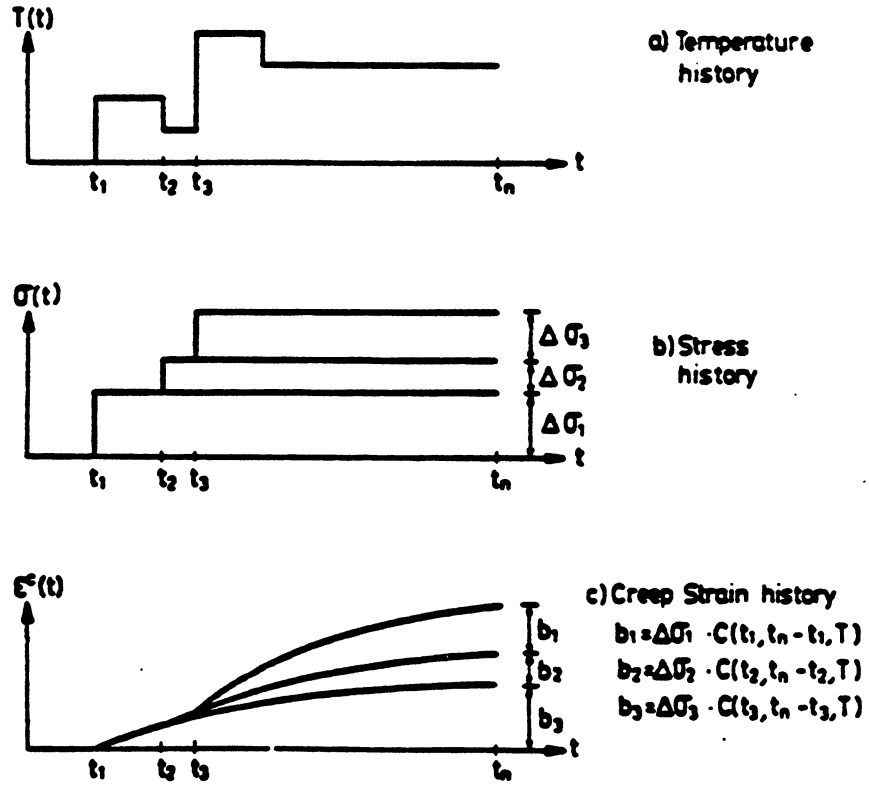

Fig. 2.2. Superposition of Creep Strain.

this study is shown in figure no. 2.1.

The following assumptions are made for this model:

1. The slope in the load reversal path in the stress-strain curve is the same as the initial tangent modulus E_i.

2. Tensile failure or cracking of concrete occurs when tensile stress exceeds its maximum tensile strength f'_t.

3. Compressive failure or crushing of concrete occurs when the compressive mechanical strain exceeds its maximum compressive strain ε_u.

4. Once the concrete has cracked it can not take any tensile stress again. But it can take compressive stress upon closing of the crack and reloading. Thus the crack is assumed to close in compression and reopen in tension without any resistance.

The parameters necessary to define this concrete stress-strain curve are the initial tangent modulus E_i, the maximum compressive strength, maximum tensile strength and ultimate strain. ACI Committee 209 |15| provides the following empirical expressions to obtain the concrete properties at time t:

$$(f'_c) = \frac{t}{a + bt} (f'_c)_{28} \qquad (2.8)$$

$$f''_c = r_c f'_c \tag{2.9}$$

$$E_i = 33w^{1.5}\sqrt{f'_c} \tag{2.10}$$

$$f'_t = r_t \sqrt{wf'_c} \tag{2.11}$$

Where: a,b, r_c and r_t are constants whose values can be obtained from ACI Committee 209 |15|.
w is unit weight of concrete p.c.f.

In the computer program developed, the concrete material state is classified into 11 different states (figure 2.1), described as following:

1. In primary tension (path OA or AO)
2. In compression not yielded (path OC)
3. In compression, yielded (path CE)
4. Cracked (beyond points A, G, I)
5. Crushed (beyond point E)
6. In load reversal path from state 2 (path BG or GB)
7. In load reversal path from state 3 (path DI or ID)
8. In compression, not yielded and once cracked (path OC or BC)
9. In compression, yielded and once cracked (path CE or DE)
10. In load reversal path from state 2 and once cracked (path BF or FB)
11. In load reversal path from state 3 and once cracked (path DH or HD).

In the above description of the eleven material states, concrete is defined as yielded when its compressive mechanical strain exceeds ε_0, the strain corresponding to the maximum compressive stress, f''_c.

The complete stress-strain relationship of concrete can be summarised in the following equations:

State 1. $$\sigma = E_i \varepsilon^m$$

$$E_t = E_i \tag{2.12}$$

States 2 and 8. $$\sigma = f''_c \frac{\varepsilon^m}{\varepsilon_0}\left(2-\frac{\varepsilon^m}{\varepsilon_0}\right) \tag{2.13}$$

$$E_t = E_i\left(1-\frac{\varepsilon^m}{\varepsilon_0}\right) \tag{2.14}$$

States 3 and 9. $$\sigma = -0.15f''_c \frac{\varepsilon^m-\varepsilon_0}{\varepsilon_u-\varepsilon_0} + f''_c \tag{2.15}$$

$$E_t = 0 \tag{2.16}$$

States 6,7,10 and 11 $$\sigma = E_i(\varepsilon^m-\varepsilon_r) \tag{2.17}$$

$$E_t = E_i \tag{2.18}$$

where ε_r is the residual strain due to unloading, as shown by point F and H of figure no. 2.1.

2.2.3 Long Time Deformation: Creep, Shrinkage and Aging

Creep is defined as the increase in strain under sustained stress, whether the stress is produced by external loading or

any other cause such as temperature changes. There are many factors influencing creep of concrete, such as age of loading, intensity of the stress, aggregate content, compressive strength, size of member, ambient humidity, temperature, etc.

Because of the number of factors influencing creep, it is difficult to predict. Based on hundreds of experiments, ACI Committee 209 |15| suggests a relatively simple equation for the prediction of creep that tries to take into account the above mentioned factors. The ACI equation, as well as any other experimental results, can be used to obtain, by a least square fit, the parameters of the analytical model of creep used in the present study.

Shrinkage of concrete is defined as a non-stress and non thermal produced time dependent volume change. Shrinkage of concrete is a function of the time t after casting of concrete, age of concrete when the completion of curing, ambient humidity, minimum thickness of element, slump, cement content, percent of fines and air content. ACI Committee 209 |15| provides an equation to obtain approximately the shrinkage strain.

Aging strain can be defined as the decrease in the mechanical strain with time due to the aging of concrete. We can consider the aging strain as a correction factor for the calculation of the current stress as a function of the current mechanical strain at any time, rather than an actual physical straining.

The increment of aging strain $\Delta\varepsilon_n^a$, occuring between time step t_{n-1} and t, assuming that the stress remains constant at σ_{n-1}, can be calculated as follows:

$$\Delta\varepsilon_n^a = g_{n-1}(\sigma_{n-1}) - g_n(\sigma_n) \tag{2.19}$$

where the subscripts n and n-1 represent time steps and the function g is a time dependent function for computing mechanical strain in terms of stress. This function can be expressed as:

$$g(\sigma) = \varepsilon^m = \frac{\sigma}{E_i} \qquad \text{In tension.}$$

$$g(\sigma) = \varepsilon^m = \varepsilon_0\left(1 - \sqrt{1-\sigma/f_c''}\right) \qquad \text{In compression.} \tag{2.20}$$

2.2.4 Deformation due to temperature effects

Concrete structures are subjected to temperature changes during their service lives. Stresses induced by this temperature changes in statically indeterminate concrete structures are often substantial and damaging to the structures.

The uniaxial thermal strain can be expressed as follows:

$$\varepsilon^t = \alpha(T - T_0) = \alpha\,\Delta T \tag{2.21}$$

Where α is the coefficient of thermal expansion, which is assumed temperature independent; T_0 is the temperature reference and T is the current temperature.

Creep strain of concrete is influenced by temperature and this effect is taken into account in this study as will be discussed next.

2.2.5 Age and temperature integral formulation of creep

Creep may be formulated in integral form as follows:

$$\varepsilon(t) = \int_0^t \bar{C}(\tau, t-\tau, T) \frac{\partial \sigma(\tau)}{\partial \tau} d\tau \qquad (2.22)$$

Where $\varepsilon(t)$ is the strain at time t, $\bar{C}(\tau, t-\tau, T)$ is the specific compliance curve or, in other words, the total stress produced strain at time t due to a unit sustained stress applied at time τ at a certain temperature T.

Equation 2.22 is a convolution integral where the principle of superposition is assumed (figure 2.2).

Specific compliance can be divided into two parts: an instantaneous part and a creep part.

$$\bar{C}(\tau, t-\tau, T) = \frac{1}{E(\tau)} + C(\tau, t-\tau, T) \qquad (2.23)$$

Where $E(\tau)$ is the modulus of elasticity at age τ and $C(\tau, t-\tau, T)$ is the specific creep at time $t-\tau$ after loading.

The creep strain $\varepsilon^c(t)$ can then be calculated as:

$$\varepsilon^c(t) = \int_0^t C(\tau, t-\tau, T) \frac{\partial \sigma(\tau)}{\sigma \tau} d\tau \qquad (2.24)$$

Using this integral formulation (eq.2.22) it can be seen that the strain at time t involves the integration of all the previous stress histories, so the computational effort and computer storage requirements in the solution process can be excessive. For this reason a proper choice of the analytical functions for the specific creep, while representing experimental or empirical creep curves accurately, must be used to overcome the necessity of storing all the stress increments of previous time steps.

A numerical formulation, developed by Kabir |18| for the evaluation of creep strain, taking into account both the effects of temperature and age of concrete is used in this study.

The inherent assumptions in this procedure are the linear superposition, additivity of the different strain components and thermorheologically simple concrete material obeying a time shift principle for a temperature variation.

The creep compliance function $c(\tau,t-\tau,T)$ takes the form of a Dirichlet series:

$$c(\tau,t-\tau,T) = \sum_{i=1}^{m} a_i(\tau)\left[1-e^{-\lambda_i \phi(T)(t-\tau)}\right] \qquad (2.25)$$

where $a_i(\tau)$ are the aging parameters depending of the age at loading τ, λ_i are the retardation times governing the shape of the logarithmically decaying creep curve, $\phi(T)$ is the temperature shift function depending on the temperature. Parameters m, $a_i(\tau)$, λ_i, $\phi(T)$ are determined by a least

squares fit to experimental or empirical curves.

A step by step method together with the Dirichlet series is used to solve for the creep strain. An efficient numerical formulation can be developed using the following definitions for incremental quantities of time steps, stresses and strains:

$$\Delta t_n = t_n - t_{n-1} \tag{2.26}$$

$$\Delta \sigma_n = \sigma_n - \sigma_{n-1} = \sigma(t_n) - \sigma(t_{n-1}) \tag{2.27}$$

$$\Delta \varepsilon^c_n = \varepsilon^c_n - \varepsilon^c_{n-1} = \varepsilon^c(t_n) - \varepsilon^c(t_{n-1}) \tag{2.28}$$

Combining equations 2.24 to 2.28, and after some extensive algebraic manipulations, the recursive relations necessary for calculating the increment of creep strain $\Delta \varepsilon^c_n$ at a time step t_n are as follows:

$$\Delta \varepsilon^c_n = \sum_{i=1}^{m} A_{i,n} \left(1 - e^{-\lambda_i \phi(T_{n-1}) \Delta t_n}\right) \tag{2.29}$$

$$A_{i,n} = A_{i,n-1} \left(e^{-\lambda_i \phi(T_{n-2}) \Delta t_{n-1}}\right) + \Delta \sigma_{n-1} a_i(t_{n-1}) \tag{2.30}$$

$$A_{i,1} = \Delta \sigma_1 . a_i(t_1) \tag{2.31}$$

A very important advantage of the above formulation is that the computation for each new creep strain increment requires only the stress history of the last time step and

not the total stress history.

The assumption of constant stress within increments is necessary in order to arrive to eq.2.29. This means that changes in stress can only occur at the beginning of a time step. For a proper choice of time intervals this assumption is justifiable.

The assumption of proportionality between creep strain and stress intensity is valid only up to a stress level of approximately 0.4 f'_c for concrete. Creep strains generally increase at an increasing rate at higher stress levels. To account for this nonlinear creep effect an effective stress is obtained by multiplying the actual stress by an appropiate magnifying factor such that the creep effect calculated by the effective stress on the basis of linear creep law would be the same as that produced by the actual stress.

The equations used for the calculation of the effective stress σ_e in this study are:

$$\sigma_e = \sigma \qquad \text{if} \quad \sigma \leq r_1 . f''_c \tag{2.32}$$

$$\sigma_e = c_1\sigma + c_2 f''_c \qquad \text{if} \quad r_1 f''_c < \sigma \leq f''_c \tag{2.33}$$

$$\sigma_e = r_2 . \sigma \qquad \text{if} \quad \sigma = f''_c \tag{2.34}$$

Where r_1 is the stress-strength ratio up to which creep strain is proportional to stress intensity and r_2 is the

magnifying factor when the stress equals the maximum compressive stress f''_c.

With given values of r_1 and r_2, c_1 and c_2 can be calculated from the two equations given below

$$c_1 = \frac{r_2 - r_1}{1 - r_1} \quad ; \quad c_2 = r_1(1 - c_1)$$

Figure 2.3 shows the relationship between σ_e and σ according with equations 2.32, 2.33 and 2.34.

2.3 Reinforcing steel

The properties of reinforcing steel, unlike concrete, generally are not dependent on environmental conditions or time. In this study a bilinear model which is symmetrical about origin, as shown in figure 2.4, is used. The only non-mechanical strain considered is thermal strain which is computed by equation 2.21 as in concrete. The coefficient of thermal expansion α of steel is only slightly different from that of concrete. The mechanical strain ε^m is then computed by substracting thermal strain ε^t from total strain ε.

The slope of the load reversal path is assumed to be the same as the initial modulus, and the load reversal path is assumed to stay within the envelope shown with dotted lines in figure 2.4.

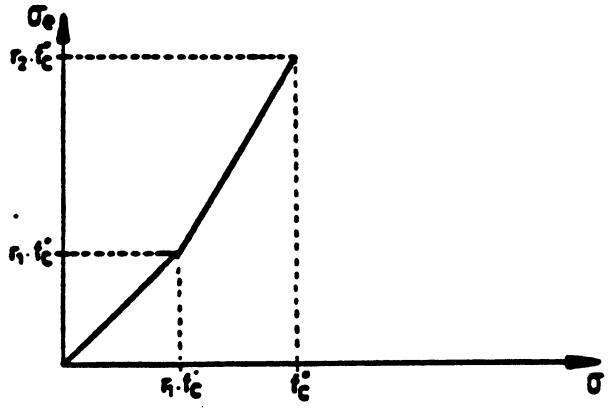

Fig.2.3 Effective stress σ_e as a function of actual stress σ for non linear creep.

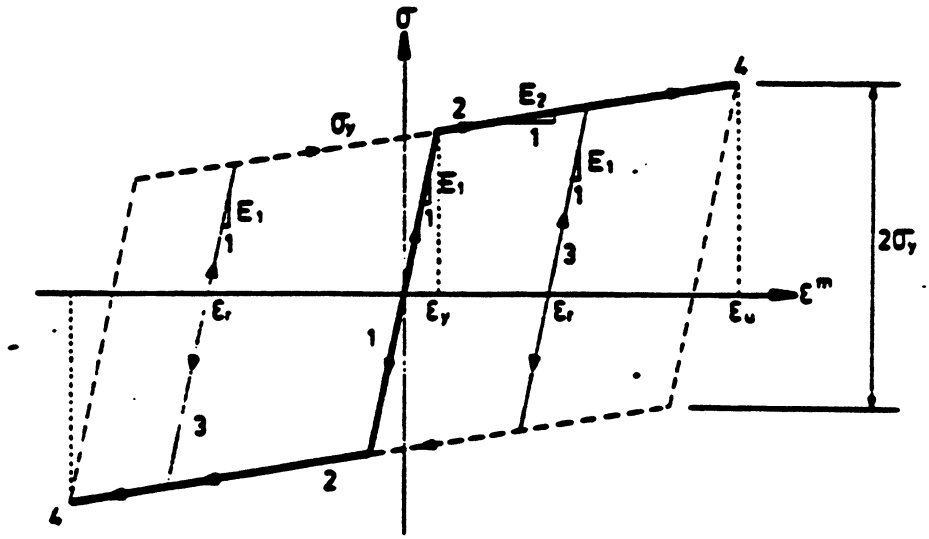

Fig.2.4. Uniaxial Stress-Strain Curve of Reinforcing steel Assumed in the Present Study.

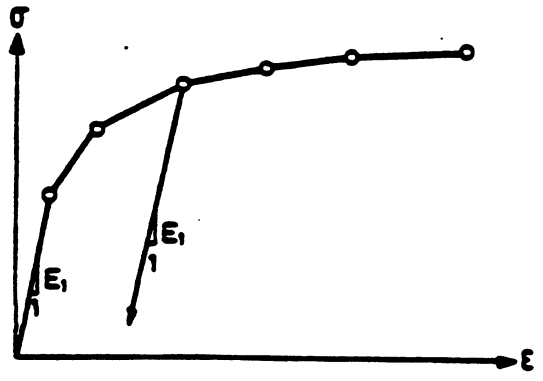

Fig.2.5. Uniaxial Stress-Strain Curve of Prestressing Steel Assumed in the Present Study.

Four different material states can be identified in the stress-strain curve. Their equations can be written as follows:

1. In primary tension or compression

$$\sigma = E_1.\varepsilon^m \quad ; \quad E_t = E_1 \tag{2.35}$$

where E_1 is the initial modulus up to yelding.

2. Yielded

$$\sigma = E_2.\varepsilon^m \pm (\sigma_y - E_2.\varepsilon_y) \tag{2.36}$$

where E_2 is the second modulus after yelding

σ_y and ε_y are yield stress and yield strain respectively.

3. In load reversal path

$$\sigma = E_1(\varepsilon^m - \varepsilon_r) \tag{2.37}$$

where ε_r is the residual strain due to load reversal (figure 2.4).

4. Failed. Failure is assumed to occur when the mechanical strain ε^m exceeds the ultimate strain ε_u.

2.4 Prestressing Steel

A multilinear stress-strain curve as shown in figure 2.5 is adopted for prestressing steel for this study.

The slope of the unloading and reloading path is assumed to be the same as the initial modulus. Since prestressing steel is never subjected to compressive stresses the compressive stress-strain curve is not considered. Also temperature strain is not considered for prestressing steel.

An important property of the prestressing steel is the relaxation of stress with time. Relaxation can be defined as the decrease in stress with time under a constant strain. The incorporation of relaxation in the analysis of prestressed concrete frames is treated in chapter no. 6.

3. MODELLING OF STRUCTURAL GEOMETRY

3.1 Geometric Definition of the Beam Element

Three dimensional reinforced and prestressed concrete frames such as the one shown in figure 3.1 are analysed in this study. The idealized structure consists of one-dimensional beam elements interconnected by joints. Each element is assumed to be prismatic with an arbitrary cross sectional shape and length L. The geometry of the beam element is shown in figure 3.2 where the global axes X,Y,Z and an element local system x,y,z with unit vectors $\vec{\xi},\vec{\eta},\vec{\rho}$ are also shown.

In order to define completely the position of the element in space, in addition to the nodal coordinates, the orientation of the cross sectional local axes must be known. This is achieved by using an auxiliary node K (figure 3.2) that together with the element joints I and J define a plane π that will be the x-z plane. Once this plane is known, the unit vector of the y axis is obtained by imposing the condition of orthogonality to the plane x-z, and the unit vector $\vec{\rho}$ of the z axis will be obtained by the vector product of the unit vectors $\vec{\xi}$ and $\vec{\eta}$ as follows:

$$\vec{\xi} = \frac{\vec{IJ}}{|\vec{IJ}|} \qquad \vec{\eta} = \frac{\vec{IJ}\times\vec{IK}}{|\vec{IJ}\times\vec{IK}|} \qquad \begin{matrix}\vec{\rho} = \vec{\xi}\times\vec{\eta} \\ \vec{\rho} = \vec{\eta}\times\vec{\xi}\end{matrix} \qquad (3.1)$$

The location of node K must not lie along the x axis and the axes y and z are the reference axes used for defining the cross section as explained next.

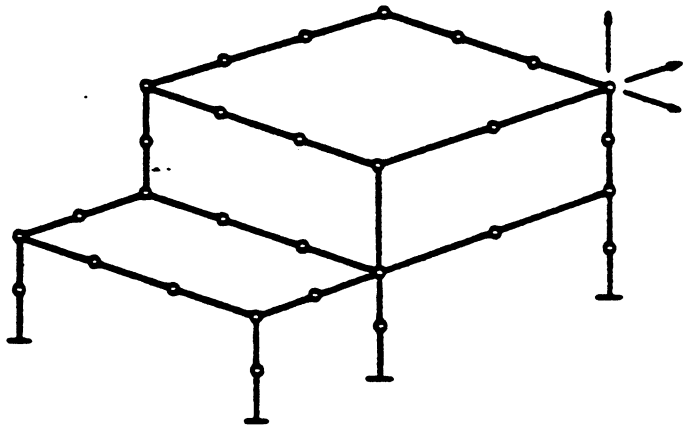

Fig. 3.1. Three Dimensional Rigid Frame.

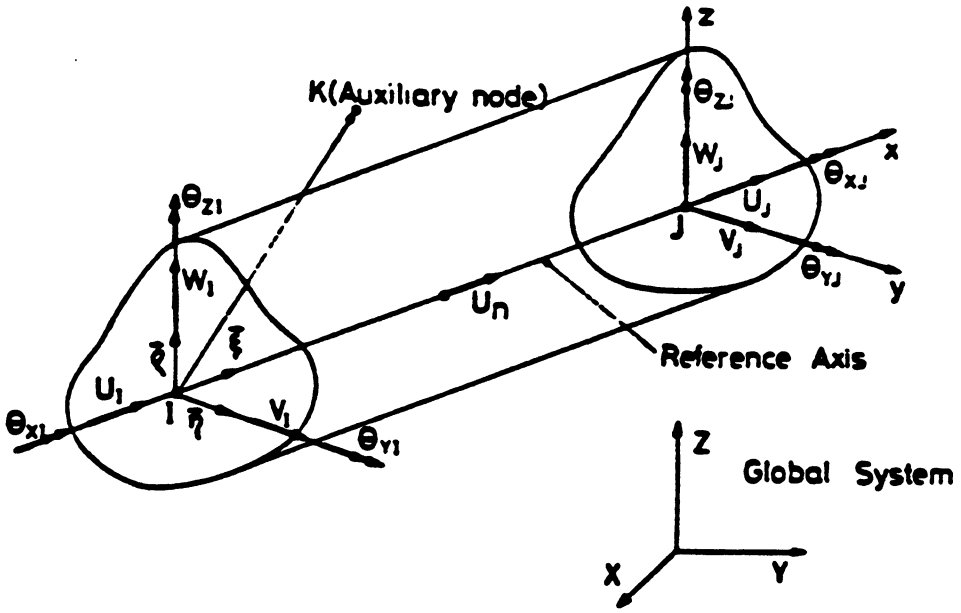

Fig. 3.2. Three Dimensional Beam-Element . Geometry and Displacement Components.

3.2 Definition of the Element Cross Section

The cross section of each element can be solid or hollow of arbitrary shape. For the definition of the cross section it is divided into a discrete number of concrete areas and the actual section is assumed to be equivalent to an ideal section having an integer number of elemental areas, as seen in figure 3.3. To find the position of each elemental concrete area, the y and z local axes must be placed. The simplest way of doing this is to consider the cross section to be inscribed in an ideal rectangle of dimensions B and H, (Figure 3.3). This rectangle is divided by a grid of m rows and n columns so that each concrete area has dimensions of b=B/n and h=H/m. The reference axes of the cross section are considered parallel to the sides of the rectangle and their distances to them are given by the values Z_{max},Z_{min},Y_{max},Y_{min} (figure 3.4). The position of each elemental concrete area (filament) is given by the coordinates of its geometric center.

If the filaments are all equal sized, the expression of the Y_i and Z_j coordinates of the concrete filament lying in the j-th row and i-th column are:

$$Z_j = -\frac{H}{m}(j-0.5)+Z_{max} \quad ; \quad Y_i = -\frac{B}{n}(i-0.5)+Y_{max} \qquad (3.2)$$

Warner |16| used a matrix A of n rows and m columns associated to the circunscribed rectangle to define the cross section. Elements A_{ij} of A matrix assume either values

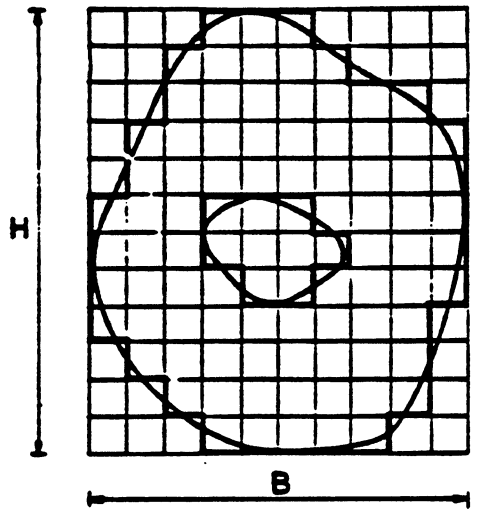

Fig. 3.3. Actual and Idealized Cross Section.

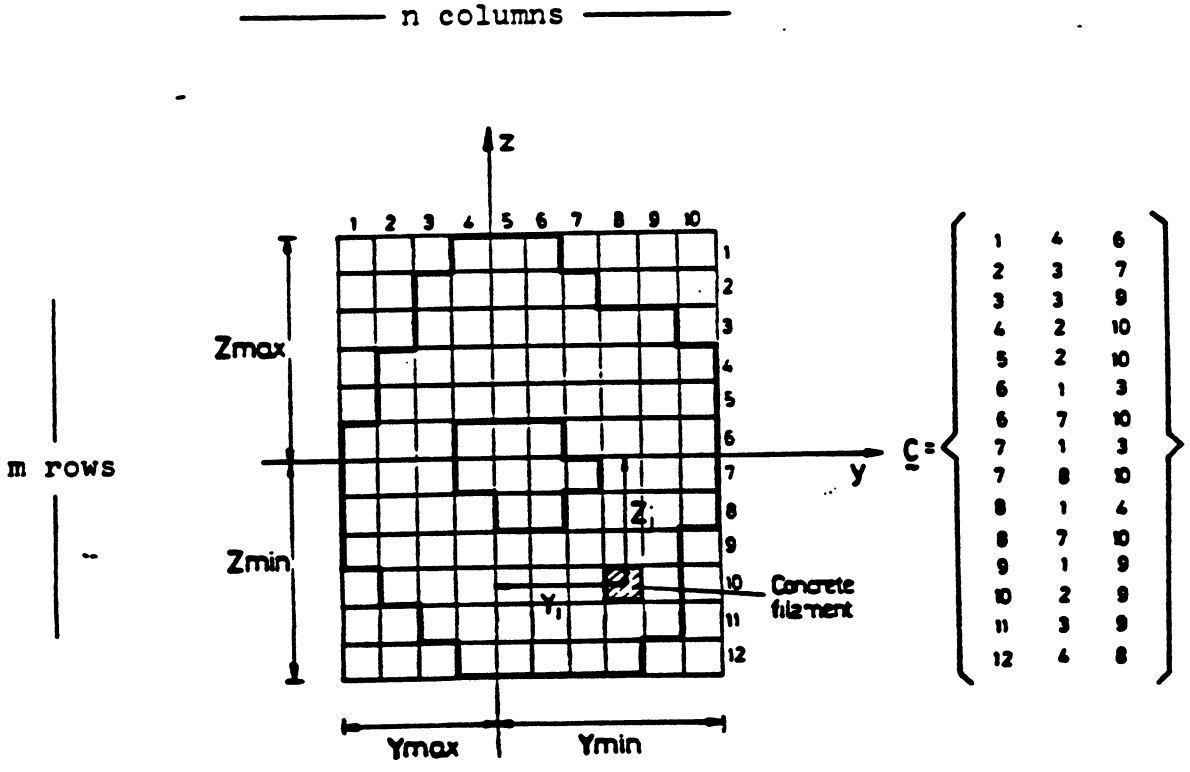

Fig. 3.4. Discretization of the Idealized Cross Section.

zero or unity depending on whether there is or not material in the position (Y_i, Z_j). Such an array is valid to define any arbitrary cross section, but presents some inconveniences as shown in the following.

When obtaining element stiffness, internal resisting load vector, initial strain load vector, internal forces, etc, numerical integration over the cross section area of certain functions must be performed. A number of expressions such as:

$$I = \iint_S \phi(Y,Z)\ f(Y,Z)dS \tag{3.3}$$

must be evaluated, where $\phi(Y,Z)$ can represent the tangent modulus $E(Y,Z)$, the stress at any point $\sigma(Y,Z)$, or the non-mechanical strain $\varepsilon^{nm}(Y,Z)$, for example; $f(Y,Z)$ is usually a polynomic function of y and/or z. (i.e. $f(Y,Z) = Y.Z$)

By using the A matrix, the numerical approach for evaluating this integral is:

$$I = \sum_{i=1}^{n} \sum_{j=1}^{m} \phi(Y_i,Z_j)\ f(Y_i,Z_j)\ \Delta Y_i\ \Delta Z_j\ a_{ij} \tag{3.4}$$

The summation is extended to all the filaments, and when $a_{ij} = 0$ the contribution of the non existing concrete areas is zero.

This procedure requires that the A matrix be explicitly defined, on the other hand, it is excessively time consuming and requires more storage than that strictly

necessary because the operations are performed even for the phisically non existing rectangles where $a_{ij} = 0$.

To avoid this problem, a more efficient alternative way of defining geometrically the cross section shape is proposed. For this purpose a $\underset{\sim}{C}$ matrix whose terms C_{ij} are associated only to the existing concrete rectangles is defined as follows:

- The first element in every row indicates the layer of the rectangular grid to which the considered filament belongs.
- The second element $C_{i,2}$ in each row i indicates the column in the grid where the cross section starts existing (or the first non empty rectangle).
- The elements in the third column $C_{i,3}$ indicate the column in the gridafter which the material no longer existsor there is discontinuity in the existence of material. In other words, $C_{i,3}$ indicates the last full rectangle before a series of new empty elements starts.

The elements in the fourth column indicate the material code for the current layer, which permits composite sections subjected to uniaxial bending to be analyzed.

It should be noted that the number of rows of $\underset{\sim}{C}$ and the number of physical layers of the rectangular grid can be different as in the case of the section shown in figure 3.4. This occurs when, due to an existing whole or due to the shape of the cross section, two or more rows of C matrix are necessary to define one physical layer of the grid.

Once the C matrix is known, the summation over the cross

section can be expressed as:

$$I = \iint_s F(y,z)ds = \sum_{i=1}^{n_c} \sum_{j=C_{i2}}^{C_{i3}} F(y_i,z_k)\Delta y_i.\Delta z_k \qquad (3.5)$$

where n_c = number of rows of $\underset{\sim}{C}$ matrix

$k = C_{i,1}$ = current layer of the filament

The summation is extended only over the actual existing filaments. This permits the storage of only the strictly necessary variables and avoids unnecessary execution time, which can be important in a nonlinear iterative procedure.

Summarizing: In order to geometrically define a reinforced concrete cross section by means of the proposed procedure it is necessary to know the following data:

- Position of the reference axes y,z in the cross section, by the values, $Z_{max}, Z_{min}, Y_{max}, Y_{min}$.
- Number of rows and columns of the grid into which the ideal circumscribed rectangle is divided.
- Matrix C defining the cross sectional shape.

3.3 Geometric definition of reinforcement and prestressing

For each element the reinforcing steel is considered constant along its length and parallel to the longitudinal local x - axis. The position of the reinforcing steel bars is defined by their eccentricities e_{sy} and e_{sz} in the element local coordinates and their area A_{si}. (Figure 3.5).

The following definitions are used for the geometric

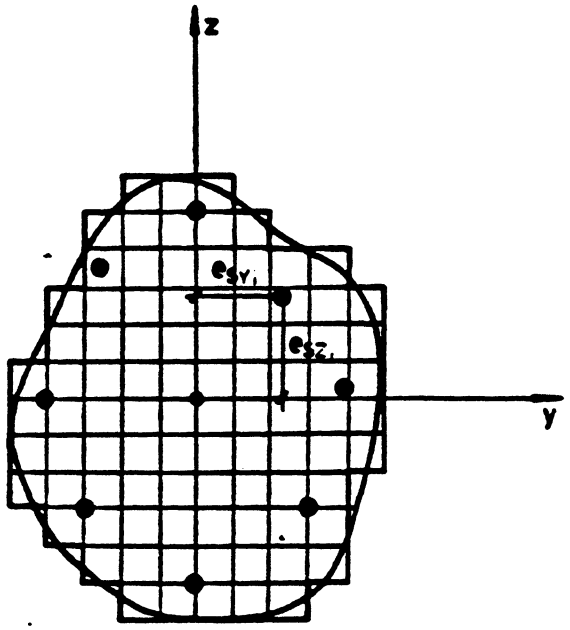

Fig. 3.5 Steel Filaments in the cross section.

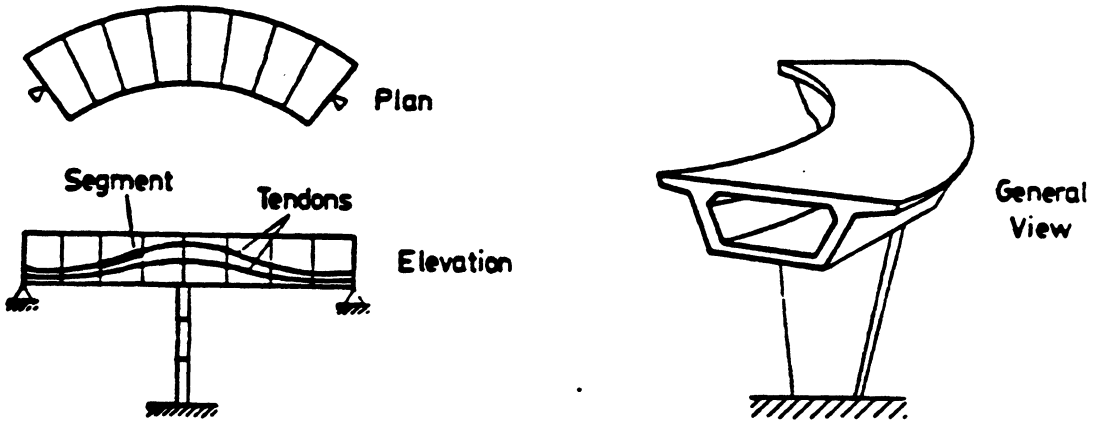

Fig.3.6. Actual and Idealized 3-D prestressed Concrete Frame.

definition of the prestressing in a 3-D prestressed concrete frame (see figure 3.6):

There is a discrete number of prestressing steel tendons in the frame, each of which has a given profile and constant sectional area along its length. A prestressing steel tendon consists of a discrete number of prestressing steel segments each of which is straight and spans a frame element. The location of the two end points of a prestressing steel segment in a frame element are defined by the eccentricities e_{yi} and e_{zi} at each end as shown in figure 3.7, where e_{yi} and e_{zi} are measured in local y and z coordinates of the element.

3.4 Boundary Conditions

Boundary conditions at the supported nodes are specified by means of support springs. Three translational springs and three rotational springs are provided for each support whose directions in space are defined by using three additional nodes as shown in figure 3.8. The four nodes S, S_1, S_2 and S_3 define a local system of coordinates (x',y',z') for the spring system. Nodes J and K are other nodes of the structure.

Spring stiffnesses (k_x',k_y',k_z',k_{rx}',k_{ry}',k_{rz}') associated with these six springs are specified to simulate the boundary conditions at the support. For a zero displacement in the specific direction a large value of the spring stiffness corresponding to that direction is specified, and for a free displacement zero value is specified for the spring stiffness.

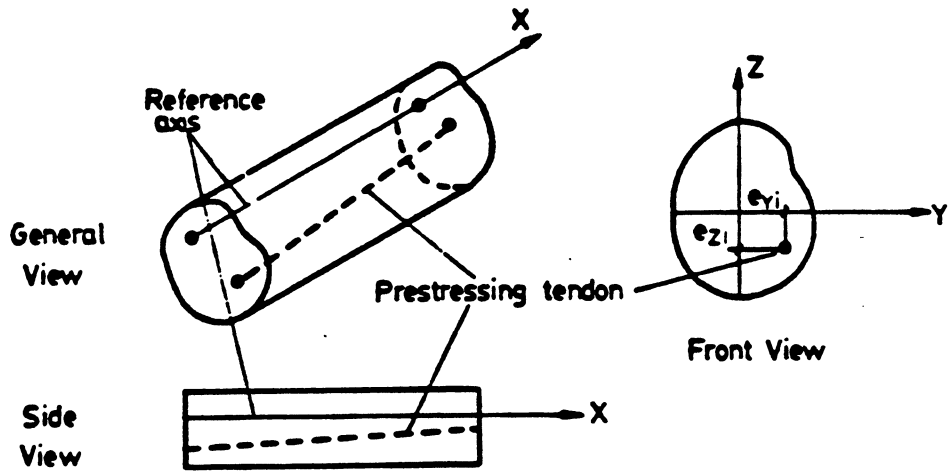

Fig. 3.7. Prestressed beam element.

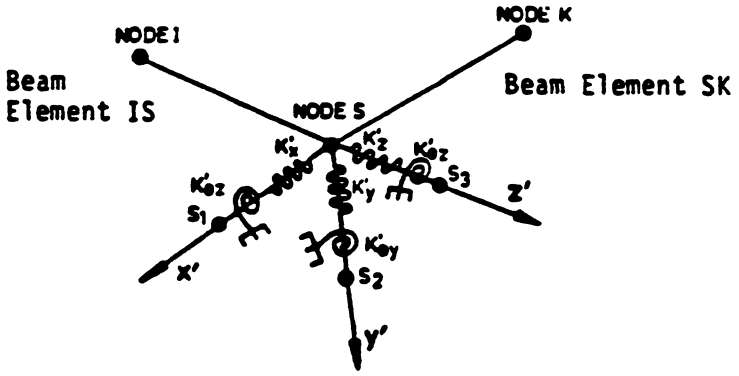

Fig. 3.8. Local Spring System for Supported Joints

Support spring stiffness matrix $\underset{\sim}{k}$ may be written in (x', y',z') coordinates:

$$\underset{\sim}{k}_s = \begin{bmatrix} k_x' & & & & & \\ & k_y' & & \text{zeros} & & \\ & & k_z' & & & \\ & & & k_{rx}' & & \\ & & & & k_{ry}' & \\ \text{Symmetric} & & & & & k_{rz}' \end{bmatrix} \tag{3.6}$$

Spring stiffness matrix $\underset{\sim}{k}_s$ in global coordinates may be obtained by:

$$\underset{\sim}{K}_s^G = \underset{\sim}{A}^T \underset{\sim}{k}_s \underset{\sim}{A} \tag{3.7}$$

where:

$$\underset{\sim}{A} = \left[\begin{array}{c|c} a_{ij} & 0 \\ \hline 0 & a_{ij} \end{array}\right] \qquad a_{ij} = \cos(x_i, x_j) \tag{3.8}$$

and a_{ij} = transformation matrix (3 × 3) between local spring system and global coordinates.

4. SOLUTION STRATEGY FOR THE TIME DEPENDENT NONLINEAR THREE DIMENSIONAL FRAME PROBLEM

4.1 Statement of the problem

Suppose we want to analyse a 3-D concrete frame idealized by beam elements interconnected by joints, with given boundary conditions. It is assumed that the loads are applied only at joints. The prestressing, joint load history, temperature history of every part of the structure and the stress-strain curve of materials at any instant of time are given. Also creep and shrinkage characteristics of the concrete are given. Then we want to find out joint displacements, internal forces for each element, strains and stresses at any point of the structure at any instant of time.

The load-displacement relationship for this structure will be nonlinear due to the nonlinearity in the stress-strain relationship, large displacement effects and time dependent effects of load history, temperature history, creep, shrinkage and aging of concrete, etc.

To incorporate these time dependent nonlinearities, the time domain is divided into a discrete number of time intervals and a step forward integration is performed in which increments of displacements and strains are successively added to the previous totals as we march forward in the time domain. At each time step a direct stiffness finite element method based on the displacement formulation is used for the

analysis in the space domain, in which the resulting equilibrium equations will be nonlinear to be valid for the current state of material properties and geometry.

To account for the geometric nonlinearity, an "Updated Lagrangian" formulation |23| for the description of motion is used in this study based on the work by Chan |14|.

For each element, a local rectangular cartesian coordinate system x,y,z is defined. The direction of this local coordinate system varies continuously as the structure deforms. Internal forces and stiffness are calculated in the local coordinate system for each element and then transformed to a fixed global coordinate system X,Y,Z where the equilibrium equations for the entire structure are set up and solved.

4.2 Solution methods for nonlinear equilibrium equations

The solution of the equation of the form

$$\underset{\sim}{k}.\underset{\sim}{r} = \underset{\sim}{R} \qquad (4.1)$$

which is nonlinear, in general, has to resort either to a step by step procedure, an iterative procedure, or a combination of the two. The solution is relatively trivial if the load is single valued in displacement. This is generally not the case for a structural system that exhibits strain softening or a snap through phenomenon where the load is multivalued in displacement. Special treatment has to be given for this cases as will be discussed later.

For concrete structures, the solution is generally path

dependent mainly due to the progressive cracking in tensile regions, so that it is desirable to use an incremental method.

For this study the combined method is used to enhance the accuracy of the solution. An option is provided to use either tangent stiffness or constant stiffness during iterations.

When a structure exhibits strain softening or snap-through, the stiffness at some point in the solution path is non-positive definite (figure 4.1). The conventional methods for solving the nonlinear set of equations are not applicable without modifications.

Various schemes have been proposed in the past to circumvent the difficulties which arise in treating the non-positive definiteness of the stiffness matrix and passing over the limit point when the determinant of the stiffness matrix changes sign. (Points A,B and B' in figure 4.1).

For this study the double step method proposed by Simmons |22| is used, as demonstrated in comparative study made by Chan |14|. The procedure consists in obtaining the solution at any instant in two steps by solving for the displacements $\underset{\sim}{r}^u$ and $\underset{\sim}{r}^e$ of two independent load conditions $\underset{\sim}{R}^u$ and $\underset{\sim}{R}^e$.

$$\underset{\sim}{R}^u = \underset{\sim}{k}.\underset{\sim}{r}^u \qquad (4.2)$$

$$\underset{\sim}{R}^e = \underset{\sim}{k}.\underset{\sim}{r}^e \qquad (4.3)$$

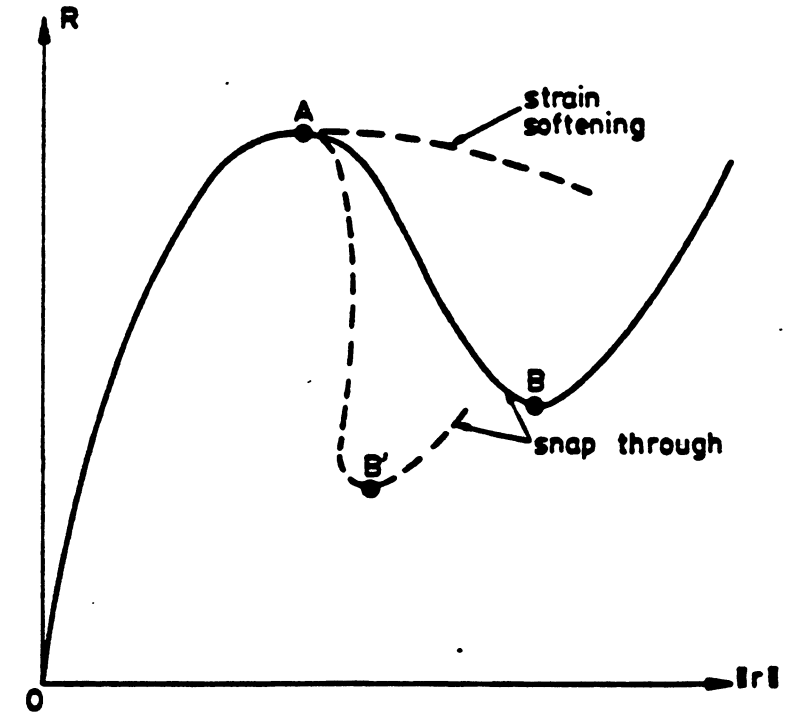

Fig 4.1 Typical load-displacement response for structure with non-positive definite stiffness matrix.

The final solution is then obtained so that a certain constraint

$$C(\underset{\sim}{r}^u, \lambda \underset{\sim}{r}^e) = \underset{\sim}{0} \tag{4.4}$$

between the displacements $\underset{\sim}{r}^u$ and $\underset{\sim}{r}^e$ is satisfied. If the constraint consists of controlling the value of a certain degree of freedom δ_j^*, then the equation 4.3 will be:

$$r_j^u + \lambda r_j^e = \delta_j^* \qquad \lambda = \frac{\delta_j^* - r_j^u}{r_j^e} \tag{4.5}$$

where λ is the scale factor.

Then the total external load vector to apply will be:

$$\underset{\sim}{R} = \underset{\sim}{R}^u + \lambda \underset{\sim}{R}^e \tag{4.6}$$

and the total displacements:

$$\underset{\sim}{r} = \underset{\sim}{r}^u + \lambda \underset{\sim}{r}^e \tag{4.7}$$

Usually $\underset{\sim}{r}^u$ is the displacement vector due to the unbalanced load $\underset{\sim}{R}^u$ and $\underset{\sim}{r}^e$ is the displacement due to some reference external load $\underset{\sim}{R}^e$.

In this method the iterative procedure is performed with variable external load $\lambda \underset{\sim}{R}^e$. If for any reason there is an external load whose value is fixed and can not be scaled, this load should be treated as an unbalanced load. That is the case of the equivalent load vector due to prestressing and the initial strain load vector due to creep, shrinkage and aging of concrete and thermal effects that, in the program presented, are treated as unbalanced loads.

4.3 Nonlinear time dependent analysis procedure

At time step t_{n-1} all joint displacements r, total strains ε, total nonmechanical strains ε^{nm}, and stresses in every part of the structure are known. The increments of non-mechanical strain $\Delta\varepsilon^{nm}$ due to creep and shrinkage of concrete and temperature changes occuring during time steps t_{n-1} and t_n are evaluated by the method described in chapter 2.

Then, the initial strain load vector ΔR_n^{nm} at time step t_n which would produce the non-mechanical strain increments $\Delta\varepsilon^{nm}$ is evaluated as shown in chapter 5 by means of the equation:

$$\Delta R^{nm} = \int_v \underset{\sim}{B}^T . E_T \, \Delta\varepsilon_n^{nm} \, dv \qquad (4.8)$$

where $\underset{\sim}{B}$ is the strain-displacement matrix

E_T is the tangent modulus

Thus, at time step t_n the load increment $\Delta\underset{\sim}{R}_n$ to be applied to the structure is obtained by adding external load increment $\Delta\underset{\sim}{R}_n^e$ and unbalanced load $\Delta\underset{\sim}{R}_{n-1}^u$ left over from time t_{n-1} to the equivalent joint load increment ΔR_n^{nm} due to non-mechanical strain:

$$\Delta\underset{\sim}{R}_n = \Delta\underset{\sim}{R}_n^e + \Delta\underset{\sim}{R}_n^{nm} + \Delta\underset{\sim}{R}_{n-1}^u \qquad (4.9)$$

If desired $\Delta\underset{\sim}{R}_n$ may be subdivided into several smaller load increments for incremetal load analysis and unbalanced load iteration which can be performed by using the following steps:

1. Form the tangent stiffness in local coordinates for each element based on current geometry and material properties. Assemble the structure tangent stiffness in global coordinates using the current displacement transformation matrix for each element.

2. Solve equations for displacement increments Δr and transform to local coordinates. Obtain increment of strain by using the nonlinear strain-displacement relationship or the equivalent procedure explained in chapter 5. Add $\Delta\varepsilon$ to previous totals to obtain current total strains ε in the concrete, reinforcing steel and prestressing steel.

3. Add displacements Δr to previous totals to get current local joint displacements. Update geometry, element local axes and lengths and element transformation matrix.

4. Substract current non-mechanical strains ε^{nm} from current total strains ε to obtain current mechanical strains ε^{n} and compute total stress σ in concrete, reinforcing steel and prestressing steel from the nonlinear stress-strain curves.

5. Compute internal resisting element forces by integrating total current stresses for each element in local coordinates and transform into global coordinates using the updated transformation matrices and assemble the internal resisting joint load R^{i}.

6. Substract the internal resisting load vector R^{i} from the

current total external joint load R^e, to obtain the unbalanced load $R^u = R^e - R^i$.

7. Set $\Delta R = R^u$ and go back to step 1. Steps 1 to 7 are repeated until the unbalanced loads R^u are within allowable tolerances. At this point, the current unbalanced loads R^u are added to the load increment ΔR for the next load step and the iterative procedure 1 to 7 is performed again.

At the end of the final load step for time t_n, proceed to next time step t_{n+1} and repeat until final time is reached or ultimate failure occurs.

4.4 Convergence criteria and termination of the solution

In the present study two convergence criteria are used as proposed by Kang |10|. The first one is a displacement criteria consisting in comparing a certain displacement ratio ρ with a displacement ratio tolerance provided by the analyst. This displacement ratio is also compared with a tolerance for changing stiffness t_c. If $\rho > t_c$, a new stiffness is formed for the next iteration. An appropriate value of t_c allows us to use either the initial stiffness method, or the tangent stiffness method for the iterative procedure.

The second criterion is an unbalanced load criterion, that provides a ceiling for the maximum unbalanced load allowed for each iteration in order to guard against the excesive violation of equilibrium even though the displacement convergence

criterion is satisfied.

In addition to these two convergence criteria a ceiling is provided to limit the number of iterations performed for each load step in case that convergence tolerances provided are too stringent.

Depending on the objective of the analysis, different criteria can be used for the termination of the solution. The criteria may be chosen to satisfy either the serviciability or safety requirements.

In the present study both criteria will be used. To find the ultimate load capacity of the structure the solution is stopped once a negative eigenvalue is detected in the stiffness matrix. To satisfy the serviciability requirements, the displacement is imposed progressively until the maximum allowable value is exceeded. Typically, this is the case in studying the postbuckling behaviour of a structure.

5. THREE DIMENSIONAL REINFORCED CONCRETE FRAMES

5.1 General Remarks

A general procedure for the geometric and material nonlinear analysis of three dimensional reinforced concrete frames including the time dependent effects of load history, temperature history, creep, shrinkage and aging of concrete was discussed in chapter 4, utilizing the mathematical model for material properties developed in chapter 2.

A description of the derivation of the tangent stiffness matrix, the internal forces and the initial strain load vector as well as the torsional models and the large displacement analysis procedure will be given in this chapter.

5.2 Definitions and assumptions regarding geometry and deformation

As explained in chapter 3, the three dimensional frame structure consists of elements interconnected by joints, in which each element is prismatic and has a cross section of arbitrary shape (figure 5.1).

In the present study a filamented reinforced concrete beam element is adopted. Each filament is assumed to be in a uniaxial stress state and perfect bond between adjacent filaments is assumed. At any cross section, the material properties of each filament can vary to accommodate material nonlinearities. The beam stiffness at some reference axes can be obtained by summing the contributions of all the

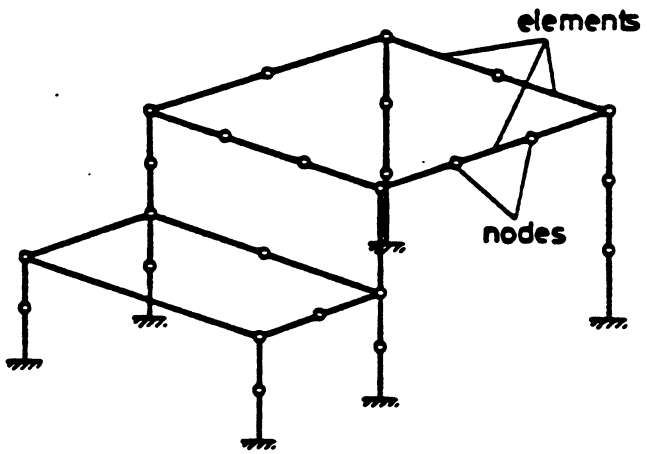

Fig 5.1. Three Dimensional Frame.

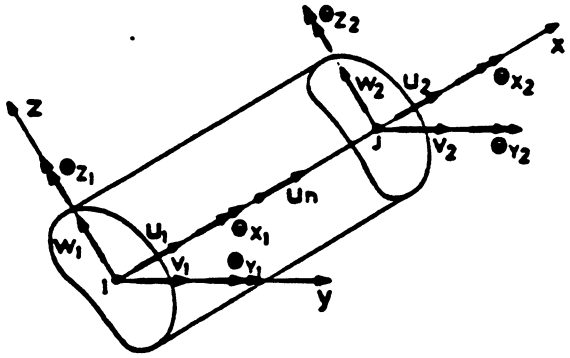

Fig. 5.2. Local Degrees of Freedom of a 3-D Beam Element.

filaments. There are 13 degrees of freedom (DOF) for the beam element (figure 5.2). Six DOF are associated with each of the two end nodes, namely $u_i, v_i, w_i, \theta_{xi}, \theta_{yi}, \theta_{zi}$, and an internal mid-side axial DOF U_n, which is eliminated at the element level leaving only 12 DOF for the beam element. As Chan |14| demonstrated, this incompatible axial displacement degree of freedom U_n, is necessary for the correct modelling of the bending stiffness so as to take into account the shifting of the neutral axis due to cracking and other material nonlinearities in a reinforced concrete beam.

5.3 Displacement fields

The displacement fields of the beam element on its local x axis are, according to the signs criteria of figure 5.2:

$$u_0 = (\lambda_1, \lambda_2, \lambda_3) \begin{Bmatrix} u_1 \\ u_2 \\ u_n \end{Bmatrix} \tag{5.1}$$

$$v_0 = (\phi_1, \phi_2, \phi_3, \phi_4) \begin{Bmatrix} v_1 \\ v_2 \\ \theta_{z_1} \\ \theta_{z_2} \end{Bmatrix} \tag{5.2}$$

$$w_0 = (\phi_1, \phi_2, -\phi_3, -\phi_4) \begin{Bmatrix} w_1 \\ w_2 \\ \theta_{y_1} \\ \theta_{y_2} \end{Bmatrix} \tag{5.3}$$

where:

$$\lambda_1 = 1-\frac{x}{L} \quad ; \quad \lambda_2 = \frac{x}{L} \quad ; \quad \lambda_3 = 4\,\frac{x}{L}\,(1-\frac{x}{L})$$

$$\phi_1 = 1 + 2(\frac{x}{L})^3 - 3(\frac{x}{L})^2 \qquad \phi_2 = 3(\frac{x}{L})^2 - 2(\frac{x}{L})^3 \qquad (5.4)$$

$$\phi_3 = L(\frac{x}{L} - 2\frac{x^2}{L^2} + (\frac{x}{L})^3) \qquad \phi_4 = -L(\frac{x^2}{L^2} - \frac{x^3}{L^3})$$

The axial displacement u_x at any point within the beam element can be obtained by assuming the Euler-Bernouilli's beam kinematics:

$$u_x = u_0 - z\,\frac{dw_0}{dx} - y\,\frac{dv_0}{dx} \qquad (5.5)$$

The axial strain is then obtained by differentiating u_x with respect to x

$$\varepsilon_x = \frac{du_x}{dx} = \frac{du_0}{dx} - z\,\frac{d^2w_0}{dx^2} - y\,\frac{d^2v_0}{dx^2} \qquad (5.6)$$

This expression has a physical interpretation that will help us to obtain the strains from the nodal displacements:

Term $\frac{du_0}{dx}$ is the axial strain of the reference axis.

$\frac{d^2w_0}{dx^2}$ is the curvature of the cross section with respect to the y axis.

$\frac{d^2v_0}{dx^2}$ is the curvature of the cross section with respect to the z axis.

The rotation θ_{x_0} about the x axis is assumed to be linear

$$\theta_{x_0} = (1-\frac{x}{L}, \frac{x}{L}) \begin{pmatrix} \theta_{x_1} \\ \\ \theta_{x_2} \end{pmatrix} \tag{5.7}$$

and the twist α along the reference axis x is:

$$\alpha = \frac{d\theta_{x_0}}{dx} = (1-\frac{1}{L}, \frac{1}{L}) \begin{pmatrix} \theta_{x_1} \\ \\ \theta_{x_2} \end{pmatrix} = \underset{\sim}{B}_\theta . \underset{\sim}{\theta}_x \tag{5.8}$$

Note that unrestrained warping torsion is assumed in equation 5.7. This leads to the uncoupling of the torsional degrees of freedom from the other degrees of freedom. Substituting equations 5.1, 5.2 and 5.3 into equation 5.6, considering also eq. 5.7 for the torsional behaviour and ordering the DOF conveniently, the resulting strain - displacement relationship is:

$$\underset{\sim}{\varepsilon} = \underset{\sim}{B} . \underset{\sim}{r} \tag{5.9}$$

where: $$\underset{\sim}{B} = |B_1, B_2, \ldots, B_{12}, B_{13}| \tag{5.10}$$

$$\underset{\sim}{r}^T = |u_1, v_1, w_1, \theta_{x_1}, \theta_{y_1}, \theta_{z_1}, u_2, v_2, w_2, \theta_{x_2}, \theta_{y_2}, \theta_{z_2}, u_n| \tag{5.11}$$

$$B_1 = -\frac{1}{L} = B_4 = -B_7 = -B_{10}$$

$$B_2 = -B_8 = \frac{6y}{L^2} (1-\frac{2x}{L})$$

$$B_3 = -B_9 = \frac{6z}{L^2} (1-\frac{2x}{L})$$

$$B_5 = \frac{2z}{L} (\frac{3x}{L}-2)$$

$$B_6 = \frac{-2y}{L}\left(\frac{3x}{L}-2\right)$$

$$B_{11} = \frac{2z}{L}\left(\frac{3x}{L}-1\right)$$

$$B_{12} = \frac{-2y}{L}\left(\frac{3x}{L}-1\right)$$

$$B_{13} = 4\left(\frac{1}{L} - \frac{2x}{L^2}\right) \qquad (5.12)$$

It will be useful to define the matrix $\underset{\sim}{B}_0$ as the one whose components are the same as $\underset{\sim}{B}$ but excluding the terms in y or z wherever they appear. So for example:

$$B_{0,2} = \frac{6}{L}\left(1-\frac{2x}{L}\right) \qquad B_{0,11} = \frac{2}{L}\left(\frac{3x}{L}-1\right)$$

and similary for the remainder terms.

5.4 Element elastic stiffness

The elastic stiffness of a reinforced concrete beam can be obtained by the expression:

$$K_e = \int_V E\,\varepsilon_x\,\delta\varepsilon_x + \int_L G\,J\,\alpha\,\delta\alpha\,dx = \int_0^L B^T\,E\,B\,dv + \int_0^L B_0^T\,G\,J\,B_0\,dx \qquad (5.13)$$

where E and ε_x are functions of the local x,y and z axes, and the torsional stiffness GJ is a function of x.

So any term of the (13 × 13) element stiffness matrix K_{ij} can be expressed either as:

$$K_{ij} = \int_V B_i E\,B_j\,dv \qquad \text{for flexural terms, or}$$

$$K_{ij} = \int_L B_{oi} GJ\, B_{oj} dx \qquad \text{for torsional terms.} \qquad (5.14)$$

The beam stiffness can be obtained explicitly if we assume that the values of E and GJ at the mid-length of the frame element represent the average value along its length. Then the integration can be performed as follows:

$$K_{ij} = \int_V B_i\, E\, B_j\, dv = \iint_S E.f(y,z)ds. \int_o^L \phi(x)dx \qquad (5.15)$$

where the first integral depends only on the sectional properties and the second is a function of x only.

This assumption is reasonable considering that the exact evaluation of the tangent stiffness matrix is not a necessary requirement for the solution of the nonlinear equilibrium equation when equilibrium correction iterations are performed.

Let's call

$$EA = \iint_S E\, ds \qquad EIY = \iint_S E\, z^2 ds$$

$$EY = -\iint E\, z.ds \qquad EIZ = \iint E\, y^2 ds \qquad (5.16)$$

$$EZ = -\iint E\, y.ds \qquad EYZ = \iint E.y\, z.ds$$

Then, the explicit expression of the element matrix stiffness is:

$$\underset{\sim}{K} = \left[\begin{array}{c:c} \underset{\sim}{K}_{ee} & \underset{\sim}{K}_{en} \\ \hdashline \underset{\sim}{K}_{ne} & \underset{\sim}{K}_{nn} \end{array}\right] \qquad (5.17)$$

$$\underset{\sim}{K}_{ee} = \left[\begin{array}{c|c} K_{ii} & K_{ij} \\ \hline K_{ji} & K_{jj} \end{array}\right] \tag{5.18}$$

where:

$$K_{ii} = \begin{bmatrix} \frac{EA}{L} & 0 & 0 & 0 & \frac{-EY}{L} & \frac{EZ}{L} \\ & \frac{12EIZ}{L^3} & \frac{12EYZ}{L^3} & 0 & \frac{-6EYZ}{L^2} & \frac{6EIZ}{L^2} \\ & & \frac{12EIY}{L^3} & 0 & \frac{-6EIY}{L^2} & \frac{6EYZ}{L^2} \\ & & & \frac{GJ}{L} & 0 & 0 \\ & & & & \frac{4EIY}{L} & \frac{-4EYZ}{L} \\ \text{symmetric} & & & & & \frac{4EIZ}{L} \end{bmatrix} \tag{5.19}$$

$$K_{jj} = \begin{bmatrix} \frac{EA}{L} & 0 & 0 & 0 & \frac{-EY}{L} & \frac{EZ}{L} \\ & \frac{12EIZ}{L^3} & \frac{12EYZ}{L^3} & 0 & \frac{6EYZ}{L^2} & \frac{-6EIZ}{L^2} \\ & & \frac{12EIY}{L^3} & 0 & \frac{6EIY}{L^2} & \frac{-6EYZ}{L^2} \\ & & & \frac{GJ}{L} & 0 & 0 \\ & & & & \frac{4EIY}{L} & \frac{-4EYZ}{L} \\ \text{symmetric} & & & & & \frac{4EIZ}{L} \end{bmatrix} \tag{5.20}$$

$$\underset{\sim}{K}_{ij} = \begin{bmatrix} \frac{-EA}{L} & 0 & 0 & 0 & \frac{EY}{L} & \frac{-EZ}{L} \\ 0 & \frac{-12EIZ}{L^3} & \frac{-12EYZ}{L^3} & 0 & \frac{-6EYZ}{L^2} & \frac{6EIZ}{L^2} \\ 0 & \frac{-12EYZ}{L^3} & \frac{-12EIZ}{L^3} & 0 & \frac{-6EIY}{L^2} & \frac{6EYZ}{L^2} \\ 0 & 0 & 0 & \frac{-GJ}{L} & 0 & 0 \\ 0 & \frac{6EYZ}{L^2} & \frac{6EYI}{L^2} & 0 & \frac{2EIY}{L} & \frac{-2EYZ}{L} \\ 0 & \frac{-6EIZ}{L^2} & \frac{-6EYZ}{L^2} & 0 & \frac{-2EYZ}{L} & \frac{2EIZ}{L} \end{bmatrix} = \underset{\sim}{K}_{ji}^{T} \tag{5.21}$$

$$K_{ne} = K_{en}^T = |0\ -\frac{8EZ}{L^2}\ -\frac{8EY}{L^2}\ \frac{4EY}{L}\ 0\ -\frac{4EZ}{L}\ 0\ \frac{8EZ}{L^2}\ \frac{8EY}{L^2}\ \frac{4EY}{L}\ 0\ \frac{4EZ}{L}| \qquad (5.22)$$

$$K_{nn} = \frac{16}{3L} EA \qquad (5.23)$$

To evaluate EA,EY,EZ,EIY,EIZ and EYZ a filament integration over the cross section at mid-length of the element is performed.

As indicated in chapter 3, each concrete filament i, is considered to have the same concrete area A_{ci}, and its position in the cross section is defined by its coordinates Y_{ci},Z_{ci}, with respect to the reference axes. The value of the tangent modulus of a concrete filament is E_{ci}.

Each steel filament has steel area A_{sj}, and coordinates Y_{sj}, Z_{sj}. The value of the tangent modulus of the j-th steel filament is E_{sj}.

Then the equations 5.16 become:

$$EA = \iint_S E\,ds = \sum_{i=1}^{n_c} E_{ci}A_{ci} + \sum_{j=1}^{n_s} E_{sj}A_{sj}$$

$$EY = -\iint_S E\,Z\,ds = -\sum_{i=1}^{n_c} E_{ci}A_{ci}Z_{ci} - \sum_{j=1}^{n_s} E_{sj}A_{sj}Z_{sj}$$

$$EZ = -\iint_S E\,Y\,ds = -\sum_{i=1}^{n_c} E_{ci}A_{ci}Y_{ci} - \sum_{j=1}^{n_s} E_{sj}A_{sj}Y_{sj}$$

$$EIY = \iint_S E\,Z^2 ds = \sum_{i=1}^{n_c} E_{ci}A_{ci}Z_{ci}^2 + \sum_{j=1}^{n_s} E_{sj}A_{sj}Z_{sj}^2 + \sum_{i=1}^{n_c} E_{ci}\cdot\frac{1}{12}\cdot\Delta Y_i\Delta Z_i^3$$

$$EIZ = \iint_S E\,Y^2 ds = \sum_{i=1}^{n_c} E_{ci}A_{ci}Y_{ci} + \sum_{j=1}^{n_s} E_{sj}A_{sj}Y_{sj} + \sum_{i=1}^{n_c} E_{ci}\cdot\frac{1}{12}\cdot\Delta z_i\Delta y_i^3$$

$$EYZ = \iint_S E\,Y\,Z\,ds = \sum_{i=1}^{n_c} E_{ci}A_{ci}Y_{ci}Z_{ci} + \sum_{j=1}^{n_s} E_{sj}A_{sj}Y_{sj}Z_{sj} \qquad (5.24)$$

where n_c is the total number of concrete filaments and n_s is the total number of steel filaments.

The last terms in the expression of EIZ and EIY are to take into account the moment of inertia of the concrete filaments with respect to their own symmetry axes.

As explained in chapter 3 the summation for all the concrete filaments is controlled by the cross section shape matrix $\underset{\sim}{C}$ that provides information for the geometric definition of the cross section shape.

The element stiffness matrix has been arranged so that the last row contains the displacement degree of freedom U_n.

$$\left[\begin{array}{c:c} \underset{\sim}{K}_{ee} & \underset{\sim}{K}_{en} \\ \hdashline \underset{\sim}{K}_{ne} & \underset{\sim}{K}_{nn} \end{array}\right]\left\{\begin{array}{c} \underset{\sim}{r}_e \\ \\ u_n \end{array}\right\} = \left\{\begin{array}{c} \underset{\sim}{P}_e \\ \\ P_n \end{array}\right\} \qquad (5.25)$$

where K_{ee}, K_{en}, K_{ne} and K_{nn} are the matrices expressed in equations 5.18 to 5.23 , and

$$\underset{\sim}{r}_e^T = |u_i, v_i, w_i, \theta_{xi}, \theta_{yi}, \theta_{zi}, u_j, v_j, w_j, \theta_{xj}, \theta_{yj}, \theta_{zj}| \qquad (5.26)$$

Using static condensation with $P_n = 0$ the final beam elastic stiffness K_e is:

$$\underset{\sim}{K}_e = \underset{\sim}{K}_{ee} - \frac{1}{K_{nn}} \underset{\sim}{K}_{en} \cdot \underset{\sim}{K}_{ne} \qquad (5.27)$$

Relating the element load P_e and the displacement $\underset{\sim}{r}_e$

$$\underset{\sim}{P}_e = \underset{\sim}{K}_e \, \underset{\sim}{r}_e \qquad (5.28)$$

5.5 Element geometric stiffness

If the nonlinear terms in the strain-displacement relationship are taken into account when calculating the element stiffness, a second matrix, usually called geometric matrix, must be included.

The nonlinear component in the strain displacement relationship can be expressed as:

$$\eta_{xx} = \frac{1}{2}\left[\frac{du_0}{dx}\right]^2 + \frac{1}{2}\left[\frac{dv_0}{dx}\right]^2 + \frac{1}{2}\left[\frac{dw_0}{dx}\right]^2 \qquad (5.29)$$

where u_0, v_0 and w_0 are the displacements of the reference axis.

The beam geometric stiffness can be obtained by substituting the assumed beam displacement fields (eq. 5.4) into equation 5.29, and evaluating the expression:

$$K_g = \int_V \sigma\, \eta_{xx}\, \delta\eta_{xx}\, dv \qquad (5.30)$$

This approach has been used by Kang |10| and Aldstedt |9|. The resulting beam geometric stiffness is:

$$K_g = N \begin{bmatrix} 0 & 0 & 0 & 0 & 0 & 0 & 0 & 0 & 0 & 0 & 0 & 0 \\ & \frac{6}{5L} & 0 & 0 & 0 & \frac{-1}{10} & 0 & \frac{-6}{5L} & 0 & 0 & 0 & 0 \\ & & \frac{6}{5L} & 0 & \frac{1}{10} & 0 & 0 & 0 & \frac{-6}{5L} & 0 & 0 & 0 \\ & & & 0 & 0 & 0 & 0 & 0 & 0 & 0 & 0 & 0 \\ & & & & \frac{2L}{15} & 0 & 0 & 0 & \frac{-1}{10} & 0 & \frac{-L}{30} & 0 \\ & & & & & \frac{2L}{15} & 0 & \frac{1}{10} & 0 & 0 & 0 & \frac{-L}{30} \\ & & & & & & 0 & 0 & 0 & 0 & 0 & 0 \\ & & & & & & & \frac{6}{5L} & 0 & 0 & 0 & 0 \\ & & & & & & & & \frac{6}{5L} & 0 & \frac{-1}{10} & 0 \\ & & & & & & & & & 0 & 0 & 0 \\ & & & & & & & & & & \frac{2L}{15} & 0 \\ & & & & & & & & & & & \frac{2L}{15} \end{bmatrix} \tag{5.31}$$

where N is the constant axial load acting on the beam element.

$$N = \sum_{i=1}^{n_c} A_{ci}\sigma_{ci} + \sum_{j=1}^{n_s} A_{sj}\sigma_{sj} \tag{5.32}$$

and

$$\underset{\sim}{P}_e = (\underset{\sim}{K}_e + \underset{\sim}{K}_g).\underset{\sim}{r}_e \tag{5.33}$$

Thus the element tangent stiffness is then obtained by adding $\underset{\sim}{K}_e$ and $\underset{\sim}{K}_g$. Chan |14| used a more simplified approach by considering that when constant axial load force is assumed in

the beam element, the beam behaves like a truss element in carrying the axial load.

Both approaches are practically equivalent and, when equilibrium iterations are performed, lead to the same result.

5.6 Calculation of strains and stresses

For each iteration in the course of the solution procedure, tangential equilibrium equations are solved for global displacement increments. The procedure for the calculation of strains and stresses at any point of the frame is the following:

1. Transform gobal displacement increments $\Delta \underset{\sim}{r}^G$ to local displacement increments $\Delta \underset{\sim}{r}$ for each element.

2. Evaluate the axial strain of the reference axis ε_{x_0}, and the curvatures of the cross section C_y and C_z by evaluating the strain-displacement matrix at the reference axis for the specific value of x corresponding to the desired cross section by substituting in the following equations:

$$\Delta\varepsilon_{x_0} = \frac{du_0}{dx} = |B_1, B_2| \begin{Bmatrix} \Delta u_1 \\ \Delta u_2 \end{Bmatrix} \tag{5.34}$$

$$\Delta C_y = \frac{d^2 \Delta w_0}{dx^2} = |B_3, B_5, B_9, B_{11}| \begin{Bmatrix} \Delta w_1 \\ \Delta\theta_{y_1} \\ \Delta w_2 \\ \Delta\theta_{y_2} \end{Bmatrix} \tag{5.35}$$

$$\Delta C_z = \frac{d^2 \Delta v_0}{dx^2} = |B_2, B_6, B_8, B_{12}| \begin{Bmatrix} \Delta v_1 \\ \Delta \theta_{z_1} \\ \Delta v_2 \\ \Delta \theta_{z_2} \end{Bmatrix} \tag{5.36}$$

3. Strain increment is then obtained by substituting $\Delta\varepsilon_{x_0}$, ΔC_y and ΔC_z in equation

$$\Delta\varepsilon_x = \Delta\varepsilon_{x_0} - \Delta C_y . Z - \Delta C_z . y \tag{5.37}$$

Total strain ε is then obtained by adding $\Delta\varepsilon$ to the previous total.

4. Mechanical strain ε^m is calculated by substracting non-mechanical strain ε^{nm} from total strain ε. Non mechanical strain ε^{nm} is due to the combined effects of creep, shrinkage, aging and temperature changes for reinforcing steel.

5. Stress σ is calculated by the nonlinear σ-ε^m curve given in chapter 2.

5.6 Element internal resisting load vectors

The internal resisting load R^i due to the stress σ_c in the concrete filaments, σ_s in the steel filaments and torque T_x in the beam can be obtained by evaluating:

$$R^i = \int_V B^T \sigma \, dv + \int_L B_\theta T_x \, dx \tag{5.38}$$

In this expression, the component B_{13} is not included in

order to force the zero force constraint for the internal degree of freedom u_n.

By assuming the stress σ in a filament to be constant at a section x, equation 5.38 can be integrated independently in longitudinal and transverse directions as follows:

$$\int_V B^T \sigma \, dv = \int_o^L \underset{\sim}{B}_o^T \left(\iint_S \sigma(y,z) \, \phi(y,z) ds \right) dx \tag{5.39}$$

Where B_o is the matrix defined in paragraph 5.3, which is a function of x. $\phi(y,z)$ is a function of y and/or z only.

Explicitly the terms of the internal resisting load vector are:

$$R_i^i = \int_o^L B_{o,i} F_i \, dx \qquad \forall_i = 4,10$$

$$R_4 = -R_{10} = \int_o^L B_\theta^T T_x \, dx = T_x \tag{5.40}$$

The values of F_i are the following:

$$F_1 = F_7 = \iint_S \sigma \, ds = \sum_{i=1}^{n_c} A_{ci}\sigma_{ci} + \sum_{j=1}^{n_s} A_{sj}\sigma_{sj} \tag{5.41}$$

$$F_2 = F_6 = F_8 = F_{12} = \iint_S \sigma \, y \, ds = \sum_{i=1}^{n_c} A_{ci}\sigma_{ci}Y_{ci} + \sum_{j=1}^{n_s} A_{sj}Y_{sj}\sigma_{sj} \tag{5.42}$$

$$F_3 = F_5 = F_9 = F_{11} = \iint_S \sigma \, y \, ds = \sum_{i=1}^{n_c} A_{ci}\sigma_{ci}Z_{ci} + \sum_{j=1}^{n_s} A_{sj}Z_{sj}\sigma_{sj} \tag{5.43}$$

In order to obtain R_i^i, numerical integration is performed by Gaussian Quadrature using two Gauss points. The functions $B_{o,i}$ must be evaluated only for the two Gauss point coordinates

$$x = \frac{L}{2} - \frac{\sqrt{3}}{6}L \quad \text{and} \quad x = \frac{L}{2} + \frac{\sqrt{3}}{6}L \ .$$

5.8 Element load due to initial strain

The equivalent load vector ΔR^{nm} due to non-mechanical strain increments are calculated by equation:

$$\Delta \underset{\sim}{R}^{nm} = \int_V B^T E \, \Delta\varepsilon_c^{nm} dv \tag{5.44}$$

in which E and $\Delta\varepsilon_c^{nm}$ are functions of x, y and z.

Following the same procedure used for the computation of $\underset{\sim}{R}^i$ and assuming E to be constant in a filament at a section x the results are:

$$\Delta R_i^{nm} = \int_o^L B_{o,i} \, \Phi_i \, dx \qquad \text{except for } i = 4, 10 \tag{5.45}$$

$$\Delta R_i^{nm} = 0 \qquad i = 4,10 \tag{5.46}$$

$$\Phi_1 = \Phi_7 = \iint_S E \, \Delta\varepsilon^{nm} ds = \sum_{i=1}^{n_c} A_{ci} E_{ci} \Delta\varepsilon_{ci}^{nm} \tag{5.47}$$

$$\Phi_2 = \Phi_6 = \Phi_8 = \Phi_{12} = \iint_S E \, y \, \Delta\varepsilon^{nm} ds = \sum_{i=1}^{n_c} A_{ci} E_{ci} y_{ci} \Delta\varepsilon_{ci}^{nm} \tag{5.48}$$

$$\Phi_3 = \Phi_5 = \Phi_9 = \Phi_{11} = \iint_S E \, z \, \Delta\varepsilon^{nm} ds = \sum_{i=1}^{n_c} A_{ci} E_{ci} z_{ci} \Delta\varepsilon_{ci}^{nm} \tag{5.49}$$

5.9 Transformation and assembly of the beam element

Before the beam's stiffnesses and the load vectors can be assembled, they must be transformed to a set of globals degrees

of freedom.

Let be $\underset{\sim}{u}_g$ the global degrees of freedom

$\underset{\sim}{u}_e$ the local degrees of freedom

$\underset{\sim}{A}$ the orthogonal matrix relating both systems

$$\underset{\sim}{r}_e = \underset{\sim}{A}\,\underset{\sim}{r}_g \tag{5.50}$$

where:

$$\underset{\sim}{r}_g = |U_i, V_i, W_i, \Theta_{xi}, \Theta_{yi}, \Theta_{zi}, U_j, V_j, W_j, \Theta_{xj}, \Theta_{yj}, \Theta_{zj}| \tag{5.51}$$

$$\underset{\sim}{r}_e = |u_i, v_i, w_i, \theta_{xi}, \theta_{yi}, \theta_{zi}, u_j, v_j, w_j, \theta_{xj}, \theta_{yj}, \theta_{zj}| \tag{5.52}$$

$$\underset{\sim}{A} = \begin{pmatrix} \underset{\sim}{T}^T & \underset{\sim}{0} & \underset{\sim}{0} & \underset{\sim}{0} \\ & \underset{\sim}{T}^T & \underset{\sim}{0} & \underset{\sim}{0} \\ & & \underset{\sim}{T}^T & \underset{\sim}{0} \\ & & & \underset{\sim}{T}^T \end{pmatrix} \tag{5.53}$$

$$\underset{\sim}{T} = \begin{pmatrix} a_{11} & a_{12} & a_{13} \\ a_{21} & a_{22} & a_{23} \\ a_{31} & a_{32} & a_{33} \end{pmatrix} \tag{5.54}$$

a_{ij} is the i-th component of the j-th vector of local system in global coordinates (director cosines).

The transformation of the matrices $\underset{\sim}{K}_e$ and $\underset{\sim}{K}_g$ are:

$$\underset{\sim}{K}_E = \underset{\sim}{A}^T . \underset{\sim}{K}_e . \underset{\sim}{A} \tag{5.55}$$

$$\underset{\sim}{K}_G = \underset{\sim}{A}^T . \underset{\sim}{K}_g . \underset{\sim}{A} \tag{5.56}$$

And the transformation of the load vectors $\underset{\sim}{R}^i$ and $\underset{\sim}{R}^{nm}$ are:

$$\underset{\sim}{R}_g^i = \underset{\sim}{A}^T \underset{\sim}{R}_e^i \tag{5.57}$$

$$\underset{\sim}{R}_g^{nm} = \underset{\sim}{A}^T \underset{\sim}{R}_e^{nm} \tag{5.58}$$

5.10 Torque-Twist relationship

The material models for the concrete and steel described in chapter two, valid for one dimensional stress state, are used. However, the material law for the torsion still remains to be defined. In the present study, the approach used by Chan [14] has been adopted and will be briefly described herein.

Bending action and torsional action are assumed to be completely uncoupled. Consequently, the interaction between the stresses from the two different sources are ignored.

A trilinear model is used to represent the torsional response of a reinforced concrete beam in terms of torque-twist relationship. The actual curve (figure 5.3) can be usually well fitted by three straight lines representing the uncracked, cracked and yielded phase, respectively.

The representative parameters in the model are:

(T_{cr}, α_{cr}) The torque at first cracking T_{cr}, and the corresponding twist.

(T_{yp}, α_{yp}) The torque at first full yielding of all the reinforcement T_{yp}, and its corresponding twist.

α_u The twist at ultimate failure.

In order to obtain this curve, experimental results must be available. Only in certain cases, such as beams with

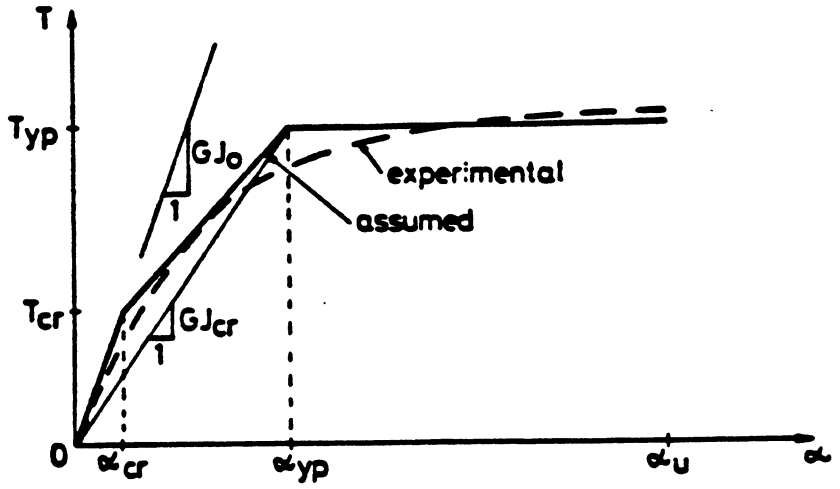

Fig. 5.3. Assumed Torque-Twist Relationship.

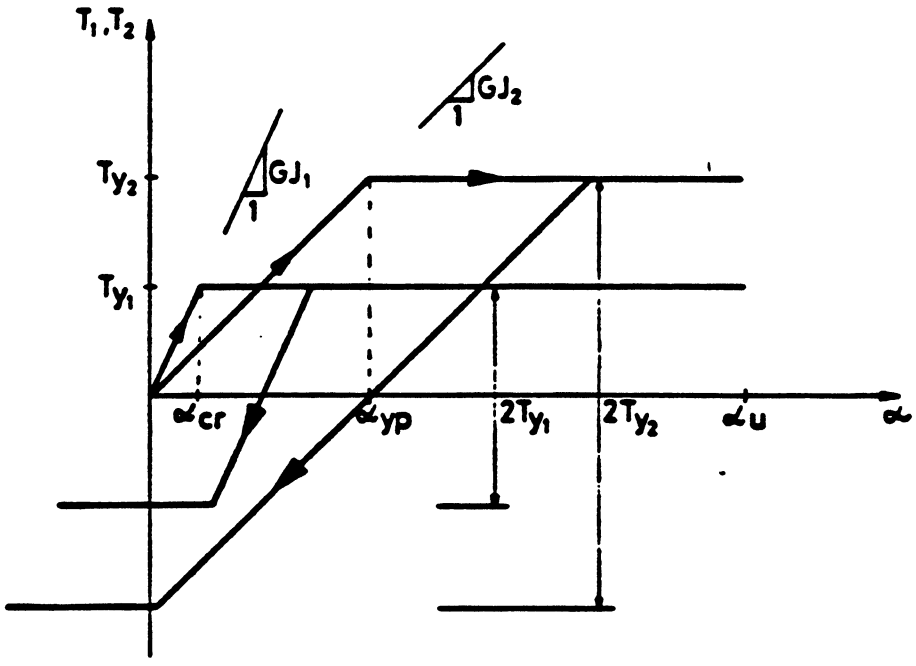

Fig. 5.4. Overlay Model for Trilinear Torque-Twist Relationship.

circular, rectangular or very simple box cross section, some analytical expressions can be deduced for representing the beam's behaviour in the cracked any yielded ranges.

In order to allow the modelling of inelastic unloading, an overlay model for torsion is used. The trilinear torque-twist response is modelled by two components, each exhibiting elasto-plastic behaviour such that the torsional stiffness GJ and the torque T of the beam are the sum of both components:

$$T = T_1 + T_2 \quad ; \quad GJ = GJ_1 + GJ_2 \tag{5.59}$$

$$GJ = \frac{T_{cr} - \Phi\alpha_{cr}}{\alpha_{cr}} \quad ; \quad J_2 = \frac{T_{yp} - T_{cr}}{\alpha_{yp} - \alpha_{cr}} = \Phi \tag{5.60}$$

$$T_{y_1} = GJ_1.\alpha_{cr} \quad ; \quad T_{y_2} = GJ_2.\alpha_{yp} \tag{5.61}$$

The use of the overlay model allows the modelling of inelastic unloading easily. It is assumed that inelastic unloading of each component is elastic with its initial stiffness (fig. 5.4).

The resulting inelastic unloading response is shown in fig. 5.5 for unloading after crack and unloading after yielded.

5.11 Large displacement analysis

The approach used in this study for the large displacement analysis, based upon average rotations of the beam element's axes is the one proposed by Chan |14|. This approach is restricted to large displacements and small rotations.

In the analysis including nonlinear geometry, the geometry of the beam and the beam's local axes x,y and z have to be

updated. It is assumed that the equilibrium configuration at step i-1 and the incremental nodal displacements at the current step i are known.

The relative displacements between the two ends of the beam element can be found from the incremental nodal displacement relative to the x^{i-1}, y^{i-1} and z^{i-1} axes. They are:

$$\begin{aligned} {}^1u &= \Delta u_j - \Delta u_i \\ {}^2u &= \Delta v_j - \Delta v_i \\ {}^3u &= \Delta w_j - \Delta w_i \end{aligned} \tag{5.62}$$

The new coordinate axes x^i, y^i, z^i at step i, with unit vectors $\hat{x}^i, \hat{y}^i, \hat{z}^i$ are obtained as a result of a series of motions. The angles α, β, γ that describe the motions can be found by simple geometry and are (figure 5.6):

$$\cos\alpha = \frac{L^{i-1} + {}^1u}{\left[(L^{i-1} + {}^1u)^2 + {}^3u^2\right]^{1/2}} \tag{5.63}$$

$$\sin\alpha = \frac{{}^3u}{\left[(L^{i-1} + {}^1u)^2 + {}^3u^2\right]^{1/2}} \tag{5.64}$$

$$\cos\beta = \frac{\left|(L^{i-1} + {}^1u)^2 + {}^3u^2\right|^{1/2}}{\left[(L^{i-1} + {}^1u)^2 + {}^2u^2 + {}^3u^2\right]^{1/2}} \tag{5.65}$$

$$\sin\beta = \frac{{}^2u}{\left[(L^{i-1} + {}^1u) + {}^2u^2 + {}^3u^2\right]^{1/2}} \tag{5.66}$$

$$\gamma = \frac{1}{2}\left(\theta_{xi} + \theta_{xj}\right) \tag{5.67}$$

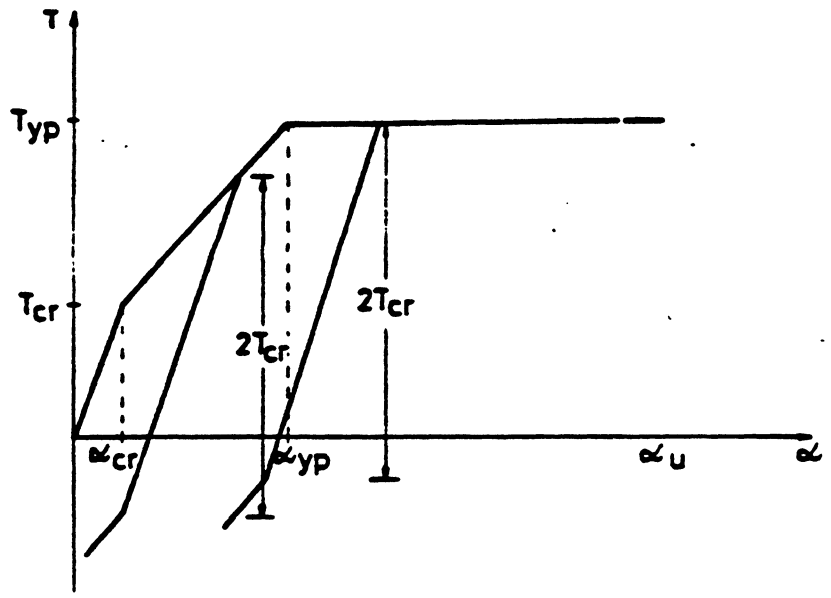

Fig. 5.5. Inelastic Unloading in Torsion for the Overlay Model.

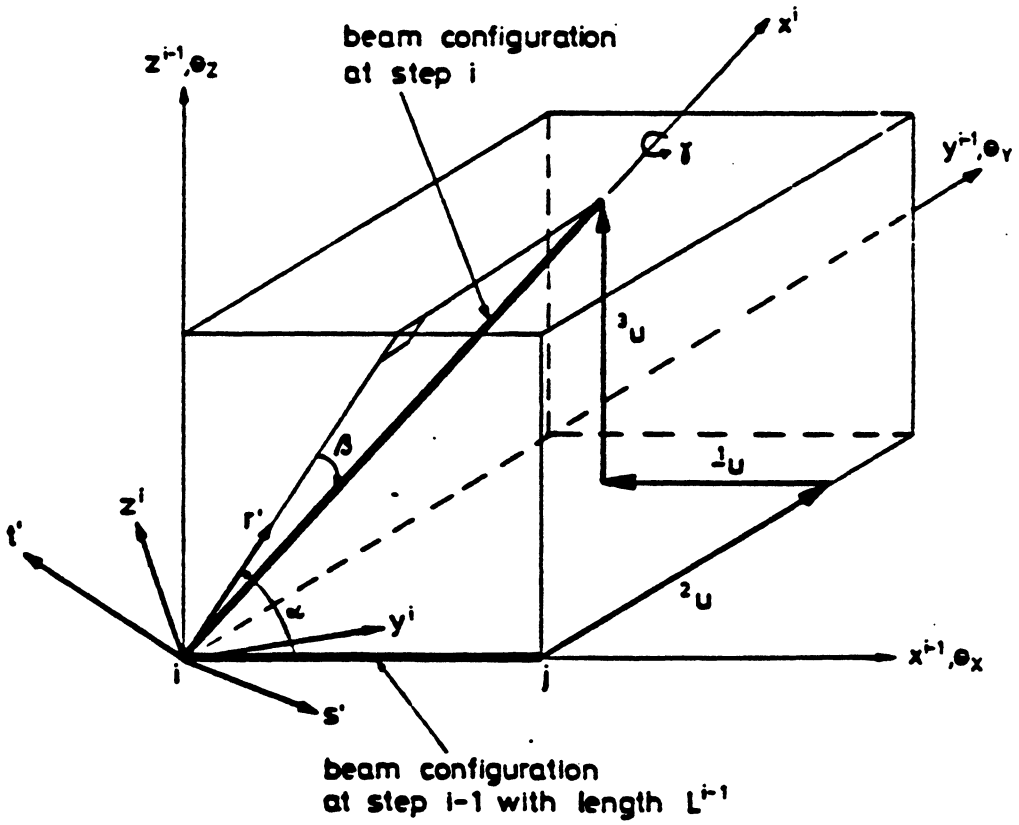

Fig. 5.6. Transformation of the Beam Local Axes in a Large Displacement Analysis.

The trasnformation between the unit vectors $\hat{x}^i, \hat{y}^i, \hat{z}^i$, at step i and the unit vectors $\hat{x}^{i-1}, \hat{y}^{i-1}, \hat{z}^{i-1}$, at step i-1 is:

$$\begin{bmatrix} \hat{x}^T \\ \hat{y}^T \\ \hat{z}^T \end{bmatrix}_i = \begin{bmatrix} \cos\alpha\cos\beta & \sin\beta & \sin\alpha\cos\beta \\ -\cos\alpha\sin\beta\cos\gamma - \sin\alpha\sin\gamma & \cos\beta\cos\gamma & -\sin\alpha\sin\beta\cos\gamma + \cos\alpha\sin\gamma \\ \cos\alpha\sin\beta\sin\gamma - \sin\alpha\cos\gamma & -\cos\beta\sin\gamma & \sin\alpha\sin\beta\sin\gamma + \cos\alpha\cos\gamma \end{bmatrix} \begin{bmatrix} \hat{x}^T \\ \hat{y}^T \\ \hat{z}^T \end{bmatrix}_{i-1} \tag{5.68}$$

The nodal point coordinates of the beam are updated once nodal displacement increments at each node j are known in the global coordinate system:

$$\begin{bmatrix} x^i \\ y^i \\ z^i \end{bmatrix}_j = \begin{bmatrix} x^{i-1} \\ y^{i-1} \\ z^{i-1} \end{bmatrix}_j + \begin{bmatrix} \Delta u \\ \Delta v \\ \Delta w \end{bmatrix} \tag{5.69}$$

The axial increment in strain due to axial elongation is, (if small strains are considered):

$$\Delta\varepsilon = \frac{L^i - L^{i-1}}{L^{i-1}} \tag{5.70}$$

where L^i is the length of the element for the step i.

In local coordinates, the axial displacement increments are:

$$u_i = 0 \quad ; \quad u_j = \Delta\varepsilon . L^{i-1} \tag{5.71}$$

6. THREE DIMENSIONAL PRESTRESSED CONCRETE FRAMES

6.1 General Remarks

Among the different types of prestressed structures, only post-tensioned bonded structures are considered in the present study. In this kind of structure the prestress is transferred gradually to the concrete while the prestressing steel is tensioned against the hardened concrete and anchored against it inmediately after the tensioning operation. The prestressing steel is grouted after the tensioning operation so that steel and concrete are bonded.

The behaviour of prestressed structures is largely dependent of the effective amount of prestress acting on them, so the determination of the variation of the stress in the prestressing steel during various stages of loading is an important factor in the analysis of prestressed concrete structures.

In post-tensioned structures, the prestress losses take place, during the tensioning operation, due to the friction between the prestressing tendon and the duct, and the anchorage slip; and after the transfer of prestress due to creep and shrinkage of concrete, the relaxation of prestressing steel and the effects of load history and temperature history.

In the present study, aim is taken in finding all the displacements, internal forces, stresses and strains for the concrete, reinforcing steel and the prestressing steel in the three dimensional post-tensioned concrete frames subjected to load history and temperature history, at any time during

their service lives by a complete analysis including material and geometric nonlinearities, and the time dependent effects of creep, shrinkage, and aging of concrete and the relaxation of prestressing steel.

In addition to the assumptions and definitions regarding geometry and deformation, given in chapters 3 and 5, some additional assumptions must be made for prestressing concrete frames:

- Each tendon is assumed to have an initial tensioning force.
- Jacking can be made from either of the two tendon ends.
- Each prestressing steel segment is assumed to have a constant force.
- Perfect bond between concrete and prestressing steel is assumed. Thus the displacement field within an element of these structures is assumed to be continuous.

6.2 Prestressing force at any point along a tendon

6.2.1 Friction losses

For post-tensioned structures the prestressing is transferred gradually to the concrete during the tensioning operation. As the prestressing force is applied from the tensioning end with initial force P_o, as shown in figure 6.1, friction takes place between the prestressing steel and the duct, resulting in the gradual decrease in the prestressing steel force away from the tensioning end. The decrease in the prestressing steel force due to the friction can be calculated

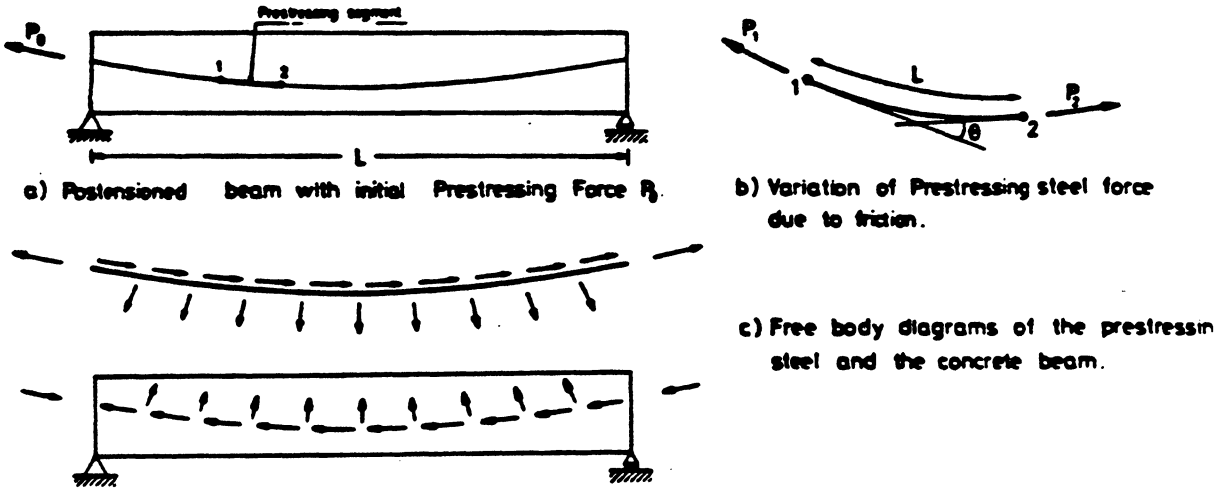

a) Postensioned beam with initial Prestressing Force P_0.

b) Variation of Prestressing steel force due to friction.

c) Free body diagrams of the prestressin steel and the concrete beam.

Fig. 6.1. Analysis of post-tensioned beam at transfer.

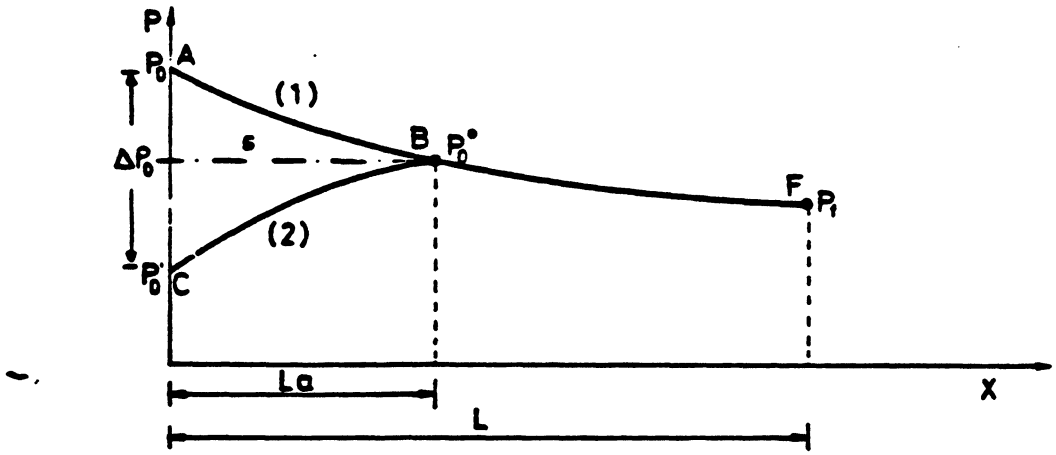

Fig. 6.2. Variation of Prestressing Force Along the Tendon With (2) and Without (1) Anchorage Slip.

by the formula:

$$P_2 = P_1 . e^{-(\mu\theta + KL)} \qquad (6.1)$$

where P_1 = Prestressing force at point 1.

P_2 = prestressing force at point 2.

L = Length of the prestressing segment

θ = Change in the slope of the prestressing steel segment, in radians, assumed to be uniformly distributed over the length.

μ = Curvature friction coefficient

K = Wobble friction coefficient.

With equation 6.1 we can calculate the prestressing force at any point along the tendon by starting from the tensioning end with given initial tensioning force P_o.

Since each prestressing steel segment is assumed to be straight and have a constant force, the force in a specific steel segment is taken as an average of the forces at the two end points of the segment.

6.2.2 Effect of anchorage slip

When there is an anchorage slip by an amount $\Delta\ell$ at the tensioning end, there is a loss of prestressing in the tendon of an amount that is gradually decreasing due to the friction force, that acts in opposite direction to the motion of the cable, and may dissapear at a certain distance, ℓ_a. This is shown in figure 6.2, where the value of the prestressing force

along the tendon, with and without anchorage slip, is presented.

In order to take into account the effect of anchorage slip, it is necessary to obtain the value of the prestressing loss at the anchorage (ΔP_o), and the length of the affected zone (ℓ_a). For that purpose the symmetry of the curves AB and CB with respect to the s axis in figure 6.2 is assumed. The physical interpretation of this asumption is that the friction acts with the same intensity for tensioning and distensioning.

On the other hand, it is known that the amount of stretching of the prestress tendon is equal to:

$$\Delta \ell = \int_0^L \frac{P(x)}{E_p A_p} dx \qquad (6.2)$$

where E_p and A_p are the elastic modulus of prestressing steel and area of prestressing tendon respectively.

This expression indicates that the value of $\Delta \ell$ is proportional to the area under the curve P(x), on the P(x)- x diagram (figure 6.2).

If this concept is applied to the case of anchorage sleep, it can be said that the area ABC is proportional to the amount of slip:

$$\Delta \ell = \frac{1}{E_p A_p} \text{ Area (ABC)} \qquad (6.3)$$

Based on these two assumptions, the problem can be solved numerically as following:

For a prestressing steel tendon the profile AF, without

considering anchorage slip losses, can be calculated by equation 6.1, so the values of prestressing force at the ends of each segment are known. Let's consider a prestressing segment with end nodes I, and J. The values of the areas A1, A2, and A3 of figure 6.3, can be obtained by the corresponding expressions of figure 6.3 a), b) and c). The area $A_3 = 2(A_1 - A_2)$ is the one that is proportional to the anchorage slip. For the exact value of ℓ_a, the following equation should be satisfied:

$$\Delta\ell = \left(\frac{A_3}{E_p A_p}\right)_{\ell = \ell_a} \tag{6.4}$$

In order to known the length of the anchorage slip effect, comparisons between the calculated area A_3 at the end of each segment, divided by $E_p . A_p$, and the value of the anchorage slip are made, starting from the beginning of the tendon, as follows:

- If $\Delta\ell > A_3/E_pA_p$ the length of the anchorage slip ℓ_a is bigger than the length of the tendon up to the current segment, ℓ_i.
- If $\Delta\ell = A_3/E_pA_p$ the length of the anchorage slip ℓ_a is equal to the length of the tendon up to the current segment.
- If $\Delta\ell < A_3/E_pA_p$ the length of the anchorage slip ℓ_a is less than the length of the tendon up to the current segment.

The numerical solution of the length ℓ_a will be found when, for the first value of i (current segment) the area A_3 divided by E_pA_p, is bigger than the anchorage slip. That indicates that

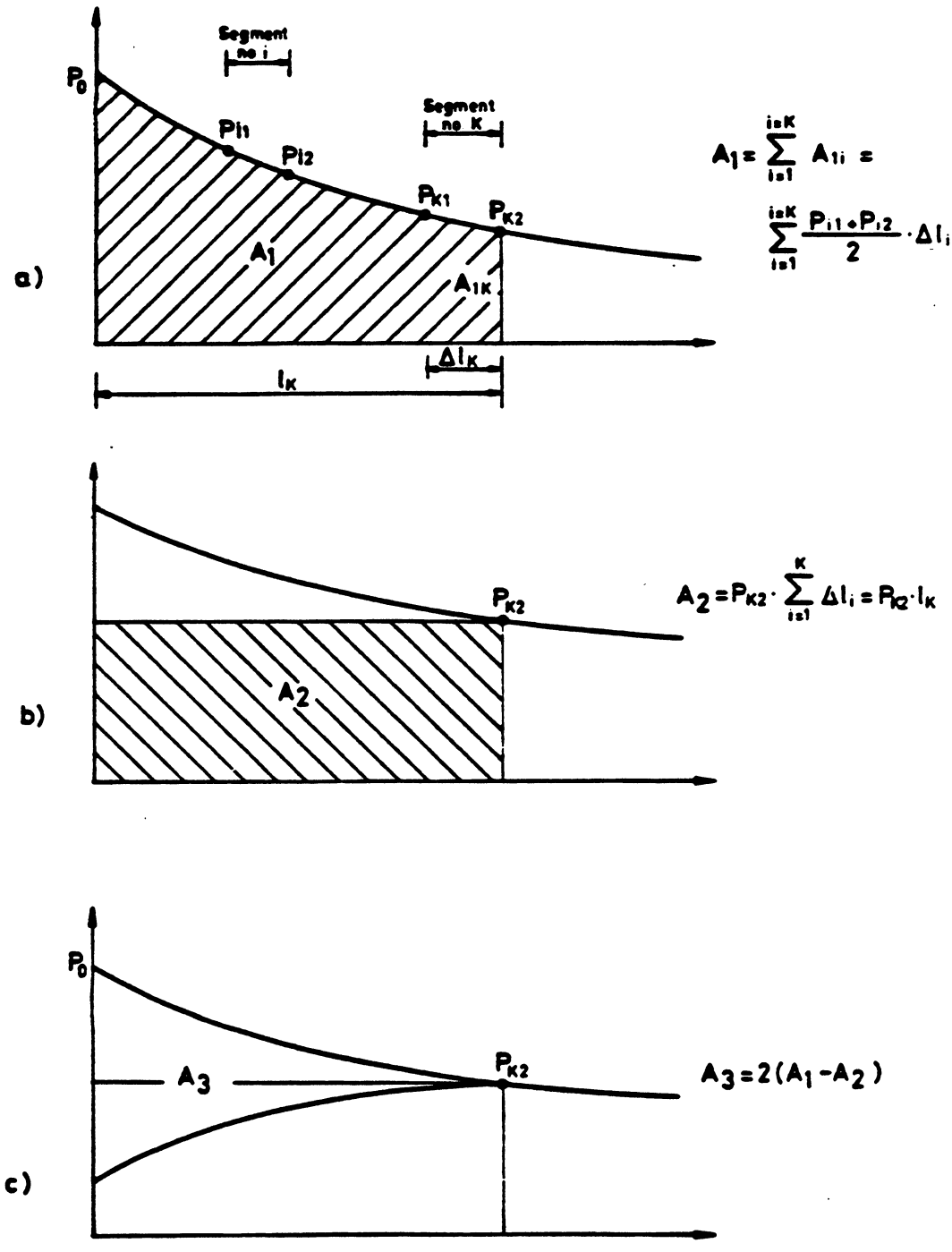

Fig. 6.3. Calculation of the Area A_3 Proportional to the Amount of Anchorage Slip.

the unknown length of the anchorage slip, has a value between the lengths of the tendon L_i and L_{i-1}. Then, linear interpolation is performed to obtain an approximate value of L_a.

The point of the prestressing tendon $L = L_a$ corresponds, hence, to the point from which the anchorage sleep does not affect the prestressing force. But before this point, the values of the prestressing forces have to be calculated, (ascending branch in figure 6.4). This is achieved by obtaining the prestressing force at $L = L_a$ and using the condition of symmetry explained above. The expressions to use for this purpose are:

$$P_o^* = P(L_a) = P_o\, e^{-(\mu\theta_a + K\ell_a)} \tag{6.5}$$

$$P_i' = P_i - 2\Delta P_i = P_i - 2(P_i - P_o^*) = 2P_o^* - P_i \tag{6.6}$$

If the anchorage slip is very big, it can affect the value of the prestressing force at the opposite end of the tendon. The above described procedure is modified, in this case. The unknown here is not the deep ℓ_a, but the value of the decrease of prestressing force at the opposite end, H (see figure 6.5). The expression that gives us the value of the prestressing force at any point, for this case is:

$$P'(x) = 2P_o^* - P(x) - H \tag{6.7}$$

The value of H is obtained by equating the total shaded area in figure 6.5 to the value $E_p A_p \Delta\ell$.

$$\text{Area} = E_p\, A_p . \Delta\ell = A_3 + H\, L \tag{6.8}$$

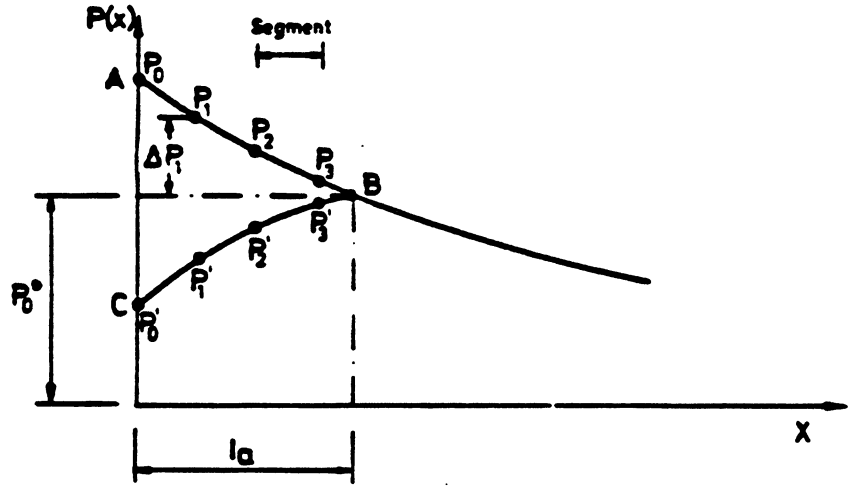

Fig.6.4. Value of the Anchorage Slip Length Effect ℓ_a and Ascending Branch of the Prestressing Force.

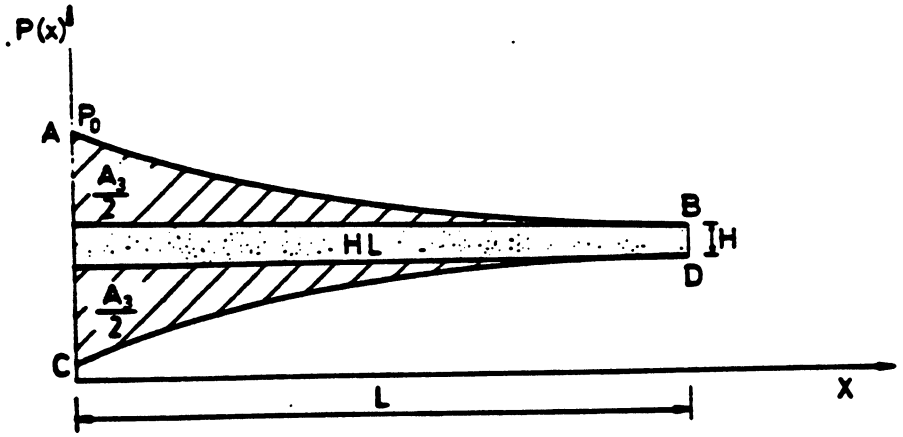

Fig.6.5. Prestressing Force When the Anchorage Slip at One End Affects the Other Tendon End.

$$H = \frac{E_p A_p \Delta\ell - A_3}{L} \qquad (6.9)$$

When the anchorage slip does not affect the other end, the expression of P(x) is the same, just substituting H for zero.

This method provides similar results to the ones obtained by Van Greunen (19), but as it is a direct method, it has the advantage that it is not necessary to iterate.

6.3 Calculation of load vector due to prestress at transfer

Once the force at any point of a prestressing tendon is known, and assuming that the force at any prestressing steel segment is constant, the interaction between prestressing steel and concrete takes place only at the ends of each prestressing segment. The load vector that prestressing introduces upon the structure is obtained as explained in the following.

Each segment introduces over the end joints of the element to which it belongs a set of forces and moments defined as indicates in figure 6.6, in local coordinates of the element.

The set of forces introduced by each prestressing steel segment are transformed to global coordinates and accumulated over the nodes. For each tendon these forces constitute a set of self equilibrated forces. The assembly of forces due to all tendons give us the load vector due to prestress at transfer.

The prestressing steel segment force is defined as the

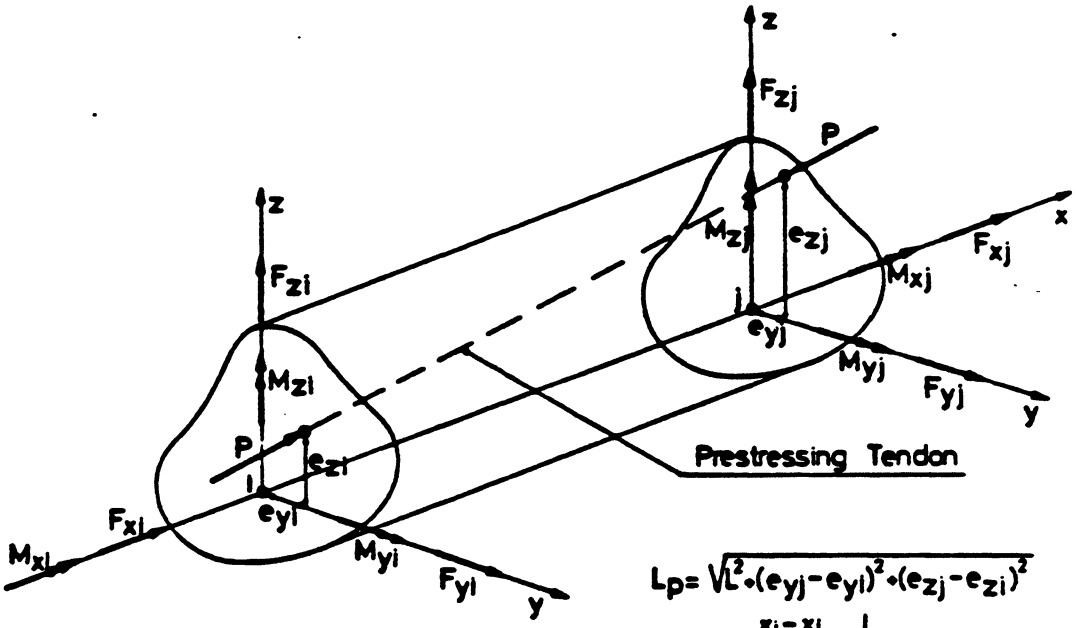

$$L_p = \sqrt{L^2 + (e_{yj} - e_{yi})^2 + (e_{zj} - e_{zi})^2}$$

$$\cos\alpha_x = \frac{x_j - x_i}{L_p} = \frac{L}{L_p}$$

$$\cos\alpha_y = \frac{e_{yj} - e_{yi}}{L_p}$$

$$\cos\alpha_z = \frac{e_{zj} - e_{zi}}{L_p}$$

$F_{xi} = P \cdot \cos\alpha_x = \frac{P \cdot L}{L_p}$ $F_{xj} = -P \cos\alpha_x = -\frac{P \cdot L}{L_p}$	$M_{xi} = F_{yi} \cdot e_{zi} - F_{zi} \cdot e_{yi}$ $M_{xj} = F_{yj} \cdot e_{zj} - F_{zj} \cdot e_{yj}$
$F_{yi} = P \cdot \cos\alpha_y$ $F_{yj} = -P \cdot \cos\alpha_y$	$M_{yi} = F_{xi} \cdot e_{zi}$ $M_{yj} = F_{xj} \cdot e_{zj}$
$F_{zi} = P \cdot \cos\alpha_z$ $F_{zj} = -P \cos\alpha_z$	$M_{zi} = F_{xi} \cdot e_{yi}$ $M_{zj} = F_{xj} \cdot e_{yj}$

Fig. 6.6. Calculation of the Joint Load Vector Due to Prestress at Transfer.

average of the values of the prestressing force of the tendon at the ends of the prestressing segment. For this reason the value of the force at the ends of any tendon, calculated in this way will be slightly different from the actual ones that can be measured when jacking. In general this difference will be small, and can be neglected. This problem is inherent to the treating of a continuous phenomenon as a discrete phenomenon.

6.4 Introduction of prestressing in the element stiffness

After grouting, the prestressing steel is bonded to the concrete so it must be taken into account when calculating the stiffness of the element. As the stiffness matrix may be not completely exact to obtain correct results in a nonlinear analysis (it will affect the number of necessary iterations to converge), an approximate value of the contribution of pretressing steel to the element stiffness is calculated. This approach consists in considering the prestressing steel segment parallel to the element x axis, with eccentricities e_y,e_z equal to the average value of the actual eccentricities at the element ends.

This contribution to the element stiffness will be taken into account only after the specified value of the age of the concrete for which the prestressing is introduced. This procedure permits the analysis of a structure as an initial reinforced concrete structure, under a load history, and after a certain interval of time, to introduce the prestressing to carry overload.

6.5 Variation of prestressing load vector with time

With the passage of time, losses in prestressing force are produced due to creep and shrinkage of concrete and relaxation of prestressing steel.

Creep and shrinkage effects in prestressing force are evaluated when calculating the internal resisting load vector due to prestress as will be shown in point 6.6. The action of the initial strain load vector due to the time dependent effects will change the length of the prestressing segments, and consequently, their stress level and force.

Relaxation is defined as the loss in stress when the strain is constant. For each prestressing steel segment, the value of the loss due to relaxation will be introduced as part of the initial strain load vector. In order to calculate the relaxation loss at any segment, the same approach used by Kang |10| has been adopted. The equation that gives the relaxation of the steel stresses, based on numerous experimental data is:

$$\frac{f_s}{f_{si}} = 1-\frac{\log t}{10}\left[\frac{f_{si}}{f_y}-0.55\right] \; ; \; \frac{f_{si}}{f_y} \geq 0.55 \qquad (6.10)$$

This equation is developed on the condition that the strain remains constant and the initial prestress is the only stress being applied. In reality various changes in the prestress take place due to other causes. The procedure used to take into account this variation of prestress can be shown

schematically in figure no. 6.7 and is explained next.

Let f_{si_0} be the initial prestress applied at time t_0. At time t_1, in addition to the stress relaxation f_{r_1} from the initial prestress f_{si_0}, the prestress drops to f_{s_1} due to other causes. Then equation 6.10 can be used to calculate a fictitous initial prestress f_{si_1} such that applied at t_0 would be relaxed to f_{s_1} at t_1. Then, on the basis of the initial prestress f_{si_1}, the stress relaxation f_{r_2} occurring during t_1 and t_2 can be calculated.

$$\Delta f_{r2} = f_{s_1} - f'_{s_2} = (f_{si_1} - f'_{s_2}) - (f_{si_1} - f_{s_1}) \qquad (6.11)$$

f_{rs} is calculated similarly after calculating a fictitious initial prestress f_{si_2} which would relax to f_{s_2} at t_2. By continuing this precess the total stress relaxation f_{rn} at time t_n can be calculated by

$$f_{rn} = \sum_{i=1}^{n} \Delta f_{ri} \qquad (6.12)$$

6.6 Calculation of prestressing steel strains and stresses and internal element forces due to prestress

In order to calculate the prestressing steel strains and stresses, the current length of each prestressing steel segment at each stage of the iterative process is calculated by first calculating the global coordinates of the two end points. Figure 6.8 shows an element with a prestressing steel segment

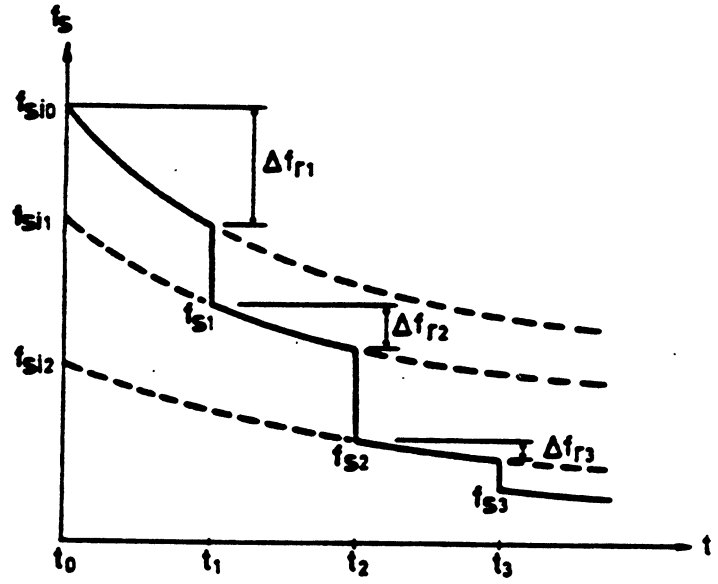

Fig. 6.7. Calculation of the Stress Relaxation.

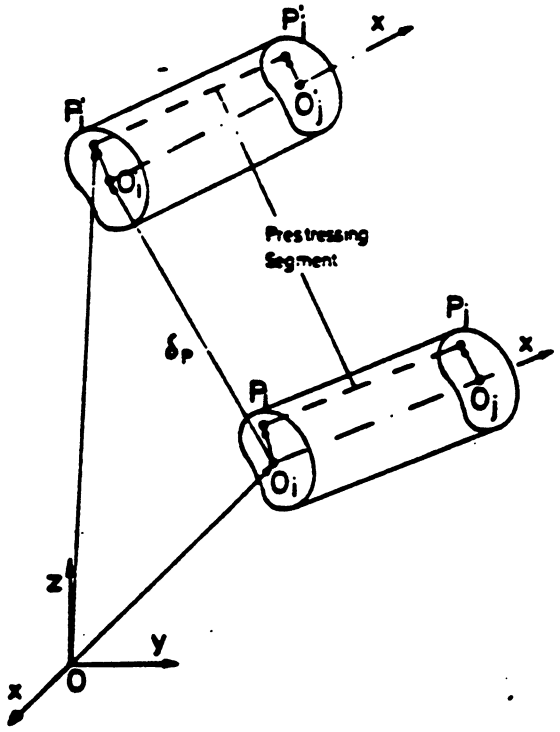

$$\overrightarrow{OP_i'} = \overrightarrow{OO_i} + \overrightarrow{O_iO_i'} + \overrightarrow{O_i'P_i'}$$
$$\overrightarrow{O_i'P_i'} = \overrightarrow{O_iP_i} + \overrightarrow{\delta_R}$$
$$\overrightarrow{O_iO_i'} = \overrightarrow{\delta_P}$$
$$\overrightarrow{OP_i'} = \overrightarrow{OO_i} + \overrightarrow{\delta_P} + \overrightarrow{O_iP_i} + \overrightarrow{\delta_R}$$

For next iteration, the initial values are

$$\overrightarrow{OO_i'} = \overrightarrow{OO_i} + \overrightarrow{\delta_P}$$
$$\overrightarrow{O_i'P_i'} = \overrightarrow{O_iP_i} + \overrightarrow{\delta_R}$$

Fig. 6.8. Calculation of the Current Global Coordinates of an End Point of the Prestressing Steel Segment.

on it, in two loading stages: A is the current stage, and B is the stage after deformation. Let be P_1P_2 the position of the prestressing segment before deformation and $P_1' P_2'$ after deformation. To obtain the global coordinates of points P_1' and P_2' we need to take into account the translation of the structure (nodal displacements) and the rotations of the end sections of the element. The position vector O_1P_1 of one segment end has global coordinates $\vec{O_1P_1} = (x_0, y_0, z_0)$. If the joint O_1 has three rotations $(\theta_x, \theta_y, \theta_z)$ and three displacements u,v,w, the position vector of point P_1, in global coordinates is:

$$\vec{OP_1} = \vec{OO_1} + \vec{O_1P_1} \tag{6.13}$$

$$\text{where } \vec{OP_1} = (x_1, y_1, z_1) \tag{6.14}$$

$$\vec{O_1P_1} = x_0, y_0, z_0 \tag{6.15}$$

Due to the rotations of joint O_1, point P_1 has suffered three translations $\Delta x, \Delta y, \Delta z$, given by the expressions:

$$\begin{aligned}
\Delta x &= z_0 \sin\theta_y + x_0(\cos\theta_y - 1) + x_0(\cos\theta_z - 1) - y_0 \sin\theta_z \\
\Delta y &= y_0(\cos\theta_x - 1) - z_0 \sin\theta_x + x_0 \sin\theta_z + y_0(\cos\theta_z - 1) \\
\Delta z &= z_0(\cos\theta_y - 1) - x_0 \sin\theta_y + y_0 \sin\theta_x + z_0(\cos\theta_x - 1)
\end{aligned} \tag{6.16}$$

if $\underset{\sim}{\delta}_r = (\Delta x, \Delta y, \Delta z)$ and $\underset{\sim}{\delta}_p = (u,v,w) = \vec{O_1O_1'}$ is the vector of nodal displacements (translations only), the final position of point P_1 will be:

$$\vec{OP}_1 = \vec{OO}_1 + \vec{\delta}_p + \vec{O_1P_1} + \vec{\delta}_r \qquad (6.17)$$

For the next iteration, the new nodal coordinates are:

$$\vec{OO}_1 = \vec{OO}_1 + \vec{O_1O}_1 = \vec{OO}_1 + \vec{\delta}_p \qquad (6.18)$$

The position vector in the section, in global coordinates is:

$$\vec{O_1P}_1 = \vec{O_1P}_1 + \vec{\delta}_r \qquad (6.19)$$

If this procedure is followed for both ends of each prestressing segment, their new global coordinates can be obtained and, consequently, the new prestressing segment length.

The procedure to obtain the stress for each prestressing segment is the following:

1. The increment of strain in the segment, measured with respect to the current state will be:

$$\Delta\varepsilon_p = \frac{L_i - L_{i-1}}{L_{i-1}} \qquad (6.20)$$

2. Add $\Delta\varepsilon_p$ to the previous total to obtain the current strain ε_p.

3. Calculate the stress corresponding to ε_p from the nonlinear stress-strain relationship for prestressing steel.

4. Substract the stress relaxation calculated by the procedure described in section 6.5 from the stress obtained in step 3 to calculate the current stress.

The internal resisting load vector R_p^i due to prestress can be expressed as follows for each element:

$$R_p^i = (R_x, R_y, R_z, M_x, M_y, M_z) \tag{6.21}$$

in which each term has been defined in section 6.3

R_p^i is transformed to global coordinates and added to the internal resisting load vector due to internal forces for the concrete and reinforcing steel, and then assembled for all the elements to form the internal resisting load vector for the structure.

7. NUMERICAL EXAMPLES

7.1 General

A number of numerical examples have been solved using the computer program PCF3D, developed in the present study, to verify the validity of the theoretical procedure. The examples also serve as a means to demonstrate the accuracy and the capability of the computer program PCF3D to predict the nonlinear material, geometric and time dependent behaviour of three dimensional prestressed and reinforced concrete frames.

In section 7.2 emphasis is placed on the verification of the present method of handling geometric nonlinearity.

In sections 7.3 and 7.4 reinforced and prestressed concrete columns of rectangular and irregular cross section, respectively, subjected to biaxial bending are presented. Both, geometric and material nonlinearities are taken into account.

In section 7.5 a reinforced concrete three dimensional frame is analysed showing the ability of the program to handle structures subjected to biaxial bending and torsion

7.2 Symmetrical Buckling of Circular Arch due to uniform pressure

An end clamped shallow circular arch subjected to a uniform pressure has been analysed to verify the capability of the program to solve a snap-through problem and the accuracy of the large displacement analysis. The load is

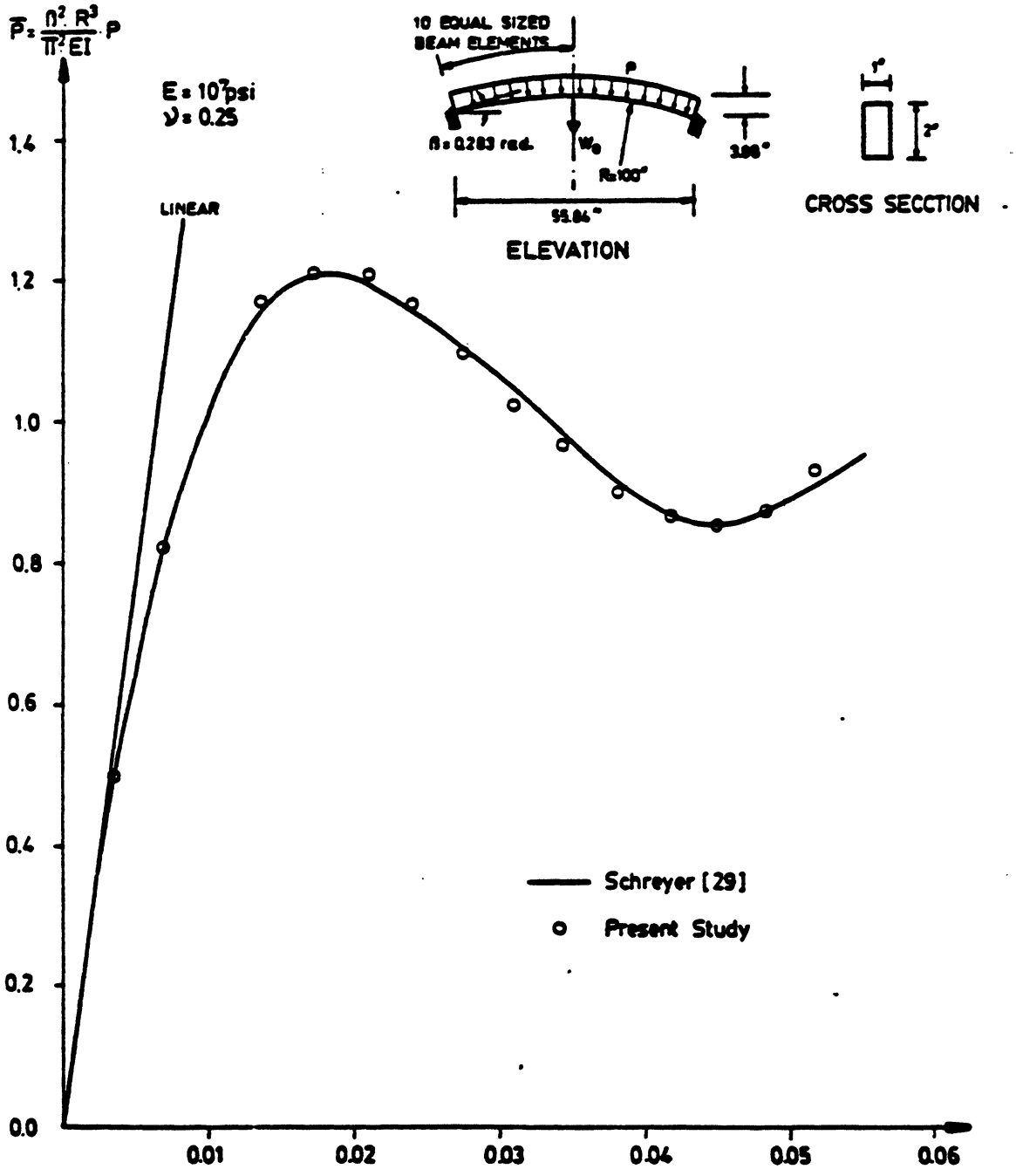

Fig.7.1. Symmetrical Buckling of Circular Arch Due to Uniform Pressure (ex.8.2) Load Vs . Central Vertical Downwards Displacement.

considered conservative and is applied only at the structure joints, by using a lumped formulation.

The geometry and the material properties of the structure are shown in figure 7.1. Due to the symmetry of the structure, one-half of the arch is modelled by 10 equal sized straight elements. The response of the structure is obtained by imposing the control vertical displacement w_0 in 15 equal displacement steps of 0.35 in. each.

The load-displacement response is shown in figure 7.1, together with the analytical solution obtained by Schreyer |29|. It can be seen that good agreement exists and that the present method of analysis predicts the correct response for relatively large load steps.

7.3 Biaxial bending of a square reinforced and prestressed concrete column

The objective of this example is to demonstrate the capability of the program to study concrete structures subjected to biaxial bending. Also the effect of prestressing in a relatively long column is studied taking into account geometric and material non-linearities.

A series of five hypothetical columns loaded eccentrically in two directions is chosen for the present analysis. They all have identical cross sectional dimensions and amounts of steel, but the first one (figure 7.2) is a reinforced concrete column with equally distributed steel along the four faces and the other four (figure 7.2) are prestressed concrete columns with only prestressing steel at the four corners of the cross section,

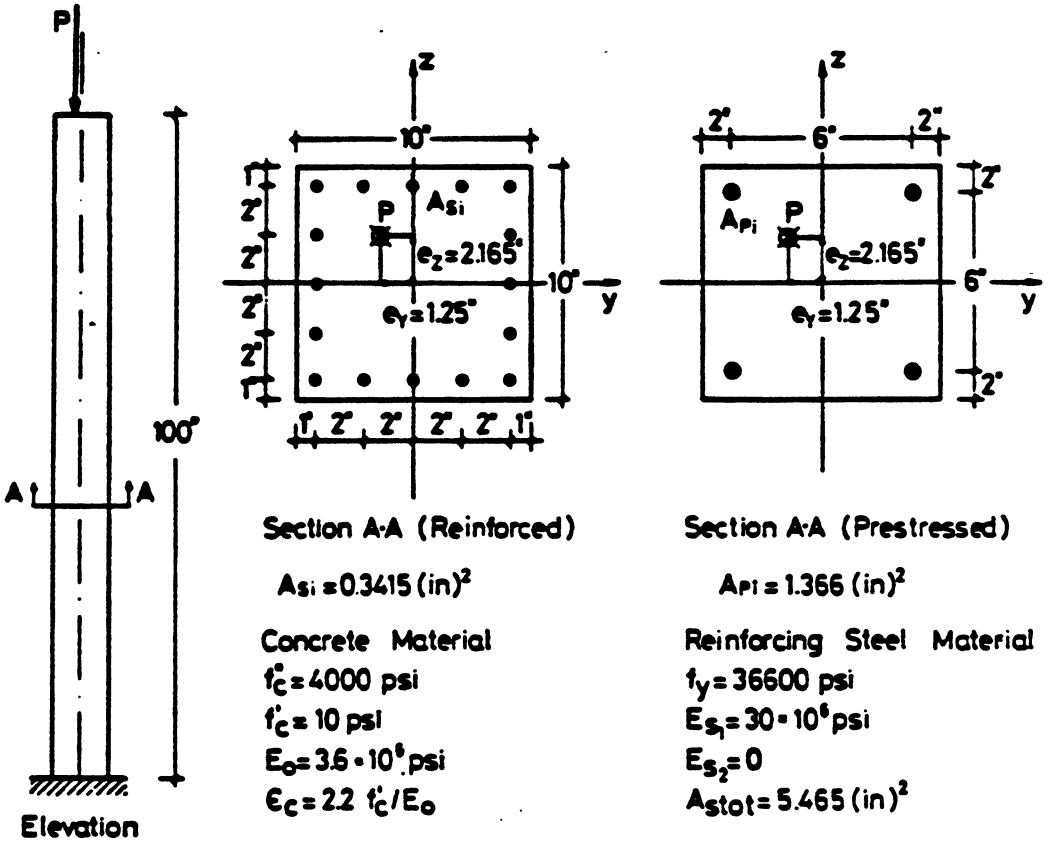

Prestressing Steel Material

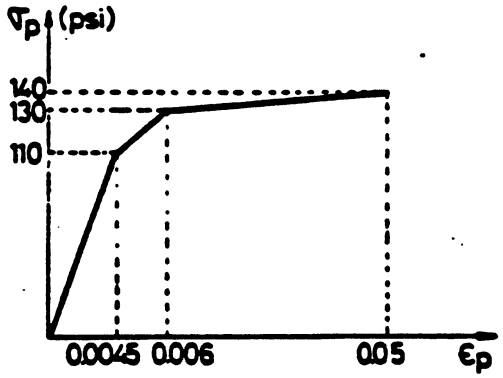

Stress (psi)	Strain
110	0.0045
130	0.0060
140	0.0500

$A_{ptot} = A_{stot} = 5.465\ (in)^2$

Fig. 7.2 Biaxial Bending of a Reinforced and/or Prestressed Concrete Column (Ex. 7.3). Geometry and Material Properties.

and each of the four with a different amount of prestressing force, without reinforcing steel.

The geometry, reinforcement and prestressing arrangement and the material properties are shown in figure 8.2. The prestressing consists of four straight prestressing cables that span the entire column length. No friction or anchorage slip losses are taken into account for the calculation of the prestressing force at each point of each tendon. The total prestressing forces are 0 kips, 120 kips, 200 kips, and 300 kips for the four prestressed concrete columns.

The cantilever column is modelled by using 10 equal sized elements. The cross section is divided into a grid of 10 x 10 filaments. Control of the Z displacement of the top of the column is used to obtain the response of the structure. The resulting load-displacement curves are presented in figure no. 7.3.

Column 1 (only reinforced) was also analyzed by Warner (16) who assumed a cosine function for the deformed shape. It is observed in figure 7.3 that good agreement exists between the results by Warner and the present study. The rest of the curves (2, 3, 4 and 5) are for the columns with only prestressing steel, but where different amounts of prestressing force are introduced. It must be remarked that although column 2 is prestressed with zero prestressing forces, and the total area of prestressing steel is equal to the total area of reinforcing steel of column 1, they are not directly comparable, because the steel properties (stress-strain relationships) and

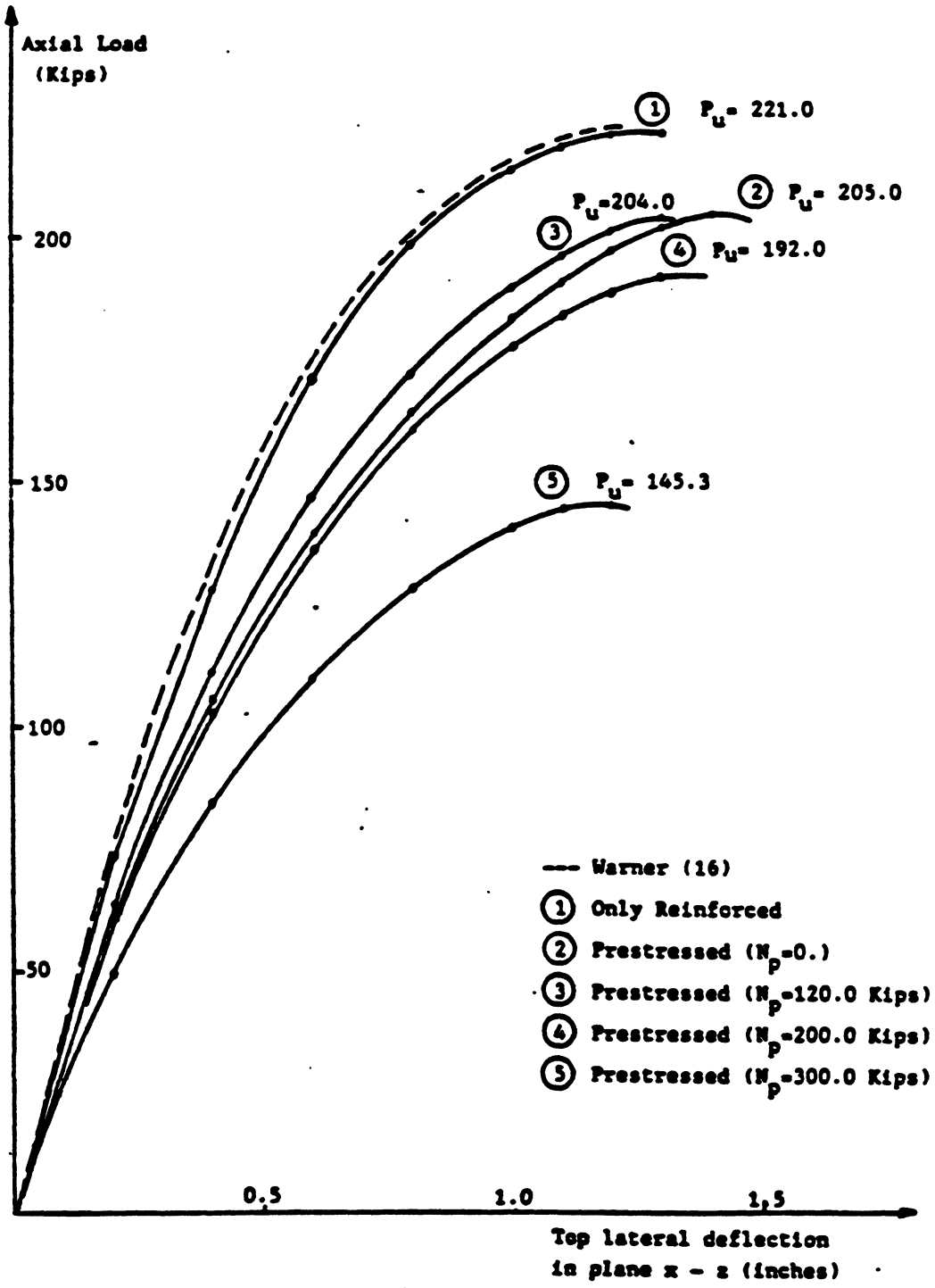

Fig. 7.3 Load-Deflection Curves for Column of Example 7.3

distribution of steel on the section are different.

However, columns 2, 3, 4 and 5 only differ in the prestressing force, so good comparisons can be made among their results in order to estimate the effect of prestressing in that column. As can be seen in figure 7.3 the increase of prestressing force does not change practically the ultimate load when a moderate prestressing force is introduced, such as $N_p \leq 200$ kips ($N_p/N_u = 0.5$, since $N_u = f''_c .b.h = 400$ kips). The stiffness of the member increases for a small amount of prestressing force (curve 3 indicates a larger stiffness than curve 2) but after a certain amount of prestressing (between 120 kips, and 700 kips for this particular case) the column becomes more flexible than the nonprestressed one.

When a large prestressing force is introduced (N_p 300 kips for column 5, which represents $N_p/N_u = 0.75$) both the ultimate load and the stiffness of the column drop considerably.

All of these phenomena can be explained by taking into account that prestressing has several effects on the column response:

First: Prestressing introduces an initial compressive axial load that delays cracking and therefore it increases the stiffness of the structure (case of column 3 where it is compared with column 2).

Second: Due to prestressing, the concrete fibers are precompressed, and because of the nonlinear stress-strain curve of the concrete, their modules of elasticity are reduced with respect to the non-prestressed column. This effect reduces the column stiffness and can be even a stronger effect than the

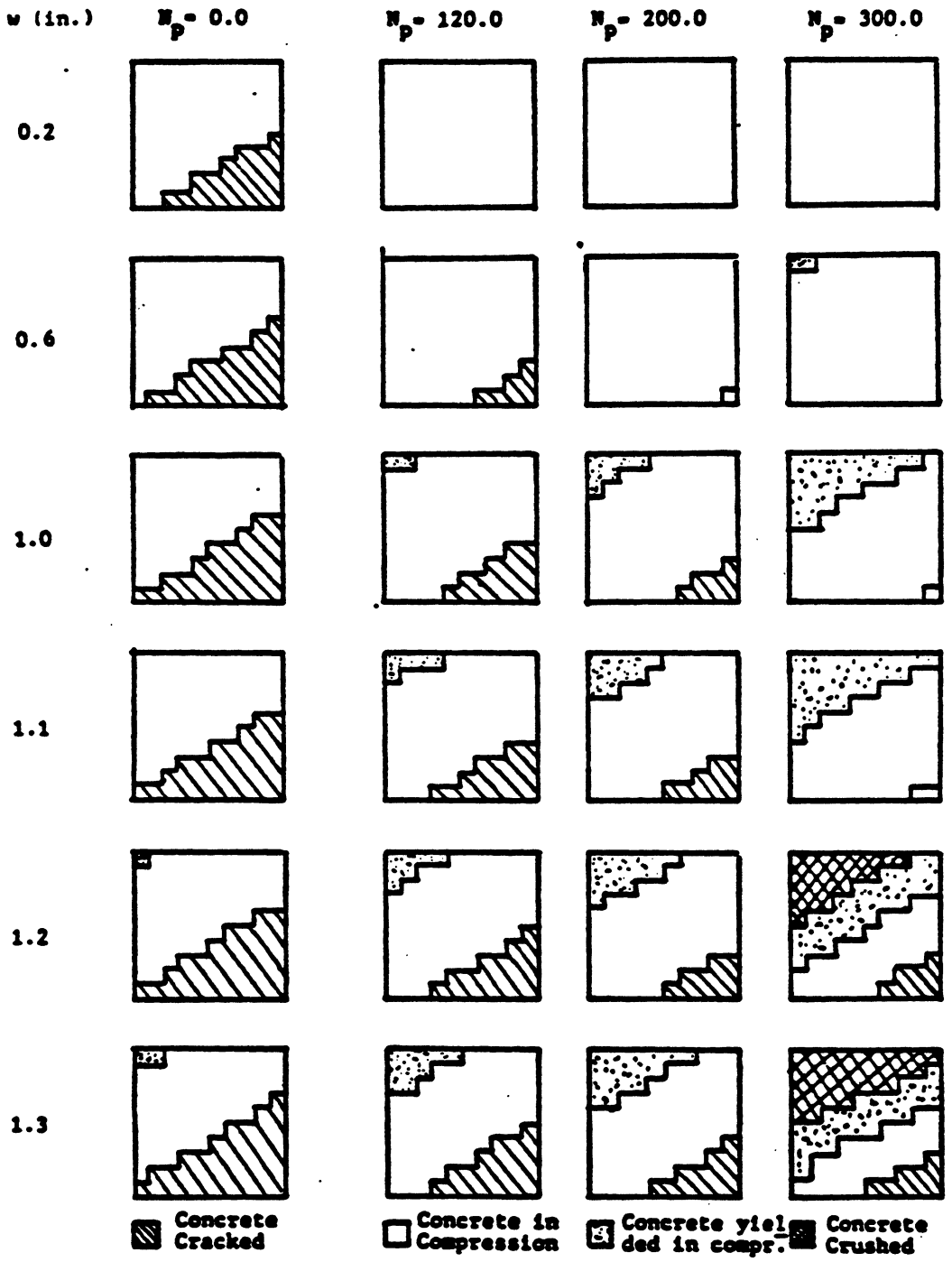

Fig. 7.4 Biaxial Bending of a Prestressed Concrete Column
Progressive crack patterns at the base section.

delaying the concrete cracking, such as occurs in column 4. Third: Prestressing is, in these columns, a concentrated compressive force on the cross section, producing a uniform compressive stress over the entire cross section that consumes part of the compression capacity of the concrete. If the prestressing force is very high (case of column 5) crushing of the concrete is produced and the load carrying capacity is drastically reduced. The progressive crack patterns at the bottom section of the four prestressed columns are shown in figure 7.4. Columns 2, 3 and 4 (moderately prestressed) show a stability failure, having part of the cross section cracked and part of the concrete yielded in compression. Column 5 fails by yielding and crushing of the concrete in compression. In none of the cases does the prestressing steel yield.

TABLE 7.1 Statical check for column of example 7.3

COLUMN	INTERNAL MOMENTS in-kips M_y	M_z	AXIAL LOAD kips	V (in.)	W (in.)	EXTERNAL MOMENTS $M=P(e_o+\delta)$ M_y	M_z
Reinforced	494.0	798.0	221.0	0.957	1.40	494.0	797.0
Prestressed N_p=0	426.1	722.6	205.0	0.851	1.35	430.7	770.6
Prestressed N_p=120	431.9	709.8	204.4	0.837	1.30	426.6	708.3
Prestressed N_p=200	383.7	665.9	192.0	0.771	1.30	388.0	665.2
Prestressed N_p=300	270.7	474.0	145.3	0.608	1.10	269.9	474.3

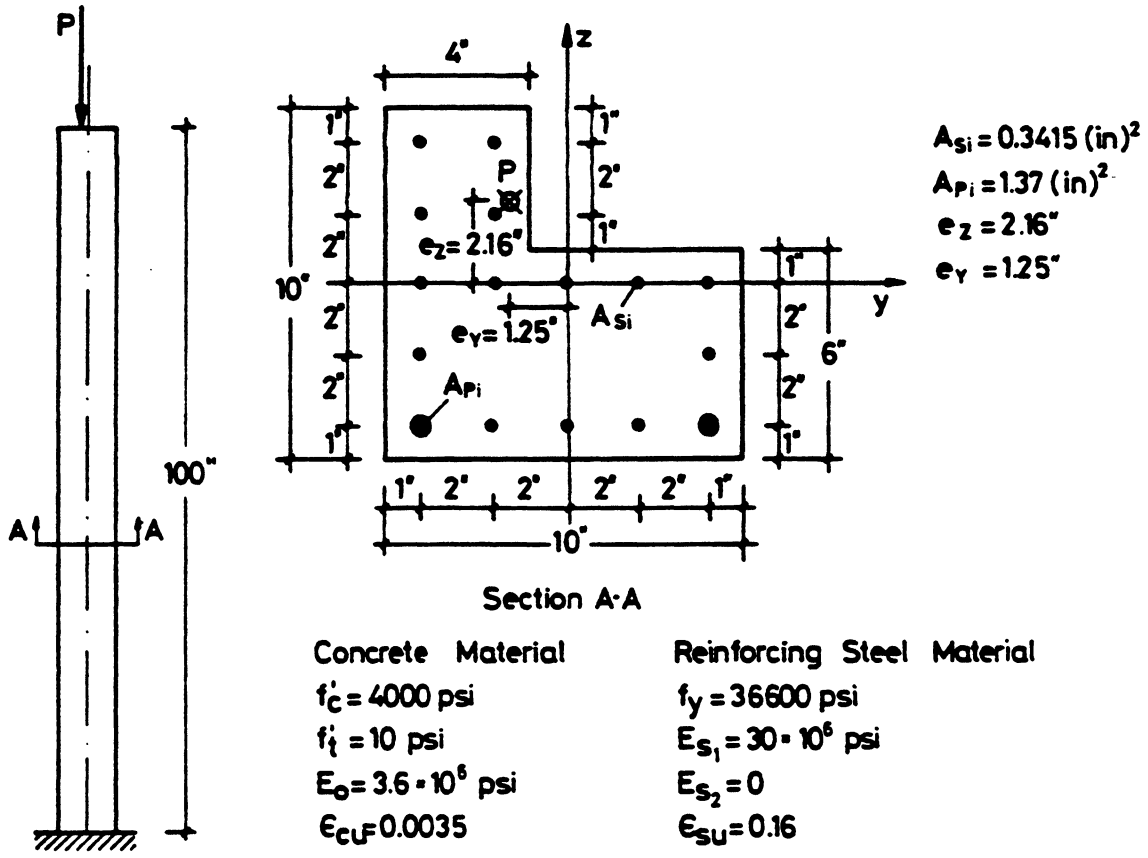

Section A-A

Concrete Material	Reinforcing Steel Material
f'_c = 4000 psi	f_y = 36600 psi
f'_t = 10 psi	E_{s_1} = 30 · 10⁶ psi
E_o = 3.6 · 10⁶ psi	E_{s_2} = 0
ϵ_{cu} = 0.0035	ϵ_{su} = 0.16

Prestressing Steel Properties

Stress	Strain	Tang. Modulus
110	0.0045	24444
130	0.0060	13333
140	0.0500	227.3
(ksi)		(ksi)

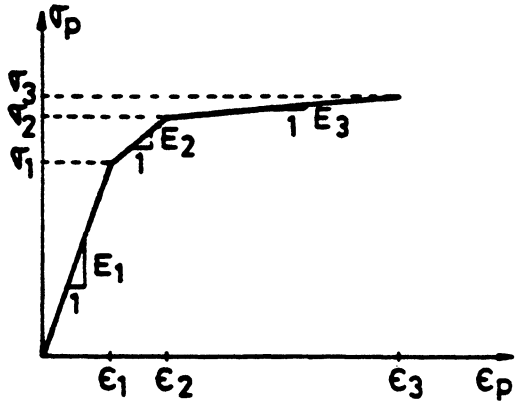

Fig. 7.5. Biaxial Bending of Prestressed Concrete Column with Irregular Cross Section. (Ex. 7.4)

The effect of prestressing on cracking is clearly shown in figure 7.4 where it can be seen that the greater the prestressing force introduced, the later cracking appears.

The orientation of the plane of bending rotates because of cracking and other material nonlinearities. The total rotation of this plane for the reinforced concrete column is 4.4° at failure (P = 221 kips). This rotation also induces a maximum torsional moment of 140 in-lb. due to nonlinear geometric effects. A statistical check has been made at the base of the column, comparing internal and external moments taking into account the P-Δ effect. The results of this check are shown in table 7.1. It can be seen that practically no unbalance exists between external and internal forces.

7.4 Reinforced and prestressed concrete column of irregular cross section

One feature of the present beam element is its ability to model members with any arbitrary cross section. It is the purpose of this example to demonstrate this capability taking into account the effect of material and geometric nonlinearities as well as the effect of prestressing applied at the tensile zone.

A series of three hypothetical columns with the same cross section is chosen for the present analysis. The first one is reinforced while the other two are prestressed with two different amounts of prestressing force (column 2 has N_p = 60 kips, and column 3 has N_p = 120 kips). There are two straight prestressing tensdons placed in the tensile zone of the column.

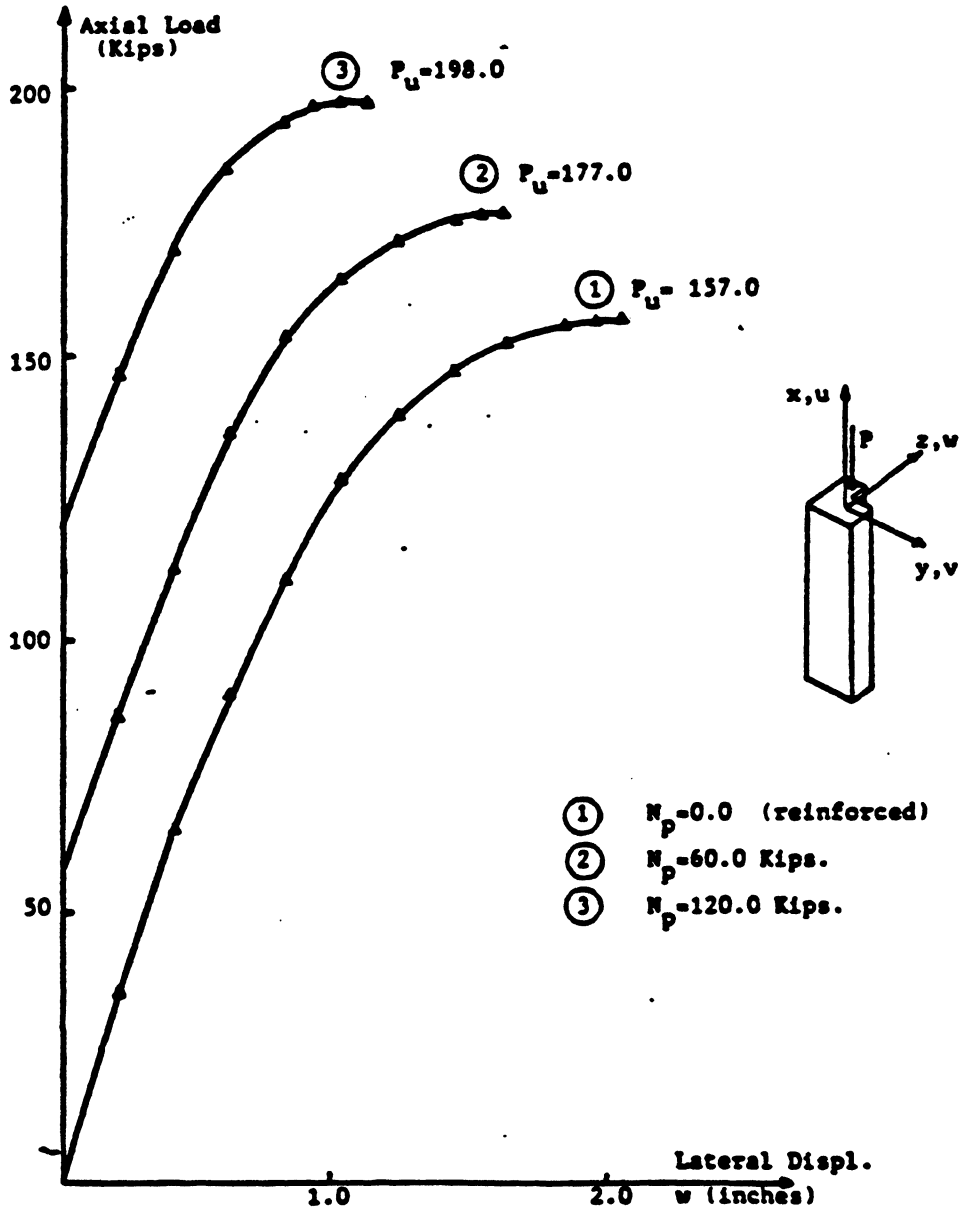

Fig. 7.6 Biaxial Bending of a Prestressed Concrete Column with Irregular Cross Section. Axial Load vs. Displacement.

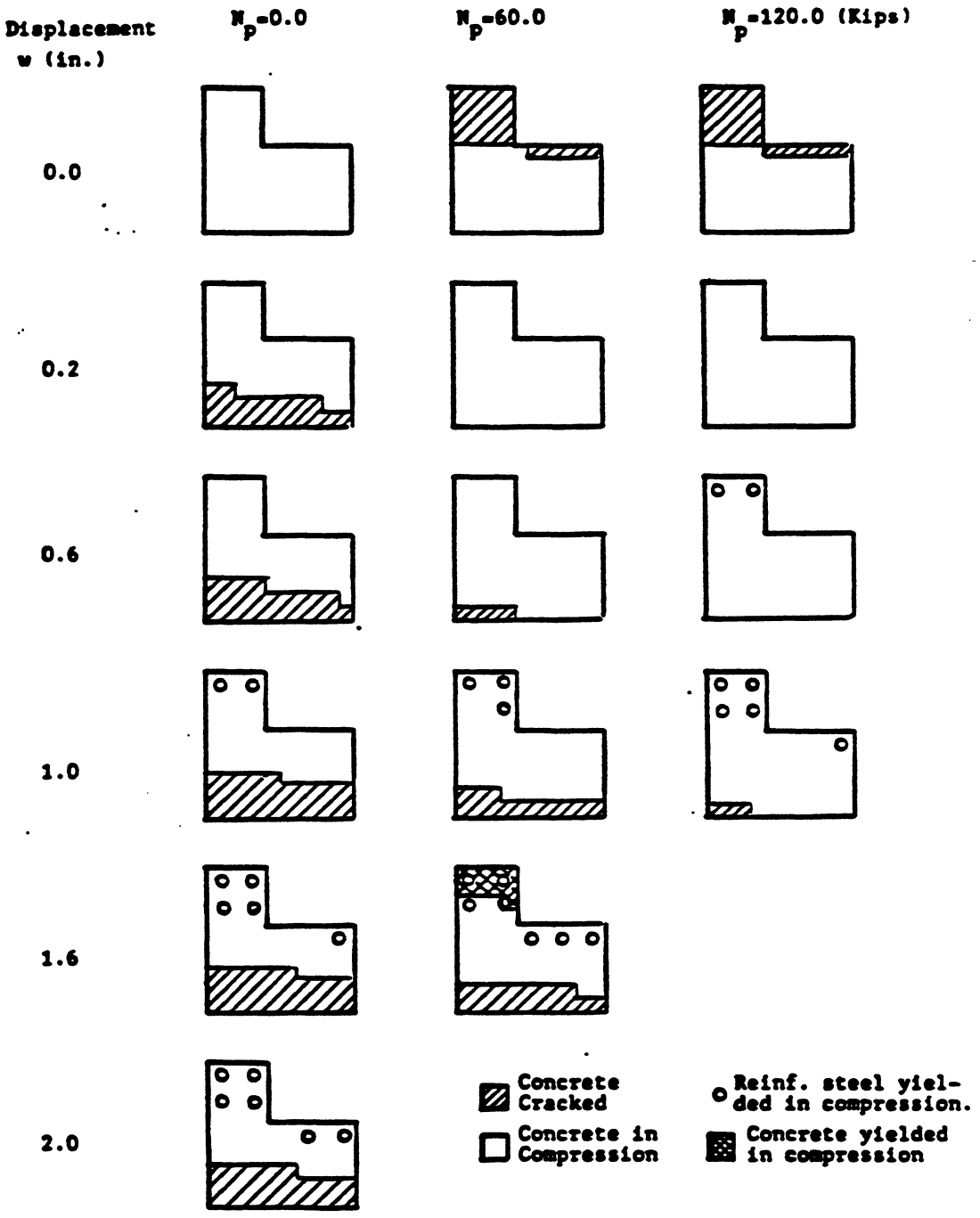

Fig. 7.7 Biaxial Bending of Reinforced and Prestressed Concrete Columns with Irregular Cross Section. Crack Patterns and Material State at the Base Section.

The geometry, reinforcement and prestressing arrangement and material properties are shown in figure 7.5.

The cross section is divided into a grid of 10 x 10 layers, having a total number of 76 concrete filaments. Again displacement control has been used to obtain the structural response. An eccentric axial load is applied at the top of the column up to failure. The load-displacement curve for the three columns is shown in figure 7.5. From these curves several remarks can be made:

1. The higher the prestressing force is, the higher load capacity the column has for this particular case.
2. The prestressed columns are stiffer than the reinforced one. Stiffness of the columns also increases with the increasing of prestressing force.
3. Instability failure occurs in the three cases. The total lateral displacement at the top of the column at failure decreases for the columns with higher prestressing forces.

This example differs essentially from the example presented in section 7.3 in that the cross sectional shape is different, and in the fact that prestressing tendons are placed in the tensile zone. The effect of prestressing in this case is very favorable because it increases substantially the stiffness of the column by reducing cracking due to external loads. In addition, prestressing does not consume in this case the compression capacity of any filament because it is placed at the tensile zone. For the same reason the tangent modulus of the compressed concrete filaments is not reduced by the prestressing

stresses. Prestressed columns 2 and 3 have negative lateral displacements v and w when only prestressing is applied. This explaines the fact that curves 2 and 3 do not pass through the origin 0 in figure 7.6. The progressive crack patterns are shown, for this example, in figure 7.7. It can be seen that when only prestressing is applied, columns 2 and 3 cracked in the upper side of the cross section. The reduction of cracking by prestressing when external load is applied can easily be seen in figure 7.7.

The maximum value of the torsional moment induced by the axial rotation of the cross section and nonlinear geometry effects is 544 in-lb.

7.5 Three-dimensional reinforced concrete frame

The objective of the present example is to show the capability of the program to analyse three dimensional concrete frames, including the torsional behaviour and to study the influence of the amount of reinforcing steel on the nonlinear behaviour of the structure. For this purpose a simple hypothetic three dimensional reinforcing concrete frame has been analysed taking into account the material nonlinearity only. The geometry of the frame, reinforcement arrangements for both cases, loading of the structure and material properties are shown in figure 7.8. Every member of the structure is divided into several equal sized beam elements of 1 m. of length.

Due to the geometry of the structure (three dimensional), the

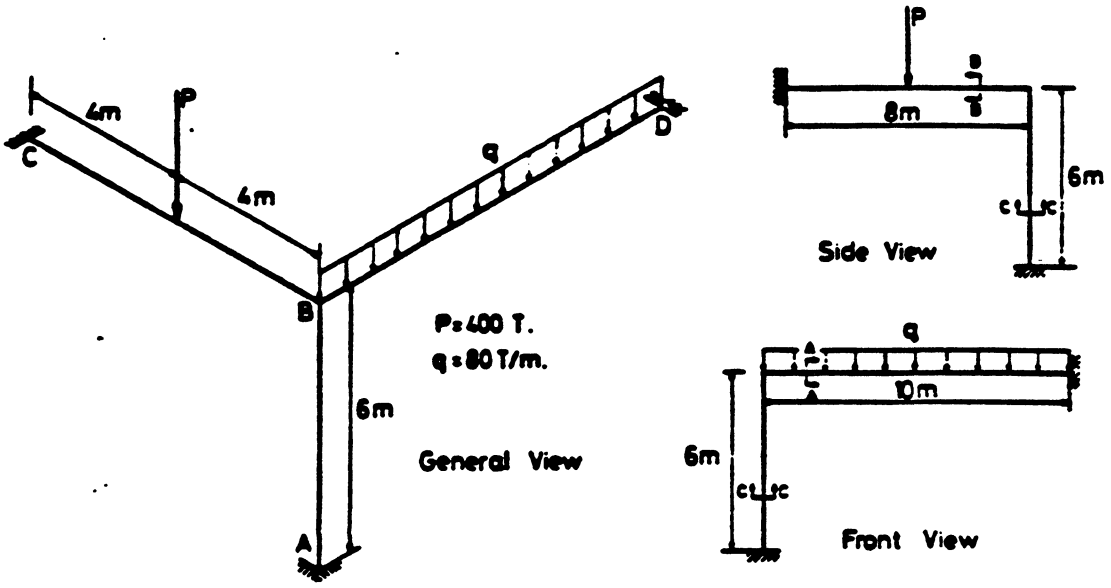

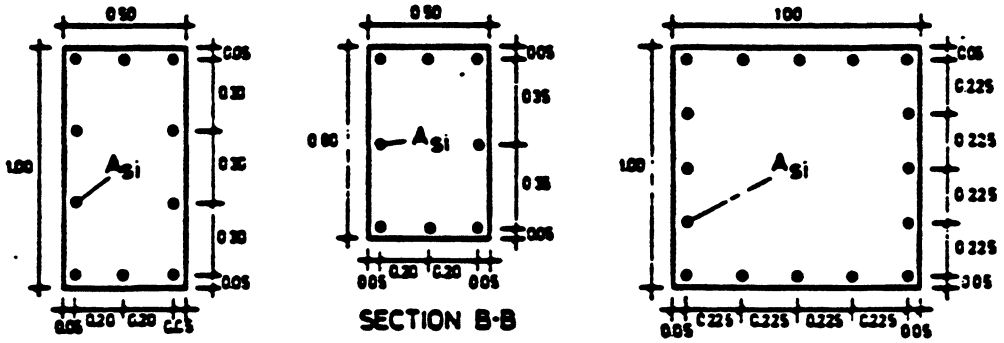

CONCRETE MATERIAL

$E_o = 3.5 \cdot 10^6$ T/m²

$f'_c = 3000$ T/m²

$f'_t = 400$ T/m²

$\epsilon_{cu} = -0.0038$

STEEL MATERIAL

$E_s = 2.1 \cdot 10^8$ T/m²

$E_s = 1.2 \cdot 10^6$ T/m²

$f_y = 50000$ T/m²

$\epsilon_{su} = 0.2$

AMOUNT OF STEEL (m^2)

SECTION	CASE 1		CASE 2	
	A_{si}	A_{stot}	A_{si}	A_{stot}
A-A	0.0008	0.008	0.0025	0.025
B-B	0.0008	0.0064	0.0025	0.02
C-C	0.0008	0.0128	0.0025	0.04

Fig. 7.8. Three Dimensional Reinforced Concrete Frame. Geometry, Loading and Material Properties. (Ex.7.5)

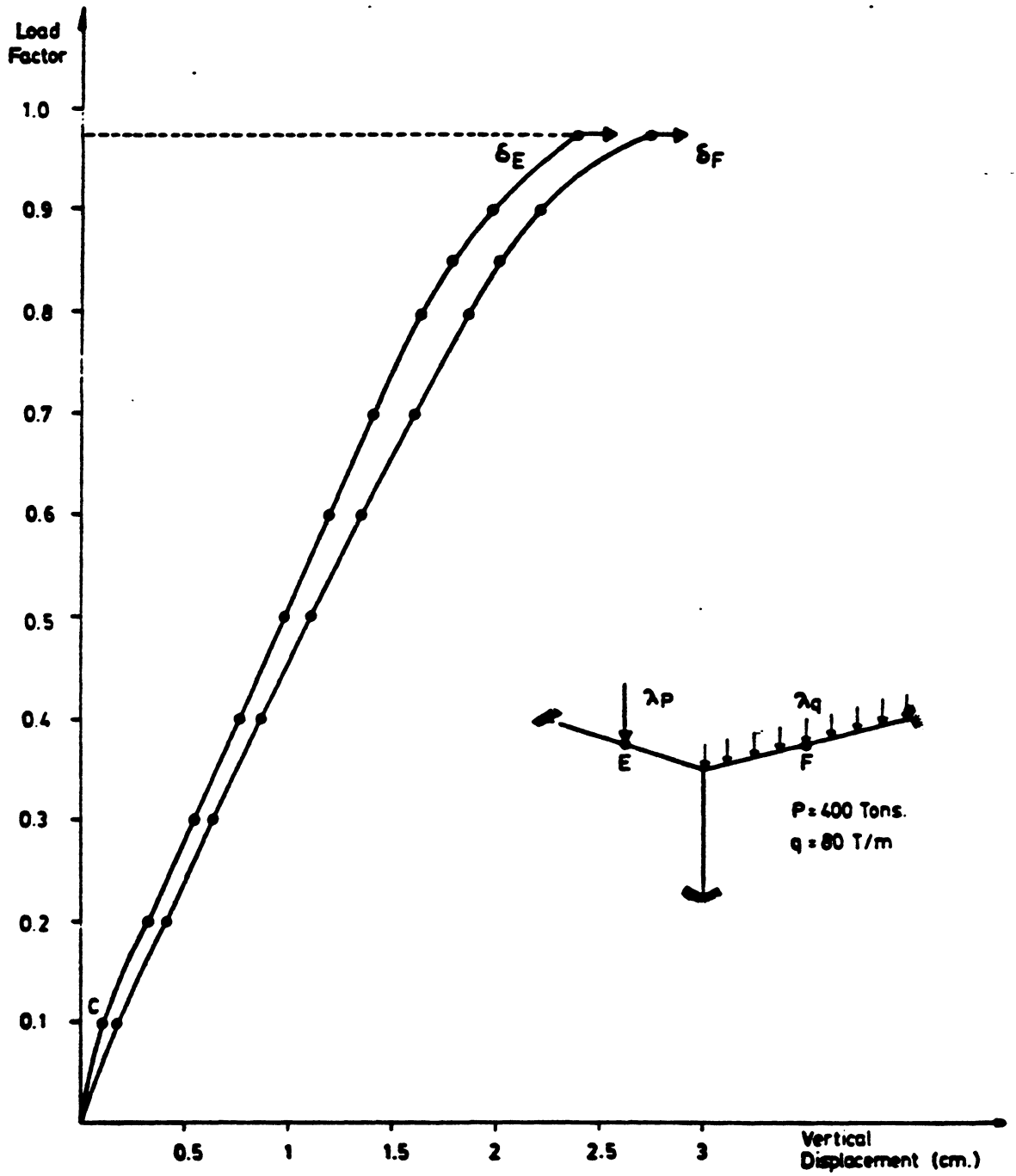

Fig. 7.9 Three Dimensional Concrete Frame (Example 7.5).
Load - Displacement curve.

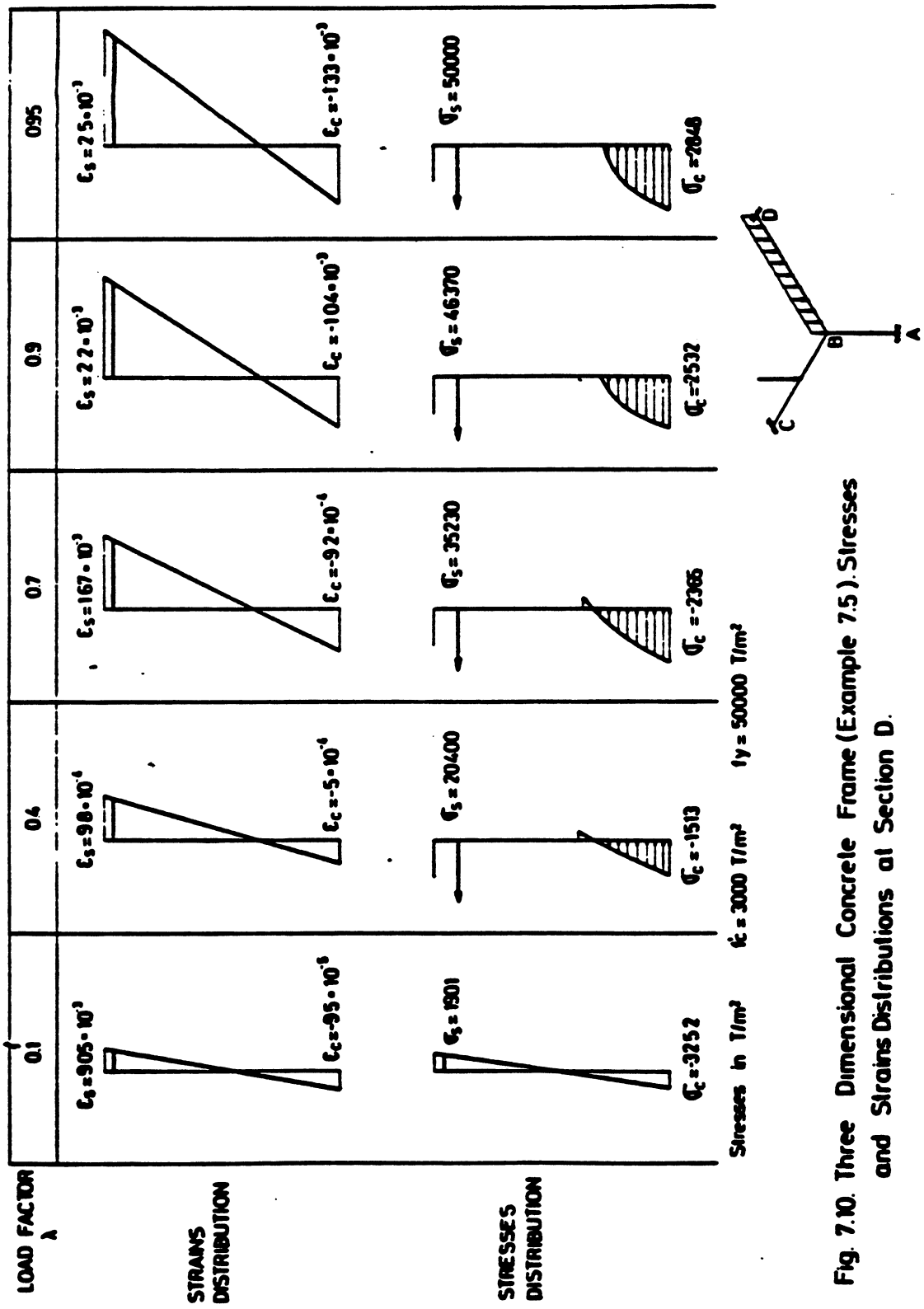

Fig. 7.10. Three Dimensional Concrete Frame (Example 7.5). Stresses and Strains Distributions at Section D.

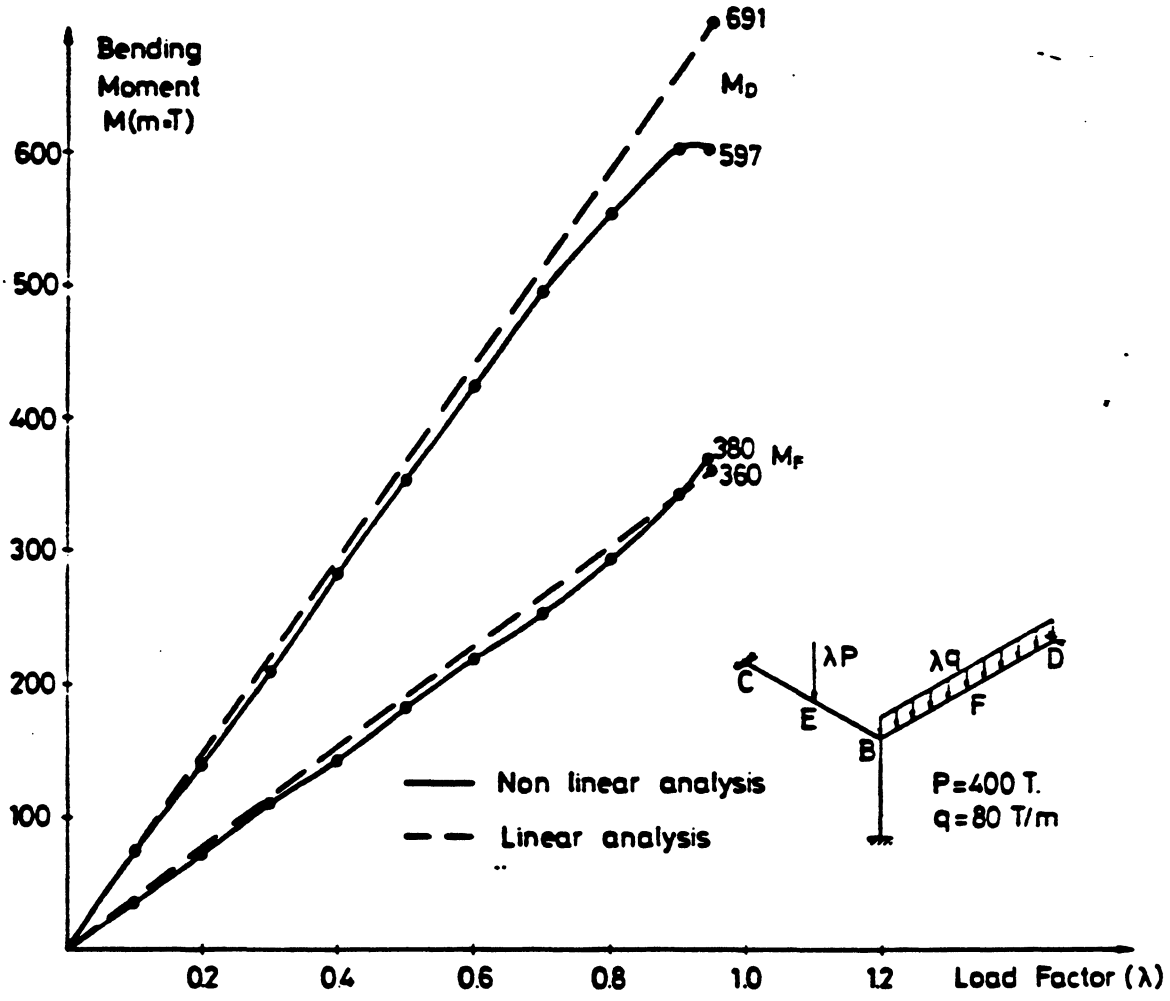

Fig. 7.11. Three Dimensional Concrete Frame (Example 7.5. Case 2). Evolution of Bending Moments at sections F and D.

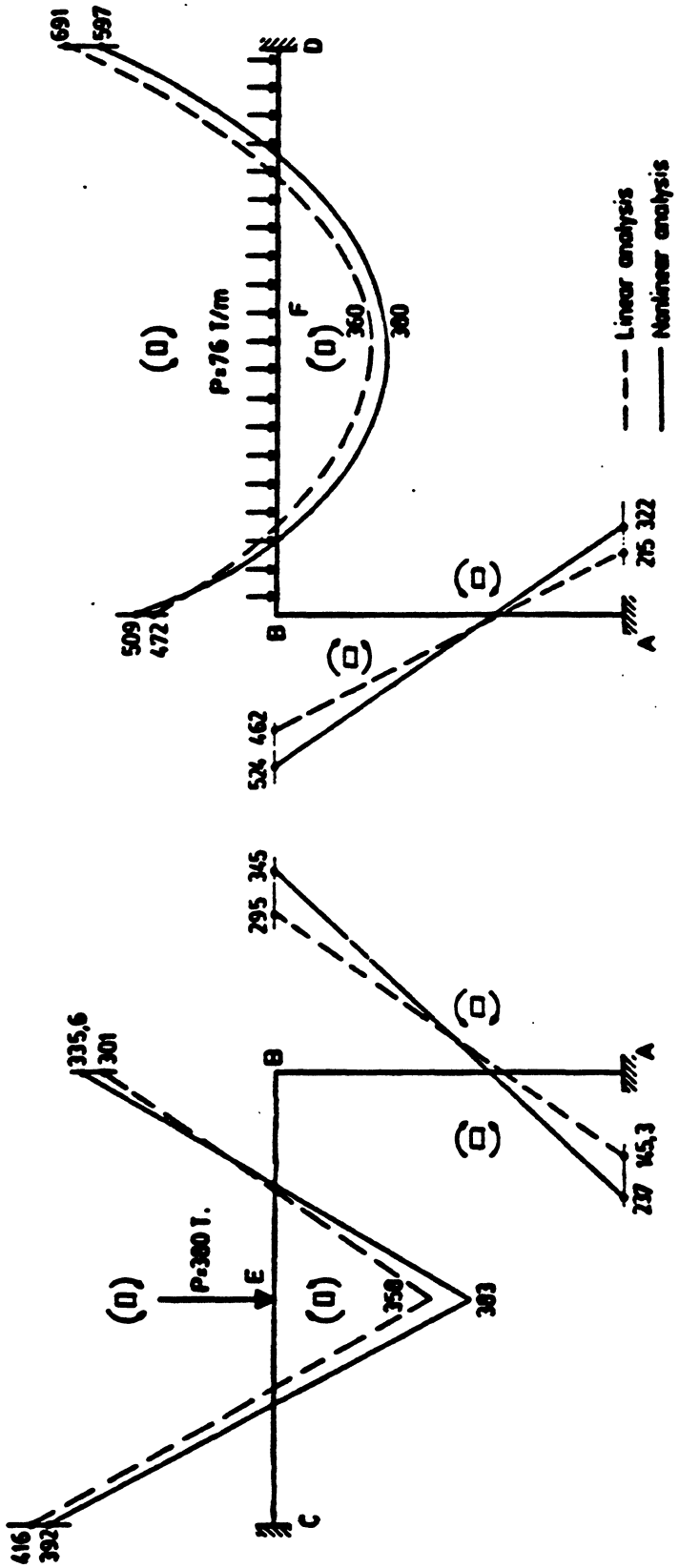

Fig. 7.12 Three Dimensional Concrete Frame (Example 7.5). Bending Moments Distribution. (Moments in txm.)

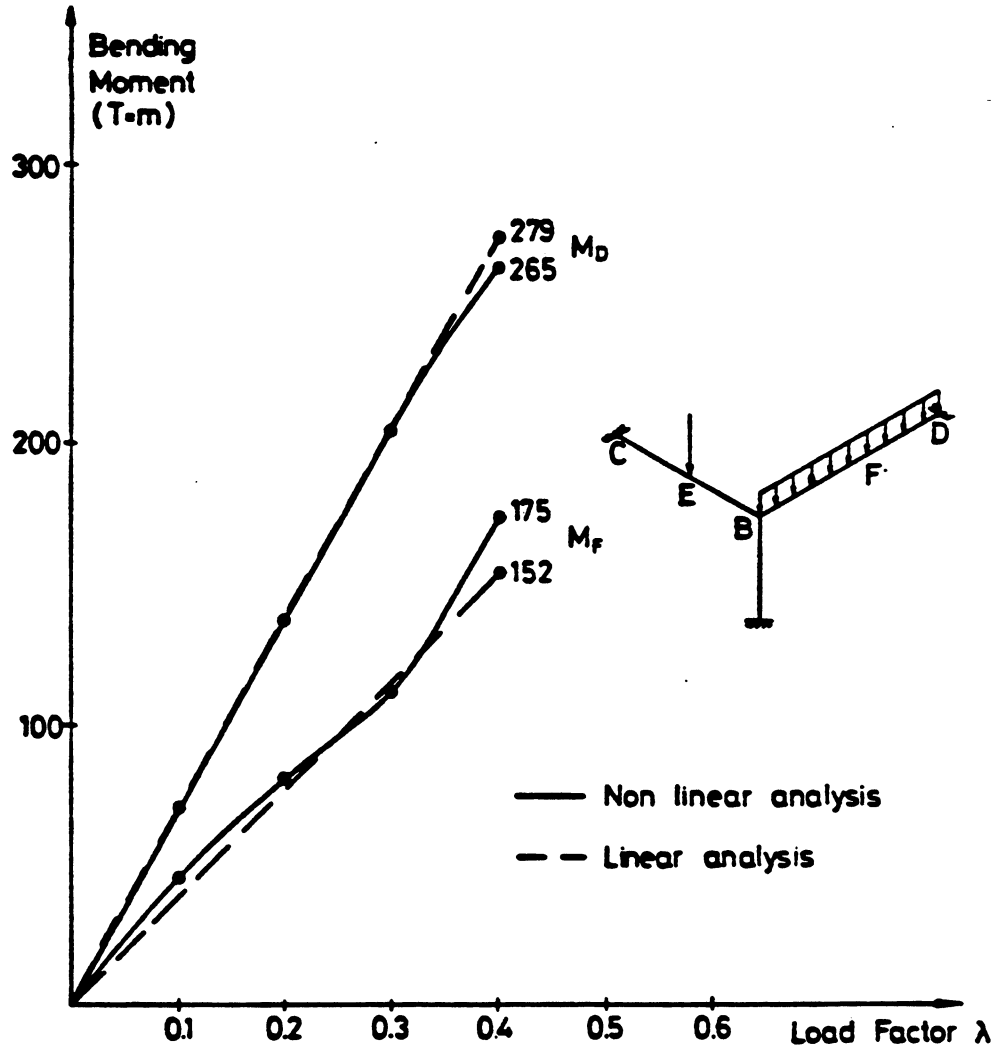

Fig. 7.13. Three Dimensional Concrete Frame (Example 7.5.Case 1). Bending Moments Evolution for Low Amount of Steel.

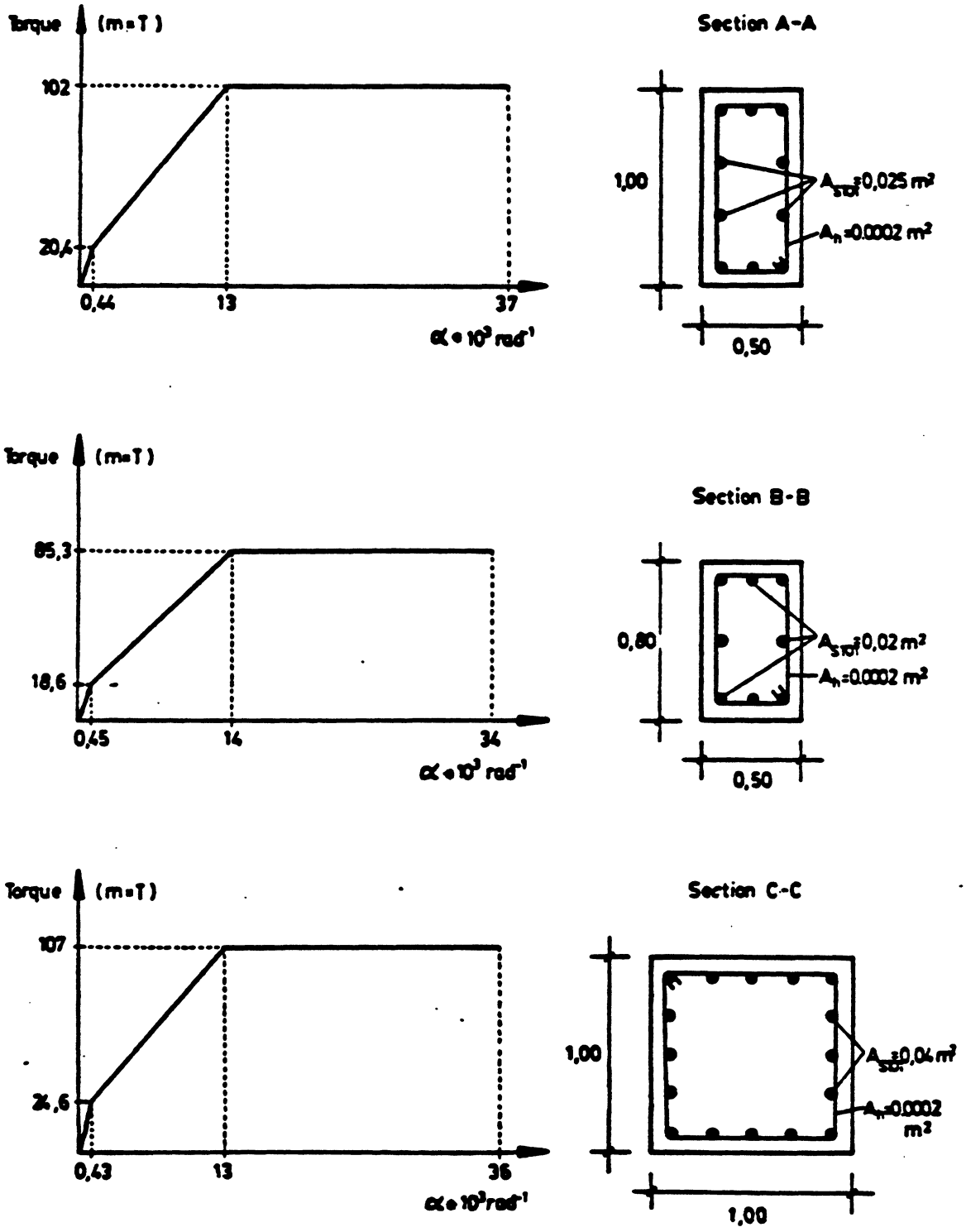

Fig 7.14 Torque-Twist relations hips for members of example 7.5, Case 2.

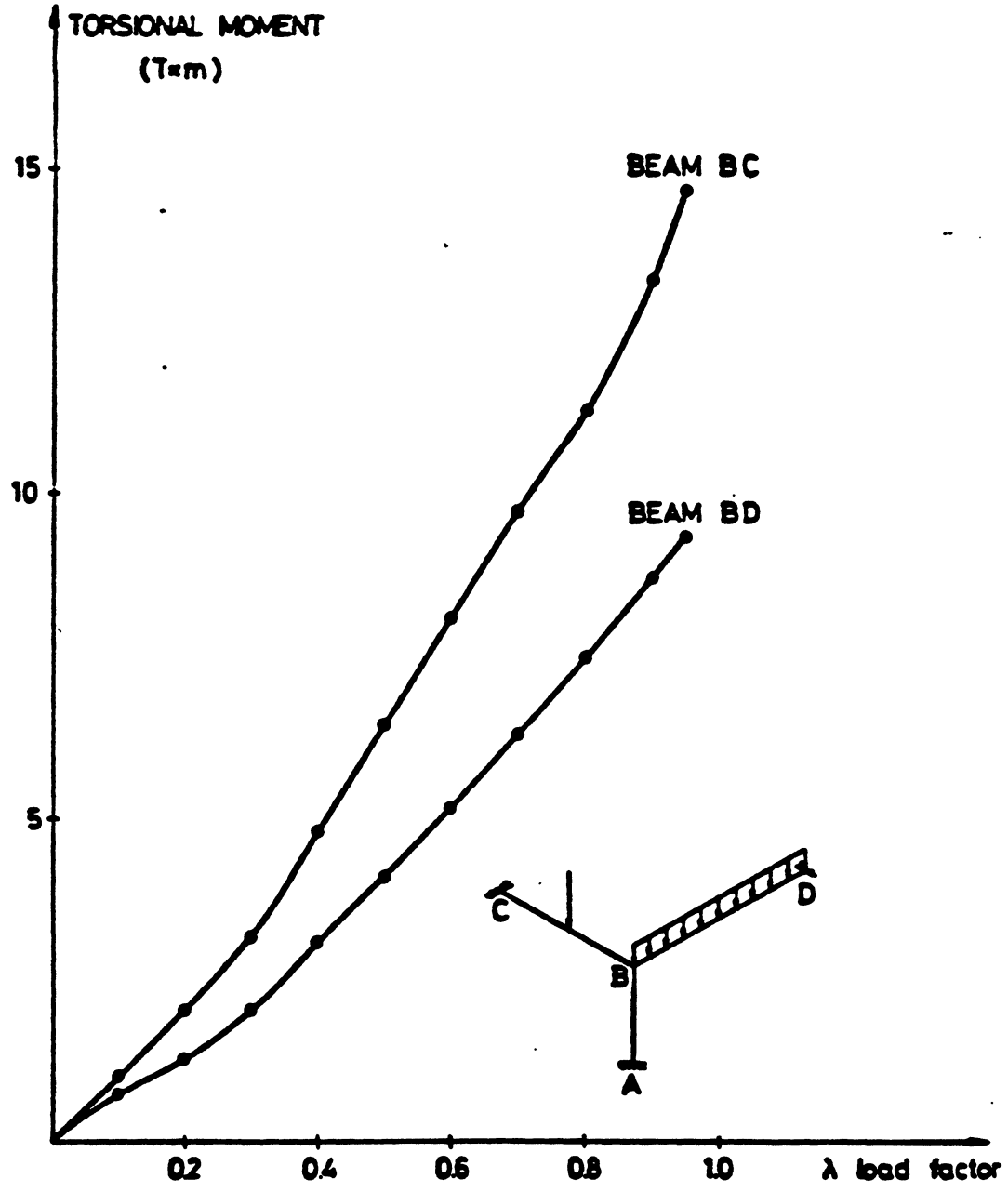

Fig. 7.15. Three Dimensional Concrete Frame (Example 7.5.Case 2). Evolution of Torsional Moments in Beams BC and CD.

kind of loading and the kind of analysis performed (only material nonlinearity), the beams are subjected to uniaxial bending and torsion, while the column is subjected to iaxial bending and torsion. For this reason the cross section of the girders are divided into a number of horizontal layers and the column cross section is divided into filaments. For the analysis of the structure, load control has been used up to the structure failure.

The load-displacement curve for the second structure is plotted in figure 7.9, where the cracking point C and the postcracking behavior (linear) of the structure can be clearly seen.

The progressive stress and strain distributions at section D are shown in figure 7.10 for several values of the load factor for the second structure analysed (higher amount of steel).

The evolution of the bending moments in the two critical sections of girder BD are shown in figure 7.11 and the final moment distribution for all the structure is shown in figure 7.12, where the linear elastic solution is also shown.

Similar results to those of figure 7.11 are presented in fig. 7.13 for the structure with the lowest amount of steel. Comparing both cases it can be seen that the moment resistribution at section D is about 5% in structure 1 and 15.75% in structure 2, while at section F, the redistributions are 15.1% for case 1 and 5% for case 2.

The torque-twist relationship of the elements are shown in figure no 7.14 for structure n 2, and the evolution of torsional moments in both girders, with the increment of load is shown in figure no 7.15. The column is subjected to a maximum torsional moment of 0.042 T×m.

8 COMPUTER PROGRAM

8.1 General Remarks

The program PCF3D is a nonlinear finite element analysis program for reinforced and prestressed three dimensional concrete frames, taking into account geometric and material nonlinearities, and the time dependent effects of load history, temperature history, creep, shrinkage and aging of concrete and relaxation of prestressing steel.

The program has been written in FORTRAN IV language, and has been developed at the IBM 4341 computer of the University of California at Berkeley.

8.2 General structure of the program and features of each subroutine

The program is composed of a main subroutine that distributes the flow to seven other subprograms, each of which can be composed by several subroutines. The architecture of the program is shown in figure 8.1, where the relationship among the subroutines is indicated.

The features of each subroutine are as follows:

MAIN Program — Distributes the flow over different main subroutines. Initializes vectors and matrices. Performs the nonlinear strategies and checks convergence and serviceability criteria.

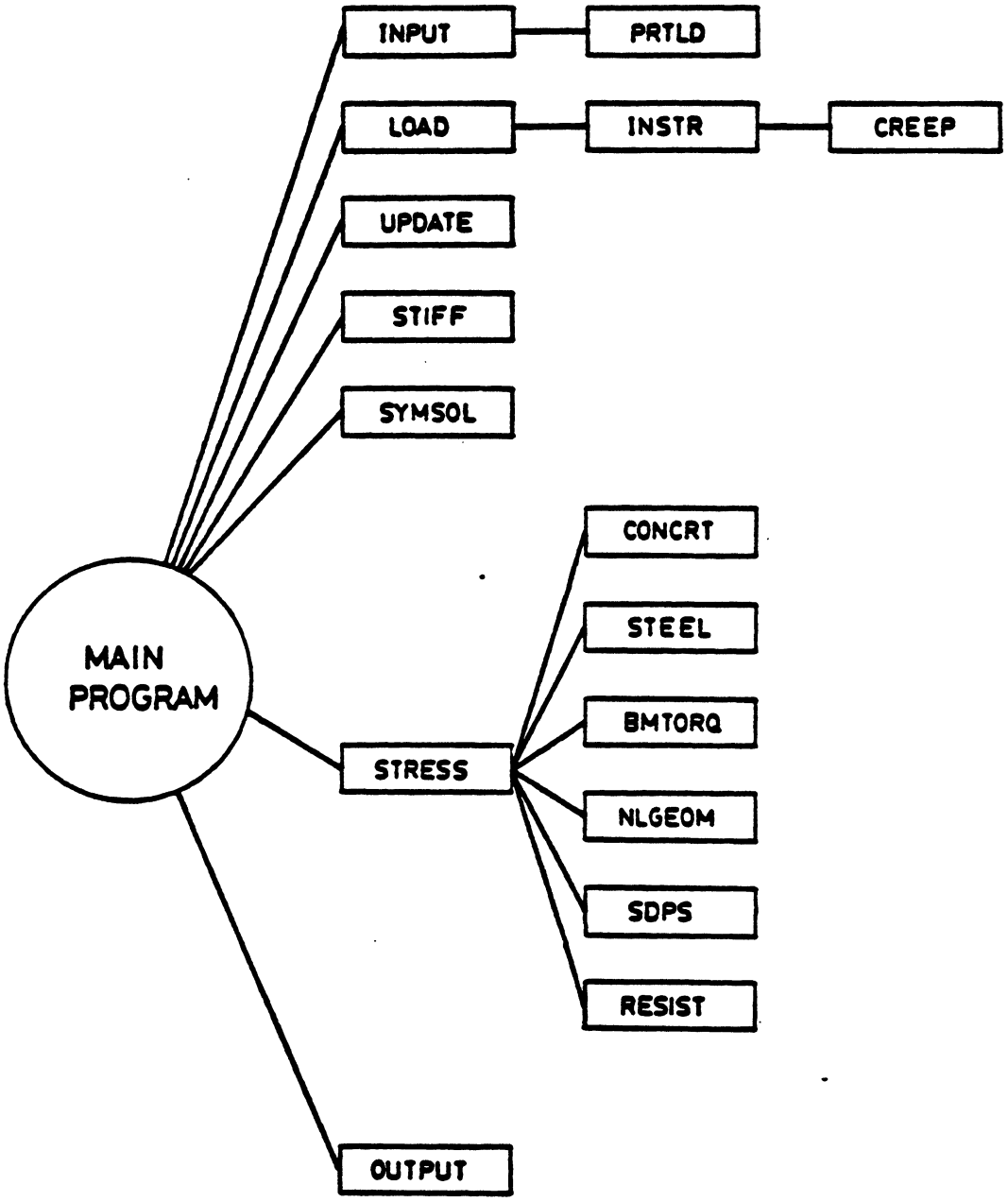

Fig. 8.1 Architecture of Program PCF3D

Subroutine INPUT	Reads input data that do not depend on time steps, load steps or iterative procedure, such as initial geometry of the structure, initial material properties, prestressing information, etc.
Subroutine PRTLD	Obtains the equivalent joint load vector due to prestressing at transfer, taking into account prestressing losses due to friction, anchorage slip, etc.
Subroutine LOAD	Inputs data corresponding to each time step, such as joint loads, material properties, load factors, nonlinear strategy to follow at the current time step. Calculates the fictitious forces due to imposed displacements at supports.
Subroutine INSTR	Obtains non-mechanical strains due to temperature variation, shrinkage and aging of concrete and relaxation of prestressing steel. Calls subroutine CREEP to obtain initial creep strain and then forms the initial strain load vector.
Subroutine CREEP	Obtains the non-mechanical strain due to creep of concrete.
Subroutine UPDATE	For each load step accumulates external joint loads, initial strain load vector and load factors.

Subroutine STIFF	Forms the element stiffness matrix, performs the static condensation, transforms to global coordinates, assembles global structural matrix and checks for structural failure.
Subroutine SYMSOL	In core banded equation solver. Obtains increments of displacements in global coordinates. Checks for singularity of the stiffness matrix. SYMSOL (1) triangularizes the newly formed stiffness matrix, while SYMSOL (2) uses the already triangularized and stored stiffness matrix.
Subroutine STRESS	Transforms global displacement increments to local element axes, updates nodal coordinates, obtains element strains, support reactions and unbalanced load vector.
Subroutine CONCRT	Obtains stresses in concrete filaments, from the stress-strain relationship. Performs state determination.
Subroutine STEEL	Obtains stresses in reinforcing steel from the stress-strain relationship. Performs state determination.
Subroutine SDPS	Obtains new length of prestressing segments, stresses and prestressing segments forces. Performs state determination.

Subroutine BMTORQ Obtains torque in the beam element, from the tri-linear torque-twist relationship.

Subroutine NLGEOM Updates element orientation matrix for large displacement analysis.

Subroutine RESIST Obtains internal resisting load vector for each element by adding the contribution of concrete, reinforcing and prestressing steel. Assembles for the whole structure.

Subroutine OUTPUT Prints results. The following information can be printed: joint displacements, support reactions, unbalanced load vector, strains, stresses and material state number for each concrete and reinforcing steel filament, element internal forces at each Gauss point, strains, stresses and forces at each prestressing steel segment.

8.3 Flow Chart

The flow chart diagram of the computer program PCF3D is the one shown in figure 8.2. The variables in the flow chart are defined as follows:

ITIME Time step counter.

NTIME Number of time steps.

LST Load step counter.

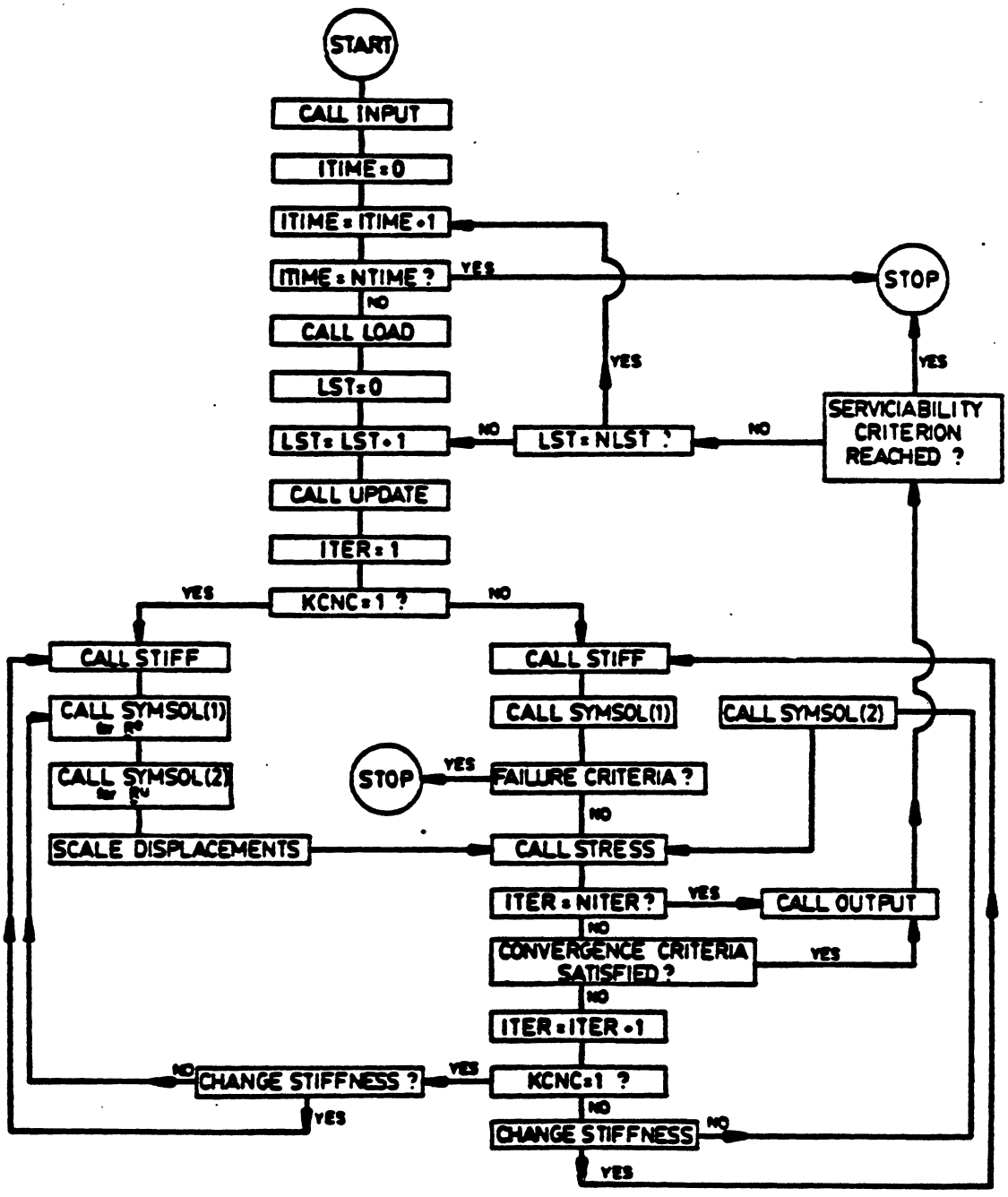

Fig. 8.2 Flow Chart Diagram of Computer Program PCF3D.

NLST Number of load steps for the current time step.

ITER Iteration counter.

NITER Maximum number of iterations allowed.

KCNT Code of nonlinear strategy adopted in the current time step. If KCNT = 1, displacement control. If KCNT = 0, load control.

8.4 Additional comments about the features and organization of the program

8.4.1 Types of analysis that can be performed

The structure can be analyzed with program PCF3D according to four different approaches. These are:

1. Linear-elastic analysis.
2. Nonlinear-material, small displacements.
3. Elastic material, large displacements.
4. Nonlinear material and geometry.
5. Any of the above posibilities with time dependent analysis.

8.4.2 Structural loading conditions

The external loads are assumed to be applied only at the joints. Distributed loads may be converted into equivalent joint loads either by the consistent load method or a lumped formulation. Imposed displacements and rotations can be applied at the supported joints.

Temperature and shrinkage distributions considered are: constant values for all the elements in the structure, different value for each element (but constant over the cross section), and planar variation for each element. This option is performed by specifying the values of the temperature or shrinkage strain, at three arbitrary points in the section boundary, together with the coordinates, in local element system, of these three points.

When incremental analysis is performed (with or without equilibrium iterations) different load factors for each load step are specified for external loads, initial strain load vector and controlled displacement, respectively.

8.4.3 Nonlinear strategies

Two different nonlinear solution schemes can be selected:

- Load control (for each load step iterations are performed with constant level of the external load). This procedure is the most usual, and is utilized to obtain the maximum load that the structure can carry.
- Displacement control (for each load step, the iterations are performed by varying the external load level and keeping the given value of the displacement controlled). This technique is used when post-buckling behaviour of a structure is to be studied.

8.4.4 Uniaxial or biaxial bending

The program has the capability of analysing planar frames with symmetric cross sections, subjected to uniaxial bending, as a particular case of a 3-D frame. For these cases the amount of storage and computer time necessary to solve a problem is much less than in a general 3-D case. Then, the cross section can be divided into layers, parallel to the y local axes, instead of filaments.

8.4.5 Data management. Intermediate variables

The number of variables to be stored in order to perform a nonlinear time dependent analysis of a reinforced or prestressed concrete frame is enormous. In the case of three dimensional concrete frames, in addition to the variables associated with joints (loads, displacements, etc.) a number of variables related to the filaments must be stored. These variables can be mechanical, nonmechanical and total strains, stresses, etc. For every concrete and steel filament, calculated at every Gauss point in every element. In order to reduce the amount of central memory occupied by these variables, out of core storage is used for the variables associated to the concrete and steel filaments.

8.5 PCF3D INPUT DATA FORMAT

1. TITLE (20A4) - 1 line

Col. 1 - 80	TITLE	Title of the problem

2. CONTROL INFORMATION (10I5,3F10.0) - One line

Col. 1 - 5	NJ	Number of joints
Col. 6 - 10	NSJ	Number of supported joints
Col. 11 - 15	NM	Number of elements
Col. 16 - 20	NSEC	Number of different types of cross sections.
Col. 21 - 25	NSTOR	Number of different torsional models.
Col. 26 - 30	IPB	Type of bending problem: IPB = 0 Biaxial bending IPB = 1 Uniaxial bending
Col. 31 - 35	NCNC	Number of different concretes
Col. 36 - 40	NSNS	Number of different reinforcing steel materials.
Col. 41 - 45	KPRT	Prestressing code: KPRT = 0 There is no prestressing KPRT = 1 There is prestressing
Col. 46 - 50	KCNC	Input code for material properties: KCNC = 1 Input ACI parameters KCNC = 2 Input experimental results
Col. 51 - 60	AGE	Age of concrete in days at time of initial loading

Col. 61 - 70	TZERO	Reference temperature (in centigrade degrees)
Col. 71 - 80	ALPHA	Coefficient of thermal expansion, (constant and equal for steel and concrete)

3. NODAL COORDINATES (I5,3F10.0) - One line per each node

Col. 1 - 5	I	Joint number
Col. 6 - 15	X(I)	X - Coordinate in globals
Col. 16 - 25	Y(I)	Y - Coordinate in globals
Col. 26 - 35	Z(I)	Z - Coordinate in globals

4. SUPPORT ORIENTATION MATRIX (I8,9F8.0) - One line per each supported joint

Col. 1 - 8	I	Supported joint number
Col. 9 - 16	XS(1)	X - Coordinate for auxiliary node in spring 1
Col. 17 - 24	YS(1)	Y - Coordinate for auxiliary node in spring 1
Col. 25 - 32	ZS(1)	Z - Coordinate for auxiliary node in spring 1
Col. 33 - 40	XS(2)	X - Coordinate for auxiliary node in spring 2
Col. 41 - 48	YS(2)	Y - Coordinate for auxiliary node in spring 2
Col. 49 - 56	ZS(2)	Z - Coordinate for auxiliary node in spring 2

Col. 57 - 64	XS(3)	X - Coordinate for auxiliary node in spring 3
Col. 65 - 72	YS(3)	Y - Coordinate for auxiliary node in spring 3
Col. 73 - 80	ZS(3)	Z - Coordinate for auxiliary node in spring 3

5. SPRING CONSTANTS (I5,6E10.0) - One line per each supported node

Col. 1 - 5	NS(I)	Supported joint number
Col. 6 - 65	SP(I,J)	Value of the spring constants at node I, J = 1,6

6. CROSS SECTION DATA - One set of lines per each different cross section

6.1 General Data (5I5,5F10.0) - One line

Col. 1 - 5	ISEC	Section type number
Col. 6 - 10	NCLY(I)	Number of concrete layers normal to y - axis
Col. 11- 15	NCLZ(I)	Number of concrete layers normal to z - axis
Col. 16 - 20	NFS(I)	Number of reinforcing steel filaments
Col. 21 - 25	NFB(I)	Number of rows of $\underset{\sim}{C}$ matrix used to define the cross section shape ($\underset{\sim}{C}$ matrix is called IB in the program).

Col. 26 - 35	YMP(I)	Maximum positive distance from center of reference to the circumscribed rectangle, in Y direction
Col. 36 - 45	ZMP(I)	Maximum positive distance from center of reference to the circumscribed rectangle, in Z direction
Col. 46 - 55	YMN(I)	Maximum negative distance from center of reference to the circumscribed rectangle, in Y direction
Col. 56 - 65	ZMN(I)	Maximum negative distance from center of reference to the circumscribed rectangle, in Z direction
Col. 66 - 75	RTJ(I)	Torsional stiffness constant

6.2 Matrix for the definition of the cross section shape (3I5)

One line for each row of the IB matrix.

Col. 1 - 5	IB(I,J,1)	Number of current physical layer
Col. 6 - 10	IB(I,J,2)	Column in which concrete starts
Col. 11 - 15	IB(I,J,3)	Column in which concrete ends.
Col. 16 - 20	IB(I,J,4)	Material code for the current layer

6.3 Definition of the steel filaments geometry (3F10.0)

One line for each steel filament. Skip if NFS(I) = 0

Col. 1 - 10	AS(I,J)	Steel area of filament J in section type I
Col. 11 - 20	ESY(I,J)	Y - eccentricity of filament J
Col. 21 - 30	ESZ(I,J)	Z - eccentricity of filament J

7. TORSIONAL PROPERTIES (5E10.0) - One line for each torsional model

Col. 1 - 10	TCR(I)	Torque at first cracking
Col. 11 - 20	TYP(I)	Torque at first yielding
Col. 21 - 30	ACR(I)	Twist at first cracking
Col. 31 - 40	AYP(I)	Twist at first yielding
Col. 41 - 50	AUL(I)	Ultimate twist

8. MEMBER DATA (6I5,3F10.0) - One line per element

Col. 1 - 5	L	Element number
Col. 6 - 10	NODI(L)	Node at I end
Col. 11 - 15	NODJ(L)	Node at J end
Col. 16 - 20	MESC(L)	Cross section type of the current element
Col. 26 - 30	KTO(L)	Torsional behaviour model of this element
Col. 31 - 40	XA(L)	Global X coordinate of orientation auxiliary node

Col. 41 - 50	YA(L)	Global Y coordinate of orientation auxiliary node
Col. 51 - 60	ZA(L)	Global Z coordinate of orientation auxiliary node

9. PRESTRESSING DATA (skip if KPRT = 0)

9.1 Control information (4I5,4F10.0) - One line

Col. 1 - 5	ITRANS	Time step when prestressing is transferred
Col. 6 - 10	NTEND	Number of tendons
Col. 11 - 16	NPS	Number of prestressing segments
Col. 16 - 20	NPT	Number of points used to define stress-strain curve of prestressing steel
Col. 21 - 30	FPSY	0.1% Offset yield stress of prestressing steel
Col. 31 - 40	ROZR	Wobble friction coefficient
Col. 41 - 50	ROZC	Curvature friction coefficient
Col. 51 - 60	CRPS	Coefficient for the relaxation loss. Use CRPS = 10 for ordinary prestressing steel.

9.2 Stress-strain curve for prestressing steel. (10E8.0)

One line

Col. 1 - 80	PSF(I)	Stress of point I
	PSE(I)	Strain of point I (I = 1,NPT, NPT<=5)

9.3 Tendon information (4I5,4F10.0) - One line for each tendon

Col. 1 - 5	I	Tendon number
Col. 6 - 10	NIN(I)	Number of element in which tendon starts
Col. 11 - 15	NFN(I)	Number of element in which tendon ends
Col. 16 - 20	INDP(I)	Jacking code: INDP(I) = 1 Jacking from I end INDP(I) = 2 Jacking from J end INDP(I) = 3 Jacking from both ends
Col. 21 - 30	AREAT(I)	Steel area of tendon I
Col. 31 - 40	PAI(I)	End force when jacking from I end
Col. 41 - 50	PAJ(I)	End force when jacking from J end
Col. 51 - 60	DESL(I)	Anchorage slip

9.4 Prestressing segment data (3I5,4F10.0) - One line for each segment

Col. 1 - 5	I	Segment number
Col. 6 - 10	MPS(I)	Element in which this segment is embedded
Col. 11 - 15	NTPS(I)	Prestressing tendon to which the segment belongs
Col. 16 - 25	EY1(I)	Y eccentricity of segment at I end
Col. 26 - 35	EZ1(I)	Z eccentricity of segment at I end
Col. 36 - 45	EY2(I)	Y eccentricity of segment at J end
Col. 46 - 51	EZ2(I)	Z eccentricity of segment at J end

NOTE: These eccentricities are in element local coordinate

10. MATERIAL PROPERTIES

10.1 Concrete properties

ACI Properties (KCNC = 1) (9F10.0) - One line per each different concrete

Col. 1 - 10	FPC28(K)	28 day strength in psi (enter with negative sign)
Col. 11 - 20	WGT(K)	Weight per unit volume in lb/cu.ft.
Col. 21 - 30	ACNC(K)	Coefficient "a" to compute $f'_c(t)$
Col. 31 - 40	BCNC(K)	Coefficient "b" to compute $f'_c(t)$
Col. 41 - 50	RCMP(K)	Ratio r_c in $f''_c = r_c.f'_c$
Col. 51 - 60	RTNS(K)	Ratio r_t in $f'_t = rt\sqrt{w.f'_c}$
Col. 61 - 70	RCRP1(K)	Ratio $r_1 = f''_c/\sigma$ up to which $\sigma_e = \sigma$ in creep calculation (usually = 0.35)
Col. 71 - 80	RCRP2(K)	Ratio $r_2 = \sigma_e/\sigma$ when $\sigma = f''_c$ in creep calculation (usually = 1.865)
Col. 81 - 90	ECU(K)	Ultimate compressive strain. Enter with negative sign.

Test Results (KCNC = 2) (2E10.0,5F10.0) - One line per each different concrete

Col. 1 - 10	ECI(K)	Initial modulus at the age of initial loading
Col. 11 - 20	G(K)	Shear modulus at the age of initial loading
Col. 21 - 30	FCDP(K)	Compressive strength f''_c. Enter with negative sign.

Col. 31 - 40	FTP(K)	Tensile strength
Col. 41 - 50	ECU(K)	Ultimate compressive strain (negative)
Col. 51 - 60	RCRP1(K)	Ratio $r_1 = f''_c/\sigma$ up to which $\sigma_e = \sigma$ in creep calculation (usually = 0.35)
Col. 61 - 70	RCRP2(K)	Ratio $r_2 = \sigma_e/\sigma$ when $\sigma = f''_c$ in creep calculation (usually = 1.865)

10.2 Steel Properties (2E10.0,2F10.0) - One card for each different steel

Skip if NSNS = 0

Col. 1 - 10	ES1(K)	First Modulus
Col. 11 - 20	ES2(K)	Second Modulus
Col. 21 - 30	FSY(K)	Yielding stress
Col. 31 - 40	ESU(K)	Ultimate strain

11. STRUCTURAL ANALYSIS CONTROL DATA. (9I5) - One line (*)

Col. 1 - 5	NTIME	Number of time steps
Col. 6 - 10	NITI	Number of iterations allowed for intermediate load steps
Col. 11 - 15	NITF	Number of iterations allowed for final load step
Col. 16 - 20	KOUT	Output code: if KOUT = 1 Output results after every iteration If KOUT = 0 Output results only at load steps.

(*) NOTE: If KPRT ≠ 0 (there is prestressing) it is convenient to use a specific time step for the introduction of prestressing force.

Col. 21 - 25	ITAN	Type of analysis code: If ITAN = 0 Linear analysis If ITAN = 1 Nonlinear material, small displacements If ITAN = 2 Nonlinear geometry, elastic material If ITAN = 3 Nonlinear material and geometry
Col. 26 - 30	KSTR	Stress output code. Number of elements in which the stresses are to be output
Col. 31 - 35	JRESP	Output code for intermediate values. Use JRESP = 0
Col. 36 - 40	KTEMP	Code for temperature effects: If KTEMP = 0 No temperature effects are considered If KTEMP = 1 Constant variation of temperature in all the structure If KTEMP = 2 Planar variation of temperature over the cross section, different for each element
Col. 41 - 45	KSHRNK	Code for shrinkage effects: If KSHRNK = 0 No shrinkage effects

If KSHRNK = 1 Constant shrinkage in the structure

If KSHRNK = 2 Planar variation for each element

12. ELEMENTS IN WHICH STRESSES ARE OUTPUT. (16I5)

Skip if KSTR = 0 (None element) or KSTR = NM (All elements)

Col. 1 - 80 KELEM(I) Element numbers. I = 1,KSTR

13. CONVERGENCE RATIO TOLERANCES. (7F10.0) - One line

Col. 1 - 10	TOLI	Displacement ratio tolerance for intermediate load steps
Col. 11 - 20	TOLF	Displacement ratio tolerance for final load step
Col. 21 - 30	TOLC	Displacement ratio tolerance for changing stiffness
Col. 31 - 40	TOLL	Maximum unbalanced load allowed
Col. 41 - 50	TOLM	Maximum unbalanced moment allowed
Col. 51 - 60	TOLD	Maximum allowable displacement
Col. 61 - 70	TOLR	Maximum allowable rotation

14. LOAD INFORMATION - One set of lines for each time step.

14.1 Control load information (7I5,F10.0) - One line

Col. 1 - 5	ITIME	Time step number
Col. 6 - 10	NLS	Number of load steps for the current time step
Col. 11 - 15	NLJ	Number of loaded joints

Col. 16 - 20	NDJ	Number of supported nodes with imposed displacements
Col. 21 - 25	KCNT	Nonlinear strategy code for the current time step: KCNT = 0 load control KCNT = 1 displacement control
Col. 26 - 30	NDC	Node with controlled displacement Use NDC=0 if KCNT=0
Col. 31 - 35	LDEG(*)	Controlled degree of freedom in node NDC. Use NDC=0 if KCNT=0
Col. 26 - 45	DDISP	Maximum value of controlled displacement. Use DDISP=0 if KCNT=0

14.2 Nodal loads in global coordinates. (I5,6F10.0) - One line

Skip if Number of loaded joints (NLJ) = 0

Col. 1 - 5	I	Loaded joint number
Col. 6 - 65	PLOAD(J)	Loads in global coordinates (J = 1,6) acting upon the joint J

14.3 Imposed displacements in global coordinates. (I5,6F10.0)

One line

Skip if there are no joints with imposed displacements (NDJ = 0)

Col. 1 - 5	NDI	Number of the node with imposed displacement

(*) NOTE: LDEG = 1, 6 depending of the dof controlled

for axial displacement (u)	LDEG=1
for transverse displacement (v)	LDEG=2
for transverse displacement (w)	LDEG=3
for rotation about x axis	LDEG=4
for rotation about x asis	LDEG=5
for rotation about z axis	LDEG=6

Col. 6 - 65 DES(NDI,J) Value of the imposed displacements for each of the six degrees of freedom (J = 1,6) of node number NDI

14.4 Load factors for load or displacement steps. (I5,3F10.0)

Provide one line for each load or displacement step in the current time step (*)

Col. 1 - 5	LS	Load step number
Col. 6 - 15	FLOAD(LS)	Factor for external loads
Col. 16 - 25	FINST(LS)	Factor for initial strain load
Col. 26 - 35	FDISP(LS)	Factor for controlled displacement This factor will scale the value of DDISP

14.5 Time increment (F10.0) - One line. Skip if ITIME = 1

Col. 1 - 10 DTIME Time increment, in days, for the current time interval.

14.6 Creep coefficients (3E10.0) - One line for each different concrete

Skip if ITIME = 1

Col. 1 - 30 XA1(M)
XA2(M)
XA3(M)

Creep coefficients a_1, a_2, a_3, for the time step t_{n-1}.

(*) NOTES: When controlled displacement is used, it is necessary to specify FLOAD=1. The program scales the external load in order to obtain the specified value of the controlled d.o.f. Prestressing can be introduced gradually by load steps. Since prestressing is treated as an initial strain load vector, its value is controlled by factor FINST (LST).

14.7 Current concrete properties. (3E10.0) - One line for each concrete

Skip if ITIME = 1

Col. 1 - 10	ECI(M)	Current initial modulus
Col. 11 - 20	FCDP(M)	Concrete compressive strength (enter negative)
Col. 21 - 30	FTP	Concrete tensile strength

14.8 Shrinkage strain increment. Skip if KSHRNK = 0

14.8.1 Constant value for all the structure. (KSHRNK = 1) (F10.0)

One line

Col. 1 - 10	DEPSS	Shrinkage strain

14.8.2 Planar Variation (KSHRNK = 2) (I8,9E8.2)

Increments of shrinkage strain for the current time step are specified at three arbitrary points of the cross section for each element. The shrinkage strain increment for each filament is automatically obtained by the program by fitting a plane surface of shrinkage strains on the section.

Col. 1 - 8	I	Current element number
Col. 9 - 16	SY(1)	Y coordinate, in locals, of first point
Col. 17 - 24	SZ(1)	Z coordinates, in locals, of first point
Col. 25 - 32	SS(1)	Shrinkage strain increment at point 1

Col. 33 - 40	SY(2)	Y coordinate, in locals, of second point
Col. 41 - 48	SZ(2)	Z coordinate, in locals, of second point
Col. 49 - 56	SS(2)	Shrinkage strain increment at point 2
Col. 57 - 64	SY(3)	Y coordinate, in locals, of third point
Col. 65 - 72	SZ(3)	Z coordinate, in locals, of third point
Col. 73 - 80	SS(3)	Shrinkage strain increment, at point 3

14.9 Temperature value. (Skip if KTEMP = 0)

14.9.1 Constant value in all the structure (KTEMP = 1)(F10.0)
One line

Col. 1 - 10	TEMP	Temperature (In centigrade degrees) (*)

14.9.2 Planar variation (KTEMP = 2) (I8,9F8.0) - One card for each element

Col. 1 - 8	I	Element number
Col. 9 - 16	YT(1)	Y - Coordinate, in locals, of first point
Col. 17 - 24	ZT(1)	Z - Coordinate, in locals, of first point

Col. 25 - 32	TT(1)	Temperature, in degrees centigrade, of first point
Col. 33 - 40	YT(2)	Y - Coordinate, in locals, of second point
Col. 41 - 48	ZT(2)	Z - Coordinate, in locals, of second point
Col. 49 - 56	TT(2)	Temperature, in degrees centigrade, of second point
Col. 57 - 64	YT(3)	Y - Coordinate, in locals, of third point
Col. 65 - 72	ZT(3)	Z - Coordinate, in locals, of third point
Col. 73 - 80	TT(3)	Temperature, in degrees centigrade, of third point.

(*) Temperature values for this option are specified at three arbitrary points of the cross section for each element. The value of the temperature at each filament is automatically obtained by the program, by fitting a planar surface of temperatures into the section.

9. SUMMARY AND CONCLUSIONS

9.1 Summary

A numerical procedure for the material and geometric non-linear analysis of three dimensional reinforced and prestressed concrete frames under short time and sustained loading has been presented. The response of such structures can be traced through their elastic, cracking, inelastic and ultimate load ranges.

A finite element displacement formulation coupled with a time step integration solution is used. An incremental load method combined with the unbalanced load iterations for each load increment is utilized for the solution of the nonlinear equilibrium equations. In addition, an iterative scheme based upon constant imposed displacement can be used so that structures with local instabilities or strain softenings can also be analyzed.

A straight beam element with an arbitrary cross-section is used. The element has six degrees of freedom at each end plus one internal axial degree of freedom at mid length that is eliminated, at element level, by static condensation.

In order to account for varied material properties within a frame element, the element is divided into a discrete number of concrete and reinforcing steel filaments which are assumed to be perfectly bonded together.

Material non-linearities due to cracking of the concrete, nonlinear stress-strain behaviour in the concrete and yielding

of the steel reinforcement are considered. Both materials, concrete and steel, are considered to be subjected to a uniaxial stress state. It is assumed that plane sections remain plane and the deformations due to shearing strains are neglected.

The integrations required to evaluate the element properties such as the stiffness matrix or the internal resisting load vector are then performed filament by filament through the surface of the cross section. By the use of the filament system, together with a special matrix, non uniform cross-sections can be modeled. An effective torsional stiffness approach has been used to represent the nonlinear torsional behaviour of the beam element.

An updated Lagrangian formulation has been used to take into account the nonlinear geometry effects due to the change in geometry of the structure. The formulation is based upon average rotations of the beam elements axes and is restricted to small strains and small incremental rotations.

Post tensioned bonded concrete frames can be analyzed with this numerical procedure.

Prestressing steel tendons are divided into a discrete number of linear segments each of which is assumed to span an element and have a constant stress along its length. The contributions of the prestressing steel to the element properties are added directly.

The effect of prestressing is introduced in the structure as an equivalent load vector obtained by equilibrating the

forces of the prestressing tendons.

Short time prestressing losses due to friction, curvature and anchorage slip are taken into account as well as long time losses due to creep and shrinkage of concrete and relaxation of prestressing steel.

An efficient procedure for the evaluation of creep strain based upon an age and temperature dependent integral formulation is incorporated. The creep strain increment at the current time step requires only the knowledge of the hidden state variables of the last time step. This is due to the use of a Dirichlet series for the specific creep function in which the coefficients can be readily determined from the available creep data.

Finally, a series of numerical examples analyzed by the computer program, based on the above principles, are presented and compared with the available theoretical and experimental results to demonstrate the applicability and validity of the present method of analysis.

9.2 Conclusions and Recommendations

The present method of analysis has been shown to be capable of predicting the nonlinear response of reinforced and prestressed concrete three dimensional frames under short time and long time loading fairly accurately.

The present modelling of material properties is capable of capturing the dominant flexural behaviour of reinforced and

prestressed concrete three dimensional frames in the elastic, inelastic and ultimate load ranges. It seems to be specially adequate to analyse the nonlinear behaviour of members with arbitrary cross section subjected to biaxial bending.

The nonlinear geometry analysis procedure is adequate to analyze structures subjected to strain softenings. On the other hand the constant imposed displacement procedure used as non linear strategy seems to present better convergence than the contant imposed load.

The amount and position of prestressing has been shown to have an important influence , not always favourable, on the behaviour of prestressed concrete columns.

The following recommendations can be made for future studies:

- A curved beam element based on the degeneration concepts could be developed.
- Interaction between flexural and torsional behaviour should be studied and incorporated in the model.
- Torsional response of arbitrary cross sections should be investigated, including also the effect of prestressing in the torque-twist relationship.
- The present study can be extended to include pretensioned and post-tensioned unbonded structures.

REFERENCES

1. Ngo, D. and Scordelis, A.C., "Finite Element Analysis of Reinforced Concrete Beams," ACI Journal, V.64, No.3, March 1967.

2. Scordelis, A.C., "Finite Element Analysis of Reinforced Concrete Structures," Proceedings of the Speciality Conference on Finite Element Methods in Civil Engineering, Montreal, June 1972.

3. Scordelis, A.C., "Analytical Models for Nonlinear Material, Geometric and Time Dependent Effects," Proceedings of The International Symposium on Nonlinearity and Continuity in Prestressed Concrete. University of Waterloo, Waterloo, Ontario, Canada, July 1983.

4. Schnobrich, W.C., "Behavior of Reinforced Concrete Predicted by Finite Element Method," Proceedings of the Second International Symposium on Computerized Structural Analysis and Design, George Washington University, Washington D.C., March 1976.

5. Bazant, Z.P., Schnobrich, W.C. and Scordelis, A.C., "Finite Element Analysis of Reinforced Concrete Structures Corso di perfezionamiento per le Costruzioni in Cemento Armato "Fratelli Pesenti," Milano, June 1978.

6. ASCE Task Committee on Finite Element Analysis of Reinforced Concrete Structures, State-of-the-Art Report on "Finite Element Analysis of Reinforced Concrete," ASCE Special Publicactions, 1982.

7. Selna, L.G., "Time Dependent Behavior of Reinforced Concrete Structures," UC-SESM Report No.67-19, Division of Structural Engineering and Structural Mechanics, University of California, Berkeley, 1967.

8. Aas-Jackobsen, K., "Design of Slender Reinforced Concrete Frames," Bericht No.48, Institut fur Baustatik, ETH, Zurich 1973.

9. Aldstedt, E., "Nonlinear Analysis of Reinforced Concrete Frames," Division of Structural Mechanics, Institute of Technology, University of Trondheim, Norway, 1975.

10. Kang, Y.J., "Nonlinear Geometric, Material and Time Dependent Analysis of Reinforced and Prestressed Concrete Frames," Ph.D. Dissertation, Division of Structural Engineering and Structural Mechanics, University of California, Berkeley, UC-SESM Report No.77-1, January 1977.

11. Hellesland, J. and Scordelis, A.C., "Analysis of Reinforced Concrete Bridge Columns Under Imposed Deformations," Proceedings of the IABSE Colloquium on "Advanced Mechanics of Reinforced Concrete," Delft, The Netherlands, June 1981.

12. Ketchum, M.A. and Scordelis, A.C., "Nonlinear Analysis of a Prestressed Concrete Bridge," Proceedings of the IABSE Colloquium on "Advanced Mechanics of Reinforced Concrete," Delft, The Netherlands, June 1981.

13. Buckle, I.G. and Jackson, A.T., "A Filament Beam Element for the Nonlinear Analysis of Reinforced Concrete Beam and Slab Structures," Department of Civil Engineering, University of Auckland, New Zealand 1981.

14. Chan, E.C., "Nonlinear Geometric, Material and Time Dependent Analysis of Reinforced Concrete Shells with Edge Beams," Ph.D. Dissertation. Division of Structural Engineering and Structural Mechanics, University of California, Berkeley, December 1982.

15. ACI Committee 209, "Prediction of Creep, Shrinkage and Temperature Effects in Concrete Structures," ACI Publicaction SP-27, 1970.

16. Warner, R.F., "Biaxial Moment Thrust Curvature Relations," Journal of the Structural Division, ASCE, No.ST5, May 1969, pp. 6564-6570.

17. Wilson, E.L., "Solid SAP - A Static Analysis Program for Three Dimensional Solid Structures," UC-SESM Report No. 71-19, University of California, Berkeley, March 1972.

18. Kabir, A.F., "Nonlinear Analysis of Reinforced Concrete Panels, Slabs and Shells for Time Dependent Effects," Ph.D. Dissertation, Division of Structural Engineering and Structural Mechanics, University of California, Berkeley, UC-SESM Report No.76-6, December 1976.

19. Van Greunen, J., "Nonlinear Geometric, Material and Time Dependent Analysis of Reinforced and Prestressed Concrete Slabs and Panels," Ph.D. Dissertation, Division of Structural Engineering and Structural Mechanics, University of California, Berkeley, UC-SESM Report No.79-3, October 1979.

20. Van Zyl, S.F., "Analysis of Curved Segmentally Erected Prestressed Concrete Box Girders Bridges", Ph.D. Dissertation, Division of Structural Engineering and Structural Mechanics, University of California, Berkeley, UC-SESM Report No.78-2, January 1978.

21. Bergan, P., "Solution Techniques for Nonlinear Finite Element Problems," International Journal for Numerical Methods in Engineering, Vol.12, 1978.

22. Simons, J.W., "Solution Strategies for Statically Loaded Nonlinear Structures," Ph.D. Dissertation, Division of Structural Engineering and Structural Mechanics, University of California, Berkeley, May 1982.

23. Bathe, K.J. and Bolourchi, S., "Large Displacement Analysis of Three Dimensional Beam Structures," International Journal for Numerical Methods in Engineering, Vol.14, 1979.

24. Bathe, K.J., Ramm, E. and Wilson, E.L., "Finite Element Formulations for Large Displacement and Large Strain Analysis," Division of Structural Engineering and Structural Mechanics, University of California, Berkeley, UC-SESM Report No.73-14, February 1973.

25. Sorensen, S.I. and Scordelis A.C., "Computer Program for Curved Prestressed Box Girder Bridges," Division of Structural Engineering and Structural Mechanics, University of California, Berkeley, UC-SESM Report No.80-10, December 1980.

26. Lin, T.Y. and Burns, N.H., "Design of Prestressed Concrete Structures," John Wiley and Sons, Third Edition, 1981.

27. Chen, W.F., "Plasticity in Reinforced Concrete," Mac Graw-Hill, 1982.

28. Bathe, K.J., "Finite Element Procedures in Engineering Analysis," Prentice Hall Inc. Englewood Cliffs N.J. 1981.

29. Schreyer, H. and Masur, E., "Buckling of shallow arches," Journal of the Engineering Mechanics Division, ASCE, V.92, No. EM4, August 1966.

```
EXAMPLE 7.4. PRETENSIONED, Np=60 Kips. (KPRT=2)
11,1,10,1,1,0,1,1,2,2,28.,0.,0.00001
1,0.,0.,0.
2,10.,0.,0.
3,20.,0.,0.
4,30.,0.,0.
5,40.,0.,0.
6,50.,0.,0.
7,60.,0.,0.
8,70.,0.,0.
9,80.,0.,0.
10,90.,0.,0.
11,100.,0.,0.
1,1.,0.,0.,0.,1.,0.,0.,0.,1.
1,1.E+10,1.E+10,1.E+10,1.E+10,1.E+10,1.E+10,1.E+10,1.E+10,1.E+10
1,10,10,16,10,5.,5.,-5.,-5.,240.
1,1,4,1
2,1,4,1
3,1,4,1
4,1,4,1
5,1,10,1
6,1,10,1
7,1,10,1
8,1,10,1
9,1,10,1
10,1,10,1
0.3415,-4.,4.
0.3415,-2.,4.
0.3415,-4.,2.
0.3415,-2.,2.
0.3415,-4.,0.
0.3415,-2.,0.
0.3415,0.,0.
0.3415,2.,0.
0.3415,4.,0.
0.3415,-4.,-2.
0.3415,4.,-2.
0.3415,-4.,-4.
0.3415,-2.,-4.
0.3415,0.,-4.
0.3415,2.,-4.
0.3415,4.,-4.
1900.,9100.,0.0044,0.013,0.036
1,1,2,1,1,0.,0.,1.
2,2,3,1,1,0.,0.,1.
3,3,4,1,1,0.,0.,1.
4,4,5,1,1,0.,0.,1.
5,5,6,1,1,0.,0.,1.
6,6,7,1,1,0.,0.,1.
7,7,8,1,1,0.,0.,1.
8,8,9,1,1,0.,0.,1.
9,9,10,1,1,0.,0.,1.
10,10,11,1,1,0.,0.,1.
1,2,20,3,130.,0.,0.,10.
110.,0.0045,130.,0.006,140.,0.05
1,1,10,2,1.37,0.,30.,0.
2,1,10,2,1.37,0.,30.,0.
1,1,1,-4.,-4.,-4.,-4.
2,2,1,-4.,-4.,-4.,-4.
3,3,1,-4.,-4.,-4.,-4.
4,4,1,-4.,-4.,-4.,-4.
5,5,1,-4.,-4.,-4.,-4.
6,6,1,-4.,-4.,-4.,-4.
7,7,1,-4.,-4.,-4.,-4.
8,8,1,-4.,-4.,-4.,-4.
9,9,1,-4.,-4.,-4.,-4.
10,10,1,-4.,-4.,-4.,-4.
11,1,2,4.,-4.,4.,-4.
12,2,2,4.,-4.,4.,-4.
13,3,2,4.,-4.,4.,-4.
14,4,2,4.,-4.,4.,-4.
15,5,2,4.,-4.,4.,-4.
16,6,2,4.,-4.,4.,-4.
17,7,2,4.,-4.,4.,-4.
18,8,2,4.,-4.,4.,-4.
19,9,2,4.,-4.,4.,-4.
20,10,2,4.,-4.,4.,-4.
3600.,1800.,-4.,0.1,-0.0035,0.35,1.865
30000.,0.,36.6,0.16
1,10,10,0,3,0,0,0,0
0.1,0.1,0.1,10.,20.,10.,10.
1,14,1,0,1,11,3,2.
11,-100.,0.,0.,0.,-216.,-125.
1,1.,1.,0.1
2,1.,1.,0.1
3,1.,1.,0.1
4,1.,1.,0.1
5,1.,1.,0.1
6,1.,1.,0.1
7,1.,1.,0.1
8,1.,1.,0.1
9,1.,1.,0.05
10,1.,1.,0.05
11,1.,1.,0.05
12,1.,1.,0.05
13,1.,1.,0.05
14,1.,1.,0.05
```

NOTE The data are in free format

APPENDIX - INPUT DATA FOR EXAMPLE NO. 3